PHYSICAL VOLCANOLOGY, PETROLOGY, AND PETROGENESIS OF THE CRETACEOUS ISACHSEN FORMATION VOLCANICS, WESTERN AXEL HEIBERG ISLAND, N.W.T.

Eric Wesely Pearson

Submitted in Partial Fulfilment of the Requirements
for the Degree of Bachelor of Science, Honours
Department of Earth Sciences
Dalhousie University, Halifax, Nova Scotia
March 1994

Distribution License

DalSpace requires agreement to this non-exclusive distribution license before your item can appear on DalSpace.

NON-EXCLUSIVE DISTRIBUTION LICENSE

You (the author(s) or copyright owner) grant to Dalhousie University the non-exclusive right to reproduce and distribute your submission worldwide in any medium.

You agree that Dalhousie University may, without changing the content, reformat the submission for the purpose of preservation.

You also agree that Dalhousie University may keep more than one copy of this submission for purposes of security, back-up and preservation.

You agree that the submission is your original work, and that you have the right to grant the rights contained in this license. You also agree that your submission does not, to the best of your knowledge, infringe upon anyone's copyright.

If the submission contains material for which you do not hold copyright, you agree that you have obtained the unrestricted permission of the copyright owner to grant Dalhousie University the rights required by this license, and that such third-party owned material is clearly identified and acknowledged within the text or content of the submission.

If the submission is based upon work that has been sponsored or supported by an agency or organization other than Dalhousie University, you assert that you have fulfilled any right of review or other obligations required by such contract or agreement.

Dalhousie University will clearly identify your name(s) as the author(s) or owner(s) of the submission, and will not make any alteration to the content of the files that you have submitted.

If you have questions regarding this license please contact the repository manager at dalspace@dal.ca.

Grant the distribution license by signing and dating below.

_____ _____

Name of signatory Date

Distribution License

DalSpace requires agreement to this non-exclusive distribution license before your item can appear on DalSpace.

NON-EXCLUSIVE DISTRIBUTION LICENSE

You (the author(s) or copyright owner) grant to Dalhousie University the non-exclusive right to reproduce and distribute your submission worldwide in any medium.

You agree that Dalhousie University may, without changing the content, reformat the submission for the purpose of preservation.

You also agree that Dalhousie University may keep more than one copy of this submission for purposes of security, back-up and preservation.

You agree that the submission is your original work, and that you have the right to grant the rights contained in this license. You also agree that your submission does not, to the best of your knowledge, infringe upon anyone's copyright.

If the submission contains material for which you do not hold copyright, you agree that you have obtained the unrestricted permission of the copyright owner to grant Dalhousie University the rights required by this license, and that such third-party owned material is clearly identified and acknowledged within the text or content of the submission.

If the submission is based upon work that has been sponsored or supported by an agency or organization other than Dalhousie University, you assert that you have fulfilled any right of review or other obligations required by such contract or agreement.

Dalhousie University will clearly identify your name(s) as the author(s) or owner(s) of the submission, and will not make any alteration to the content of the files that you have submitted.

If you have questions regarding this license please contact the repository manager at dalspace@dal.ca.

Grant the distribution license by signing and dating below.

_____ _____

Name of signatory Date

Dalhousie University

Department of Earth Sciences
Halifax, Nova Scotia
Canada B3H 3J5
(902) 494-2358
FAX (902) 494-6889

DATE April 25, 1994

AUTHOR Eric Wesely Pearson

TITLE Physical Volcanology, Petrology, and Petrogenesis of the Cretaceous Isachsen Formation Volcanics, Western Axel Heiberg Island, N.W.T.

Degree BSc. (Honours) Convocation May Year 1994

Permission is herewith granted to Dalhousie University to circulate and to have copied for non-commercial purposes, at its discretion, the above title upon the request of individuals or institutions.

Abstract

New data from Bjarnasson Island and Bals Fiord on western Axel Heiberg Island provide insight into the physical volcanology, petrology, and petrogenesis of Cretaceous Isachsen Formation magmatism. The Bjarnasson Island section is the oldest volcanogenic sequence of the Isachsen Formation. The lower stratigraphic position of the Bjarnasson Island section may be the result of erosional incision or faulting. The Bals Fiord section contains a thick basal sequence of interbedded pyroclastic (hydrovolcanic), distal epiclastic (mass-flow), and thin sedimentary (fluvial) deposits, that mark an initial explosive phase of volcanism in a fluvial-deltaic setting. Volcanic deposits at Bals Fiord change abruptly from pyroclastics to a thick flow sequence with interbedded fluvial-deltaic sedimentary units. Petrographically the Bals Fiord and Bjarnasson Island samples are tholeiites or olivine-tholeiites, and occur in two distinct textural varieties: (i) fine-grained porphyritic and glomeroporphyritic flows from Bjarnasson Island, and (ii) seriate-textured flows from Bals Fiord. Three geochemically distinct populations of Isachsen Formation samples exist, each population consisting mainly of Bjarnasson Island, Bals Fiord, or Bunde Fiord samples. Petrogenetic evaluation of all available Isachsen Formation volcanic samples reveals that at least two magmas, which shared a common parental composition similar to the Bjarnasson Island basalts (primitive flows from an early eruptive event) and distinct fractionation histories, contributed to Walker Island Member volcanism. Variations in the proportion of clinopyroxene fractionation, or the introduction of magnetite fractionation in the Bals Fiord source, may account for the compositional variation between Walker Island Member sources. The Bals Fiord section is the thickest, most proximal, and western-most Walker Island Member volcanogenic sequence, all of which suggests that the source region lies off the west coast of present-day Axel Heiberg Island.

Key Words: Walker Island Member, tholeiite, Bals Fiord, Bjarnasson Island, volcaniclastics, fractionation

TABLE OF CONTENTS

ABSTRACT i

TABLE OF CONTENTS ii

TABLE OF FIGURES vi

TABLE OF TABLES ix

ACKNOWLEDGEMENTS x

CHAPTER 1: INTRODUCTION

1.1 Opening Statement 1

1.2 Background 1

1.3 Purpose of Study 5

1.4 Scope of Investigation 5

1.5 Organization 6

CHAPTER 2: TECTONOMAGMATIC DEVELOPMENT OF THE SVERDRUP BASIN

2.1 Introduction 7

2.2 Tectonic Development of the Sverdrup Basin 7

2.3 Magmatism in the Sverdrup Basin

2.31 Late Paleozoic Magmatism 8

2.32 Cretaceous Magmatism 16

2.4 Summary 12

CHAPTER 3: VOLCANOLOGY AND PALEOENVIRONMENT OF THE ISACHSEN VOLCANIC EVENT

3.1 Introduction 13

3.2 The Bals Fiord Section

3.2.1 Introduction 13

3.2.2 Volcaniclastic Deposits 15

3.2.2.1 Introduction 15

3.2.2.2 Observations 20

3.2.2.3 Regional interpretation 26

3.2.3 Volcanic Flows and Associated Intrusives 31

3.2.3.1 Introduction 31

3.2.3.2 Observations 31

3.2.3.3 Interpretation 35

3.2.4 Sedimentary Units 37

3.2.4.1 Introduction 37

3.2.4.2 Observations 37

3.2.4.3 Interpretation 38

3.3 Bjarnasson Island Section 39

3.4 Summary 42

CHAPTER 4: PETROLOGY AND GEOCHEMISTRY

4.1 Introduction 44

4.2 Petrography

4.2.1 Introduction 44

4.2.2 Mineralogy 44

4.2.3 Textures 51

4.2.4 Petrographic Classification 51

4.3 Geochemistry

4.3.1 Introduction 53

4.3.2 Alteration 53

4.3.3 Geochemical Classification 56

4.4 Summary 59

CHAPTER 5: PETROGENETIC INTERPRETATION OF ISACHSEN FORMATION MAGMATISM

5.1 Introduction 63

5.2 Major and Trace Element Variation

5.2.1 Introduction 63

5.2.2 Incompatible and Immobile Elements 64

5.2.3 Major Elements 67

5.2.4 Trace Elements 69

5.2.5 Summary 69

5.3 Petrogenetic Interpretation

5.3.1 Introduction 71

5.3.2 Trend Analysis 72

5.3.3 Summary 77

CHAPTER 6: DISCUSSION AND CONCLUSIONS 79

REFERENCES 86

APPENDIX A: PETROGRAPHIC DESCRIPTIONS A1

APPENDIX B: GEOCHEMICAL DATA B1

TABLE OF FIGURES

Figure 1.1. Diagram showing the age relationships between tectonic events and volcanism in the Sverdrup Basin. 2

Figure 1.2a. Location of the study area within the Canadian Arctic Archipelago, and within the present-day outline of the Sverdrup Basin. 3

Figure 1.2b. Detailed location map showing the location of Isachsen Formation volcanogenic sections on western Axel Heiberg Island. 4

Figure 2.1. Areal distribution and thickness of the Cretaceous volcanic deposits (Embry and Osadetz 1988). 10

Figure 2.2. Schematic Cretaceous stratigraphy of the northeastern Sverdrup Basin showing the four T-R cycles of Embry and Osadetz (1988). 11

Figure 3.1. Stratigraphic section of the Isachsen Formation volcanogenic sequence at Bals Fiord. 14

Figure 3.2. Volcaniclastic classification scheme (after Cas and Wright 1987). 16

Figure 3.3. Photomicrograph of Unit 2a in PPL. 22

Figure 3.4. Photomicrograph of Unit 2b in PPL. 22

Figure 3.5. Photomicrograph of Unit 4 in PPL. 25

Figure 3.6. Photograph of a common pyroclastic bomb from Unit 5a. 25

Figure 3.7. Photomicrograph of quartz-rich matrix from the bomb horizon in Unit 5a. 27

Figure 3.8. Photomicrograph of the immature quartz sandstone (fluvial) typical of the Bals Fiord section. 27

Figure 3.9a. Photomicrograph of quartz-rich pyroclastic material from Unit 2b in PPL. 28

Figure 3.9b. Photomicrograph of a partially resorbed detrital quartz grain in the base of Flow #5 in PPL. 28

Figure 3.10a. Photograph of the tree stump in the base of Flow #5. 34

Figure 3.10b. Tracing of the photograph in Figure 3.10a. 34

Figure 3.11. Photograph of the top of the tree stump in Figure 3.10a. 35

Figure 3.12. Photograph of the tree fragment on the east side of the stump in Figure 3.10a. 36

Figure 3.13. Photograph of the sand-flame structure in the base of Flow #11. 36

Figure 3.14 Photograph of the shallow marine trace fossil Diplocraterion, from the sandstone above Flow #8. 41

Figure 3.15. Photograph of Flow #3 from Bjarnasson Island showing vertical to sub-horizontal column development. 41

Figure 4.1. Photomicrograph of a large plagioclase phenocryst in Flow #6. 46

Figure 4.2a. Photomicrograph showing the common mineral assemblage and seriate texture of the Bals Fiord samples in PPL. 47

Figure 4.2b. As in Figure 4.2a., in XN. 47

Figure 4.3a. Photomicrograph showing the common mineral assemblage and fine-grained porphyritic to glomeroporphyritic texture of the Bjarnasson Island samples, PPL. 48

Figure 4.3b. As in Figure 4.3a., in XN. 48

Figure 4.4a. Photomicrograph of fresh glass in the Bals Fiord samples. 50

Figure 4.4b. Photomicrograph of palagonite-replaced glass in the Bals Fiord samples. 50

Figure 4.5. Petrographic classification scheme (after McKenzie et al. 1982). 52

Figure 4.6. Major element alteration plots for selected Bals Fiord samples. 57

Figure 4.7. Trace element alteration plots for selected Bals Fiord samples. 58

Figure 4.8. Geochemical classification scheme of Le Bas et al. (1986) showing the location of the Isachsen Formation samples. 60

Figure 4.9a. Geochemical classification scheme of Irvine and Baragar (1971) showing the tholeiitic nature of the Isachsen Formation samples. 61

Figure 4.9b. Geochemical classification scheme of Irvine and Baragar (1971) showing the subalkaline nature of the Isachsen Formation samples. 61

Figure 5.1. Variation diagram (Zr-Nb) for the Isachsen Formation samples. 65

Figure 5.2. Variation diagram (Zr-TiO_2) for the Isachsen Formation samples. 66

Figure 5.3. Variation diagrams for various other major elements against Zr for the Isachsen Formation samples. 68

Figure 5.4. Variation diagrams for various other trace elements against Zr for the Isachsen Formation samples. 70

Figure 5.5. Variation diagram (log Zr-log Nb) for the Isachsen Formation samples. 73

Figure 5.6. Variation diagram (log Zr-log TiO_2) for the Isachsen Formation samples. 75

Figure 6.1. Detailed location map showing the Isachsen Formation volcanogenic sections on western Axel Heiberg Island and possible edifice locations for Walker Island Member volcanism. 83

TABLE OF TABLES

Table 3.1. Epiclastic classification scheme of Smith (1986). 18

Table 3.2. Table of lithological data for the volcaniclastic deposits from the Bals Fiord section. 19

Table 4.1. Summary geochemical statistics for the Isachsen Formation samples. 54

ACKNOWLEDGEMENTS

First and foremost I would like to thank all who made the production of this thesis possible. I would like to thank Dr. Gunter Muecke for his support throughout the development of this document, and for giving me the opportunity to experience Arctic geology first-hand. Next I would like to thank Dr. Barrie Clarke for his time and effort in making revisions and significant contributions to this document. I also must thank my one-man technical support staff, Bradley McCallum, without whom this document would not exist. I would like to thank all of my professors and classmates for making my time at Dalhousie University memorable. Finally I thank Krista for her patience, love, and understanding throughout my undergraduate studies. An NSERC grant to Dr. Muecke provided financial support for this project, and field work was made possible by the Polar Continental Shelf Project.

CHAPTER 1: INTRODUCTION

1.1 Opening Statement

Volcanism in the Sverdrup Basin occurred in two stages: (i) Middle Carboniferous-Early Permian activity related to the formation of the Sverdrup Basin; and (ii) Early-Middle Cretaceous activity related to the opening of the Amerasian basin (Fig. 1.1). Isachsen Formation volcanism belongs to the later of the two episodes. This thesis describes in detail the Isachsen Formation volcanogenic sequences at Bals Fiord and on Bjarnasson Island (Figs. 1.2a,b). Data collected from Bals Fiord and Bjarnasson Island allows the description of paleoenvironment and physical volcanology for this volcanic episode. The petrogenetic interpretation of the Isachsen volcanic episode involves a combination of previous geochemical data from Bunde Fiord (Williamson 1988, Hinds 1991), and new data from Bals Fiord and Bjarnasson Island (this study).

1.2 Background

Two stages of alkali basalt volcanism accompanied the formation of the Sverdrup Basin (Fig. 1.1): (i) Late Carboniferous syn-rift volcanics of the Audhild Formation (Ritcey 1989), and (ii) Permian post-rift volcanics of the Esayoo Formation (Cameron 1989). This early volcanism in the Sverdrup Basin is of low volume and limited areal extent.

Early Cretaceous to Early Tertiary magmatism in the Sverdrup Basin coincides with rifting events related to the opening of the Amerasian Basin to the north

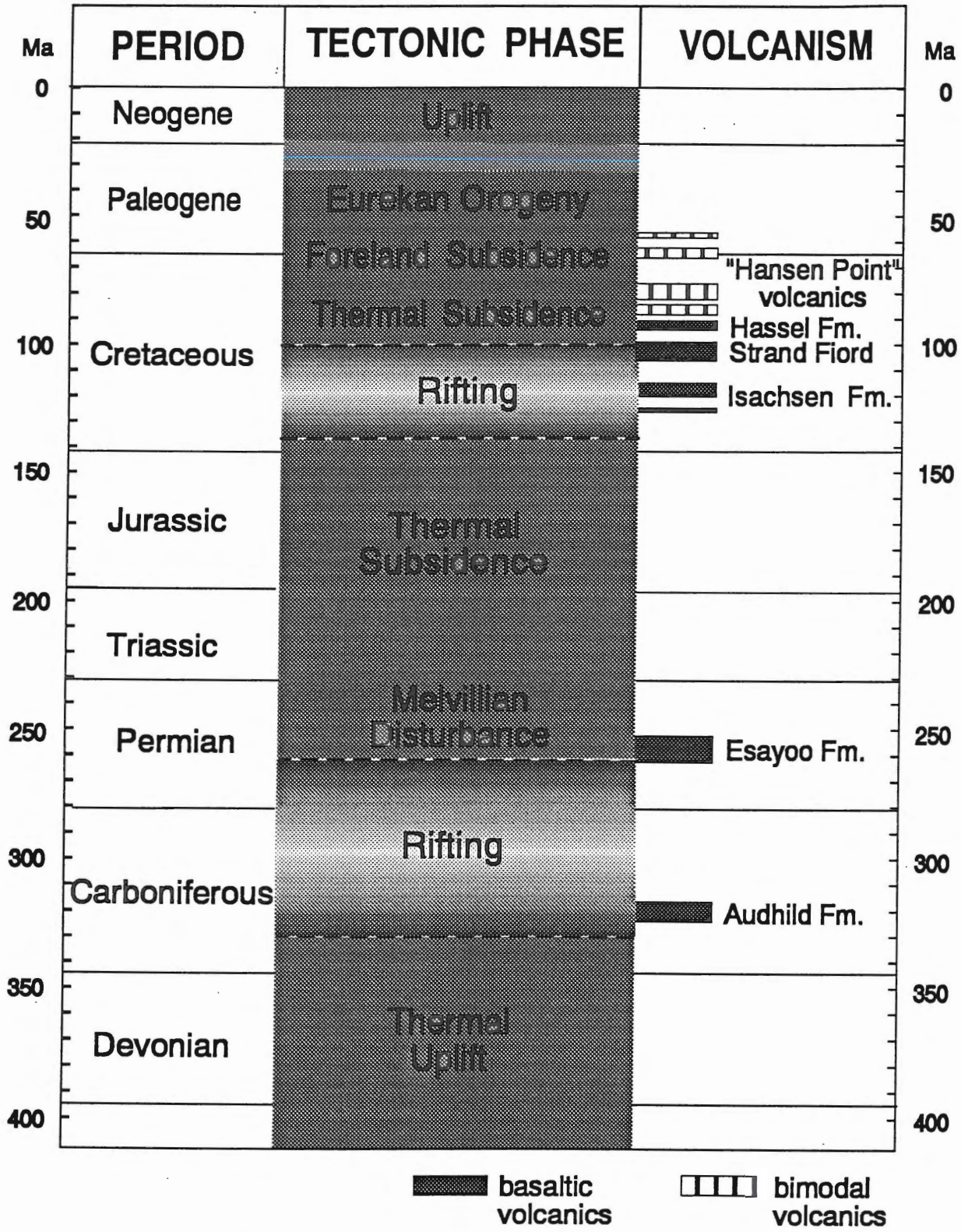

Figure 1.1. Diagram showing the age relationships between tectonic events and volcanism in the Sverdrup Basin.

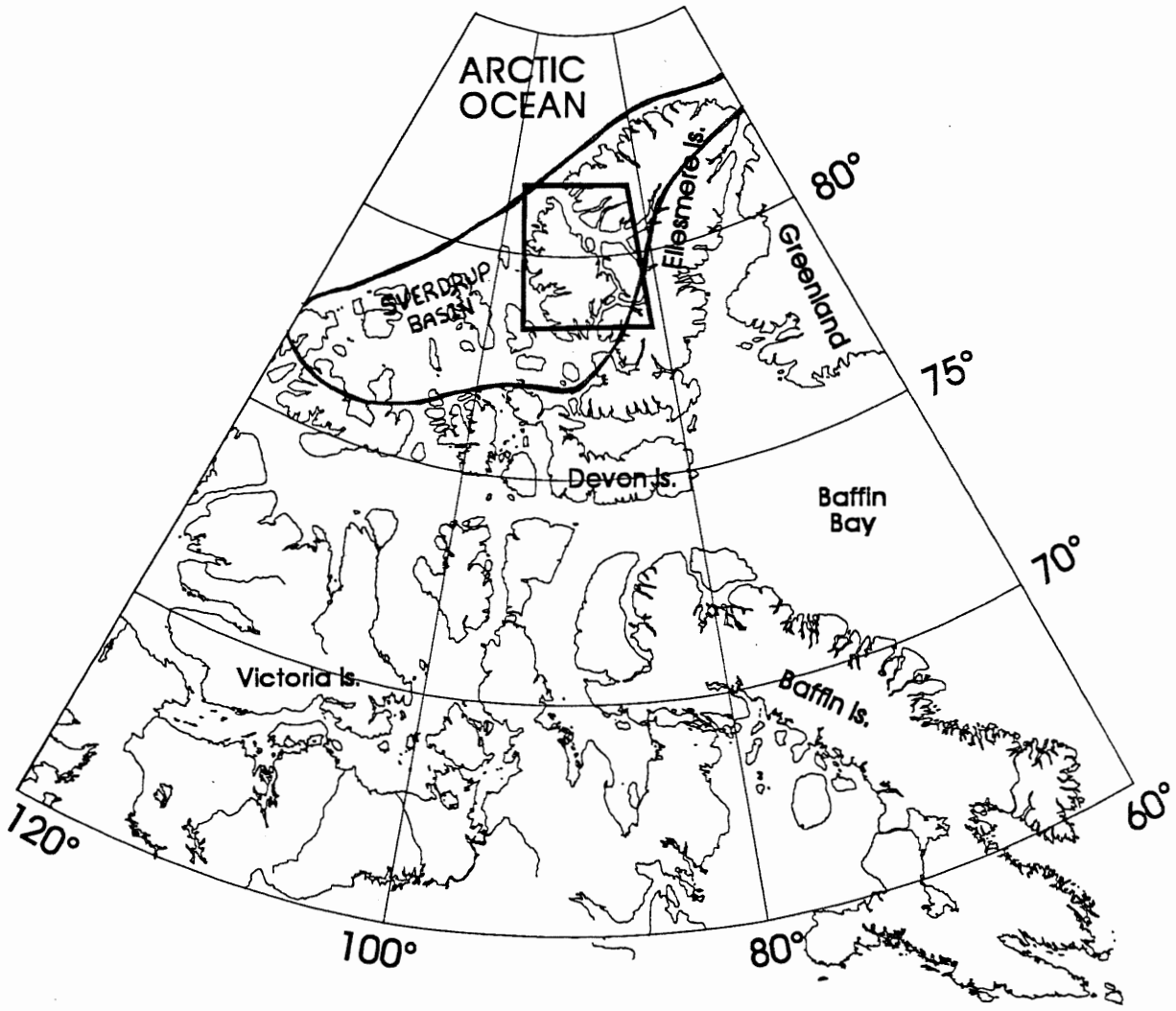

Figure 1.2a. Location of the study area within the Canadian Arctic Archipelago, and within the present-day outline of the Sverdrup Basin.

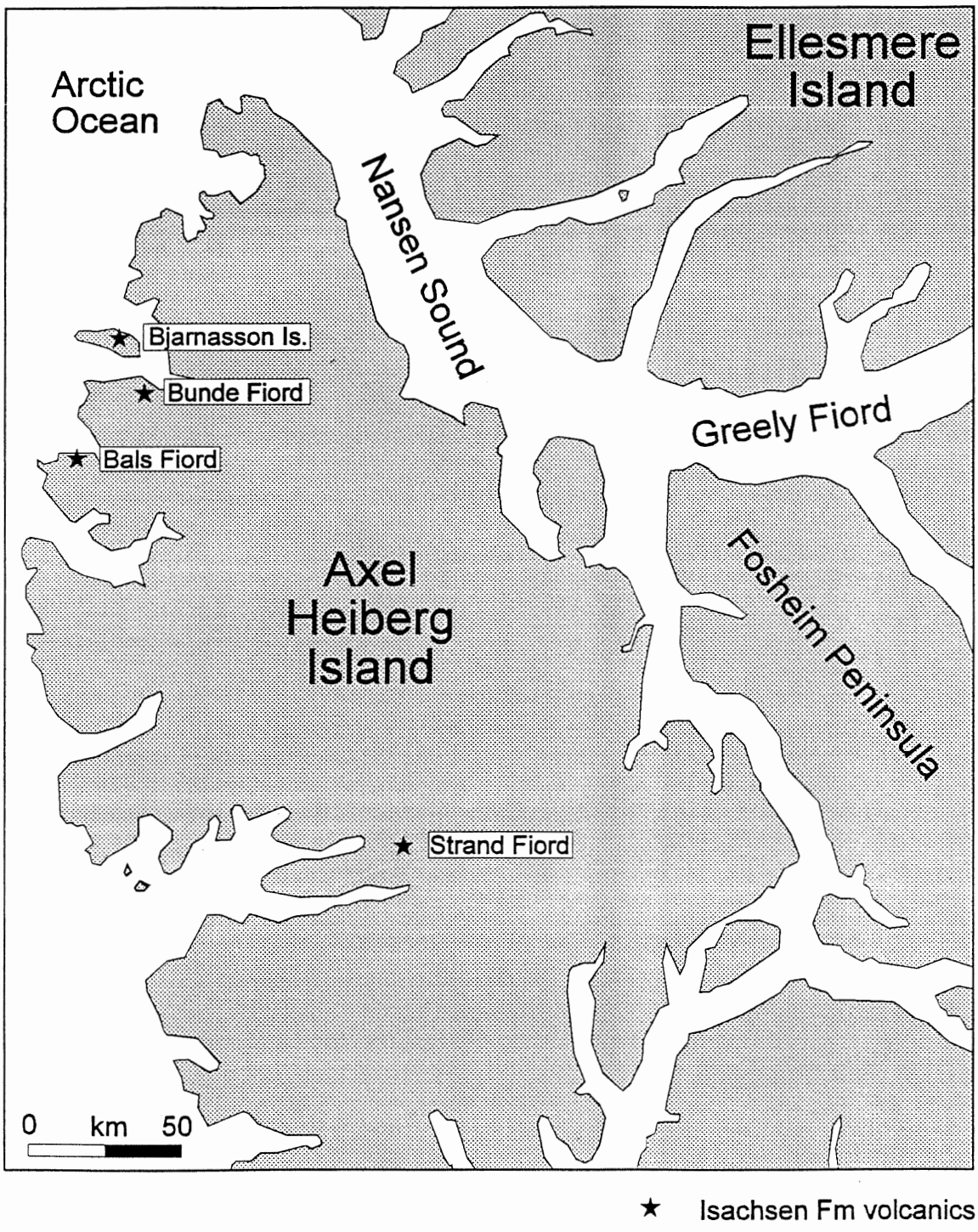

Figure 1.2b. Detailed location map (see Fig. 1.2a) showing the location of the Bals Fiord, Bjarnasson Island, Bunde Fiord, and Strand Fiord section locations.

(Embry and Osadetz 1988, Trettin 1989). The Cretaceous Isachsen and Strand Fiord formations contain thick mafic volcanic sequences, the product of renewed lithospheric extension and melt production below the Sverdrup Basin (Williamson 1988). Younger bimodal volcanics, present at several locations in the northeastern Sverdrup Basin, are not genetically or temporally related to the earlier Mesozoic events (Merrett and Muecke 1989, Muecke et al. 1990).

1.3 Purpose of Study

This study of Isachsen Formation volcanism includes two main parts: (i) the presentation of new stratigraphic, petrographic, and geochemical data, focusing mainly on the extensive section preserved at Bals Fiord, and (ii) a petrogenetic interpretation of Isachsen Formation volcanism involving a combination of new and previous geochemical data. Detailed study of the Bals Fiord volcanogenic sequence aids in the determination of paleoenvironment and physical volcanology for the Isachsen volcanic episode. Petrogenetic interpretation of all available Isachsen data provides insight into the evolution of the source for all Isachsen volcanics.

1.4 Scope of Investigation

The detailed physical description of Isachsen Formation volcanism involves stratigraphic analysis of the Bals Fiord section, with occasional reference to other Isachsen Formation volcanogenic sequences. The presentation of petrographic and geochemical data includes only new samples, collected in 1992, from Bals Fiord and Bjarnasson Island. Geochemical analyses include a suite of 10 major elements and 15

trace elements. The geochemical investigation does not include rare earth elements (REE) or isotopes. Petrogenetic studies involve the evaluation of major and trace element concentration variations in a data set including all available Isachsen Formation basalt analyses.

1.5 Organization

The following chapter summarises the tectonomagmatic history of the Sverdrup Basin, and the surrounding region. Chapter 3 includes descriptions of the Bals Fiord and Bjarnasson Island sections, and a discussion of the paleoenvironment and physical volcanology of Isachsen Formation volcanism. Chapter 4 presents the petrographic and geochemical data for the Bals Fiord and Bjarnasson Island basalts. A combination of new geochemical data with analyses from other Isachsen sections provides a large data base with which to evaluate petrogenesis in Chapter 5. Finally, Chapter 6 summarizes the results of this study, and provides some conclusions based on these results.

CHAPTER 2: TECTONOMAGMATIC DEVELOPMENT OF THE SVERDRUP BASIN

2.1 Introduction

The Sverdrup Basin, a large intracratonic basin, served as the major depocenter in the Canadian Arctic Islands from the Carboniferous to the early Tertiary (Balkwill 1978). The Sverdrup Basin is 1300 x 400 km in its greatest dimensions, and contains up to 12 km of sediments (Trettin 1989). This chapter describes the tectonic development of the Basin, and associated magmatic events.

2.2 Tectonic Development of the Sverdrup Basin

The Sverdrup Basin is approximately triangular in its surface expression, bounded to the south and east by stable cratonic regions, and to the north by the Sverdrup Rim, a horst of continental crust (Trettin 1989). The Basin suffered two stages of extension, discussed in chronological order below (Fig. 1.1).

Deposition in the Sverdrup Basin began in the Early Carboniferous as syn-rift sediments of the Emma Fiord Formation, and Audhild Formation volcanogenic deposits accumulated in graben and half-graben structures (Trettin 1989). Concentric, basin-wide depositional sequences in the latest Early Carboniferous mark the end of rifting, and the onset of thermal relaxation (Trettin 1989). The Permian Esayoo Formation volcanogenic deposits occur locally near the top of the Paleozoic sedimentary sequence (Trettin 1989).

The next phase of deposition in the Sverdrup Basin began with the renewed extension of the crust below the Basin during the Early Cretaceous opening of the Amerasian Basin to the north (Trettin 1989) (Fig. 1.1). The renewed extension in the Sverdrup Basin led to the production of very large volumes of mafic magma, as manifested by the thick Cretaceous volcanic sequences present in the northeastern parts of the Basin (Trettin 1989, Williamson 1988, Embry and Osadetz 1988) (Fig. 1.1).

Williamson (1988) suggests the combined evolution of parallel rift basins as a model for the tectonic development of the Sverdrup Basin. The older basin in this model experiences two phases of extension: (i) an initial rifting event, and (ii) renewed extension related to the opening of an adjacent basin. The sequence of events for the older basin in the parallel rift basin model resembles the tectonic history of the Sverdrup Basin (Williamson 1988) (Fig. 1.1). The following section summarizes magmatism in the Sverdrup Basin, which is closely linked to the tectonic development.

2.3 Magmatism in the Sverdrup Basin

2.3.1 Late Paleozoic Magmatism

Volcanism occurred in two episodes of low volume and limited areal extent during the Late Paleozoic development of the Sverdrup Basin (Fig. 1.1). Middle Carboniferous Audhild Formation volcanism, associated with the earliest rifting in the Basin, resulted in the deposition of subaerial volcaniclastics and alkaline basalt flows within the basal rift sedimentary sequence (Ritcey 1989, Trettin 1989). The Permian Esayoo Formation volcanogenic deposits occur within the early post-rift sedimentary

sequence, and consist of alkaline to transitional basalt flows and volcaniclastics up to 300 m in total thickness (Cameron 1989, Trettin 1989).

Late Paleozoic volcanism in the Sverdrup Basin resulted from partial melting of the asthenosphere below the Basin during rifting (Williamson 1988). Although volumetrically small, this melting event likely caused a significant depletion of incompatible elements in the asthenosphere below the Sverdrup Basin. This depletion has implications for the determination of source composition, and the melt-generation mechanism for Cretaceous volcanism.

2.3.2 Cretaceous Magmatism

Cretaceous magmatism in the Sverdrup Basin is highly voluminous, but restricted in areal extent to the northeastern part of the Basin. This magmatism reflects renewed extension of the Sverdrup Basin, related to the opening of the Amerasian Basin to the north (Williamson 1988, Trettin 1989).

Embry and Osadetz (1988) suggest that mafic volcanism accompanied each of four transgressive-regressive (T-R) sedimentation cycles in the Sverdrup Basin (Figs. 2.1 and 2.2). Data collected in 1992 contributes significantly to the understanding of Cretaceous volcanism. A section on northern Bjarnasson Island contains basalt flows within the Lower Isachsen Formation sediments of T-R cycle #1 (Figs. 2.1 and 2.2), however these units are of limited areal extent. This Bjarnasson Island volcanic sequence may be continuous into the Upper Isachsen Formation, related to T-R cycle #2 (Figs. 2.1 and 2.2). Several Isachsen Formation basalt units occur on the south side of Bjarnasson Island, only one of which occurs within the Lower Isachsen Formation.

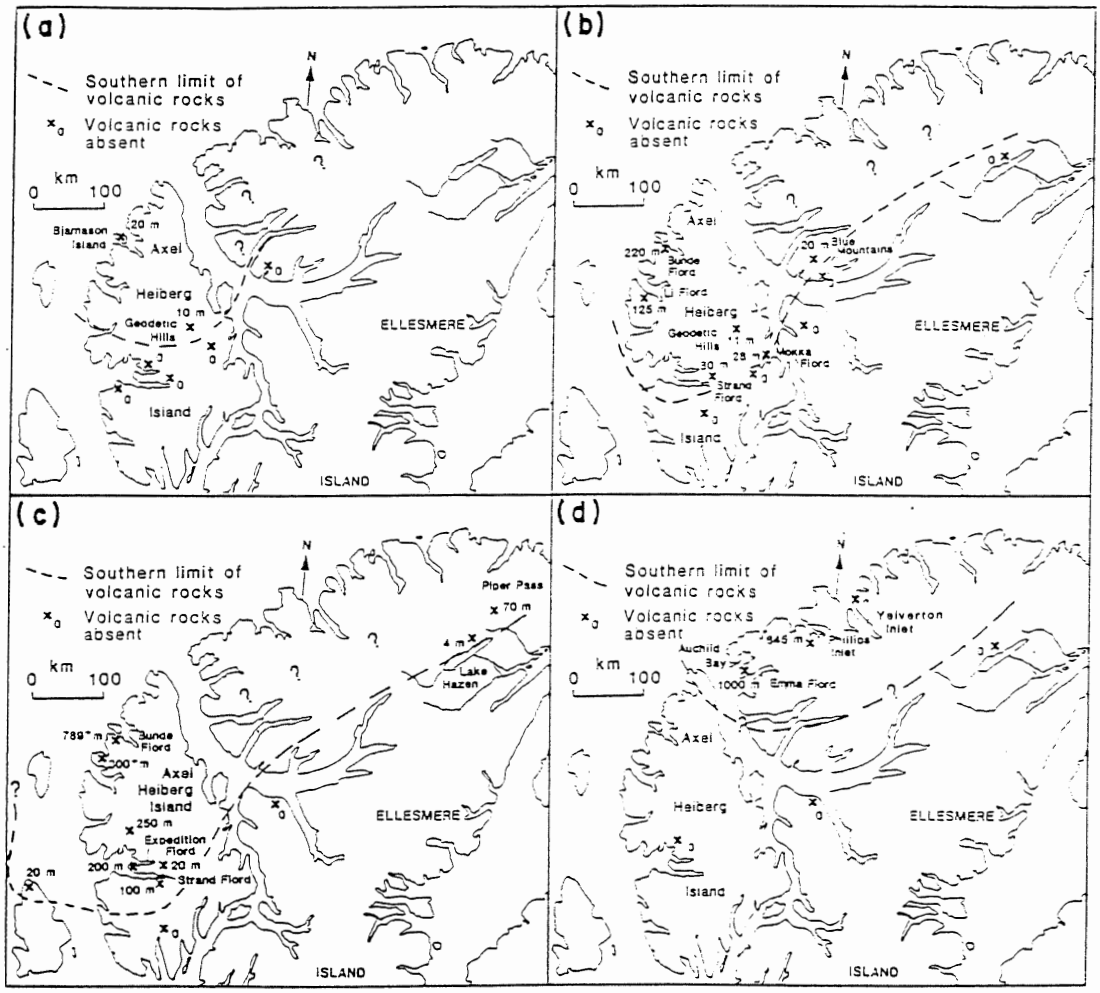

Figure 2.1. Areal distribution and thickness of the Cretaceous volcanic deposits believed to be associated with the four transgressive-regressive cycles proposed by Embry and Osadetz (1988): a) Lower Isachsen Formation, b) Upper Isachsen Formation, c) Strand Fiord Formation, and d) "Hansen Point Volcanics" (Embry and Osadetz 1988).

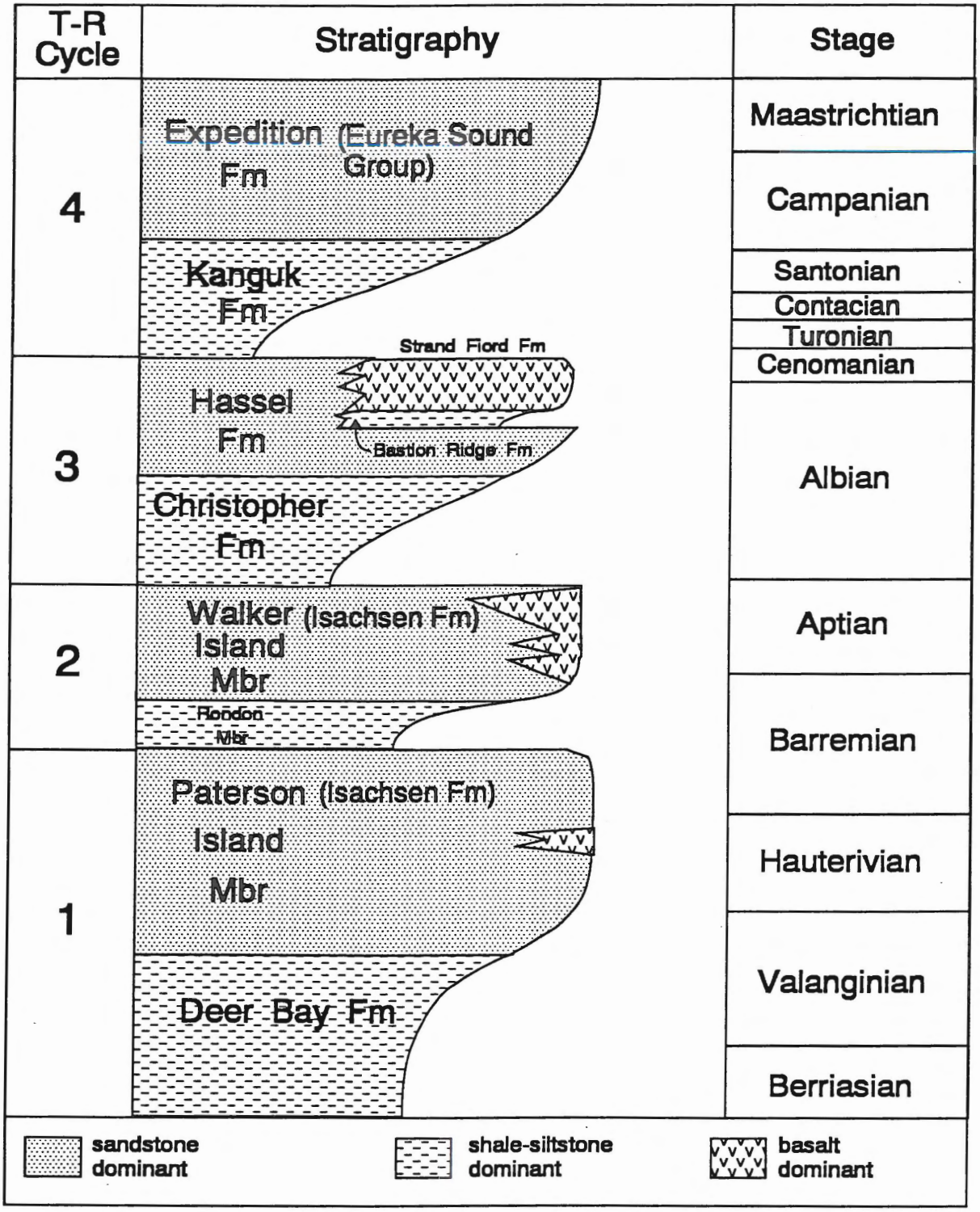

Figure 2.2. Schematic Cretaceous stratigraphy of the northeastern Sverdrup Basin showing the four transgressive-regressive cycles of Embry and Osadetz (1988), and their associated volcanic episodes, excluding the "Hansen Point Volcanics" (after Embry and Osadetz 1988).

The Bals Fiord basalt flows lie within the Upper Isachsen Formation, but the stratigraphic position of the basal volcaniclastic sequence is uncertain. T-R cycle #3 of Embry and Osadetz (1988) contains the Strand Fiord and Hassel Formation volcanics (Figs. 2.1 and 2.2). Embry and Osadetz (1988) associate the bimodal "Hansen Point Volcanics" in the northeastern Sverdrup Basin with T-R cycle #4 (Figs. 2.1 and 2.2). Work by G.K. Muecke and students has led to the subdivision of the "Hansen Point Volcanics," which display a much greater variability in age than previously believed, extending into the Paleogene (Merrett and Muecke 1989).

2.4 Summary

The Sverdrup Basin experienced two extensional events, each accompanied by mafic magmatism. Volcanic activity during the formation of the Sverdrup Basin was of limited volume and areal extent. Renewed extension led to voluminous, more extensive volcanic activity. This study focuses on Isachsen Formation volcanism, related to the second extensional event.

CHAPTER 3: VOLCANOLOGY AND PALEOENVIRONMENT OF THE ISACHSEN VOLCANIC EVENT

3.1 Introduction

This chapter begins with a description of the Isachsen section at Bals Fiord. A brief summary of the Bjarnasson Island section follows, but detailed stratigraphic information is not available. A discussion of the physical volcanology and paleoenvironment of Isachsen Formation volcanism, as preserved in these two sections, follows the presentation of new data. The summary incorporates stratigraphic data from Isachsen Formation volcanogenic sequences at Bunde and Strand fiords (Hinds 1991, Williamson 1988) with the new data from Bals Fiord and Bjarnasson Island (this study) (Fig. 1.2b).

3.2 The Bals Fiord Section

3.2.1 Introduction

The Isachsen Formation section on the south coast of Bals Fiord (Figs. 1.2b, 3.1) contains the thickest and most complete section of Isachsen Formation volcanogenic material known to date (G.K. Muecke pers comm). This 570 m thick sequence consists of volcaniclastics, 12 thick basalt flow units, and minor sedimentary horizons. The volcanic flow sequence (Fig. 3.1) lies within the Walker Island Member of the Isachsen Formation, but the stratigraphic position of the volcaniclastic material is unknown. The following discussion summarizes lithological data for the

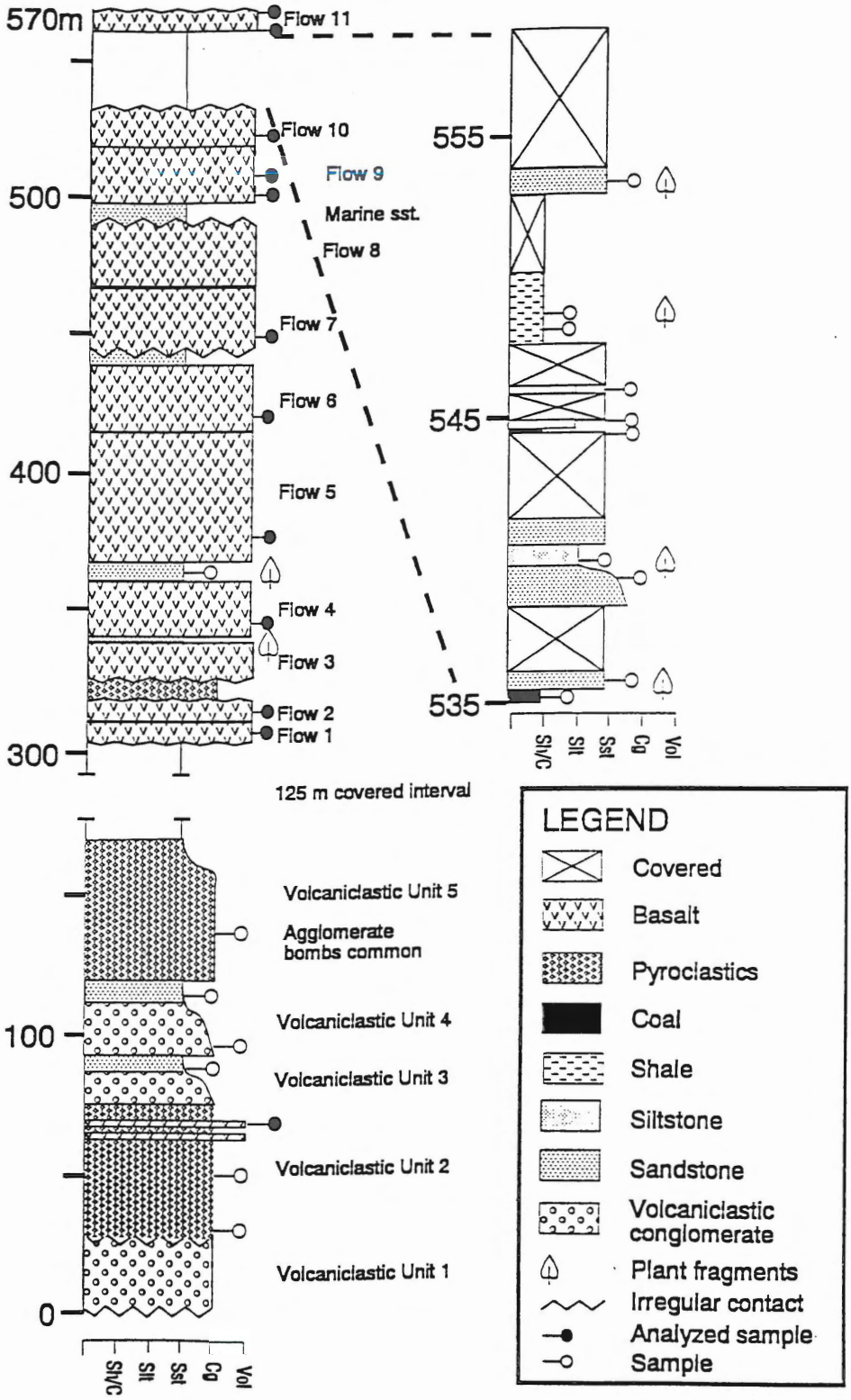

Figure 3.1. Stratigraphic section of the Isachsen Formation volcanogenic sequence at Bals Fiord.

volcaniclastic, volcanic, and sedimentary units at Bals Fiord and provides paleoenvironmental and volcanological interpretations where possible.

3.2.2 Volcaniclastic Deposits

3.2.2.1 Introduction

The basal 169 m of the Bals Fiord Isachsen volcanogenic sequence consists of volcaniclastic material (Volcaniclastic units 1-5) (Fig. 3.1). One other volcaniclastic unit occurs between flows #2 and #3, in the lower part of the main flow sequence (Fig. 3.1).

Ancient volcaniclastic material is inherently difficult to study because of limited exposure, intense alteration, and the lack of any spatial relationship to a known source (Lajoie 1984, Cas and Wright 1987). The best approach in studying this type of deposit is by non-genetic lithological classification, followed by genetic interpretation based on the occurrence of specific lithological criteria.

Figure 3.2 outlines the approach to volcaniclastic classification used in this study (after Cas and Wright 1987). This classification scheme involves the systematic division of various volcaniclastic units based on lithological criteria including: grain size, clast angularity, and framework type (open or closed). Open framework coarse-grain volcaniclastic material is in matrix support, and closed framework material is in clast support. This classification scheme results from work on fresh material, but the Isachsen Formation volcaniclastic material is highly altered. For this reason the descriptions of all volcanic material in the following discussion are made with

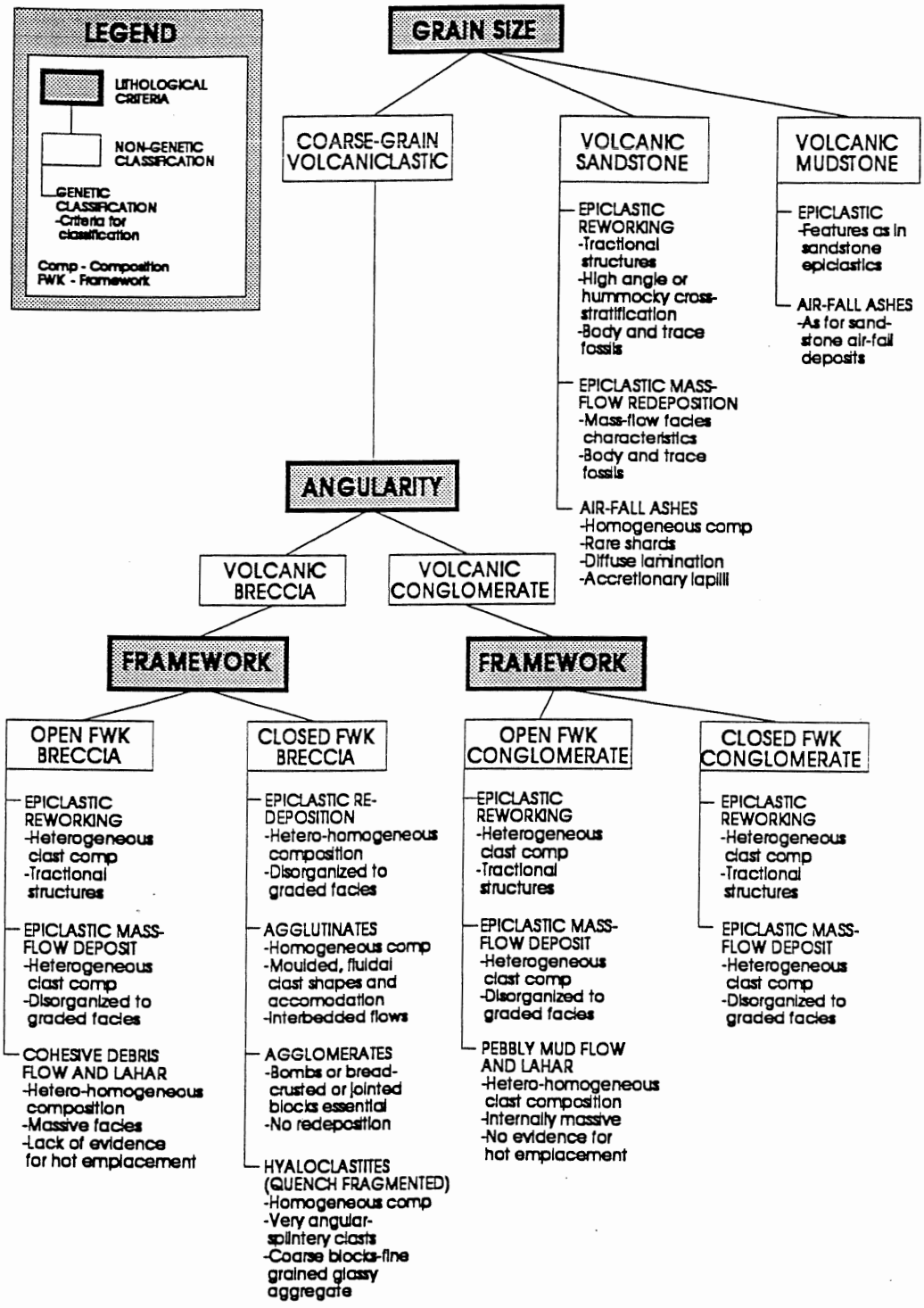

Figure 3.2. Volcaniclastic classification scheme (after Cas and Wright 1987), with emphasis on deposits possible in the Bals Fiord volcanogenic sequence.

reference to the original volcanic products. For example, material described as basaltic glass in this section is pervasively altered to palagonite.

The origins of epiclastic deposits range from dilute stream-flow to viscous debris flows (Smith 1986). The various mechanisms for transport control the sedimentary features of each deposit (Table 3.1). Debris flows behave plastically and deposit material *en masse* as the flow wanes, whereas stream flows are turbulent and their deposits more closely resemble fluvial sedimentation (Smith 1986). Hyperconcentrated flood flow deposits are transitional between debris flow and stream flow deposits, where turbulence is not the only mechanism of transport, and deposition is not *en masse* (Smith 1986). The depositional characteristics of various epiclastic units, using Table 3.1, allow the determination of flow type for each unit.

The following section summarizes field and thin section data for the volcaniclastic deposits, and provides both non-genetic and genetic classifications for each unit following the scheme presented in Figure 3.2. Table 3.2 provides a summary of important lithological data for each volcaniclastic unit, following the criteria outlined in Cas and Wright (1987). An interpretation section discusses volcanological and paleoenvironmental conclusions based on evidence taken from the volcaniclastic units in the Bals Fiord sequence.

Characteristics of flow	Debris flow	Hyperconcentrated flood flow	Normal stream flow
1. Flow type	1. Laminar at time of deposition but may be turbulent on steep slopes.	1. Partly turbulent at all times; however, high sediment load dampens out small eddies.	1. Fully turbulent
2. Sediment support mechanism(s)	2. Matrix strength, grain dispersive pressure, buoyancy.	2. Turbulence, grain dispersive pressure, buoyancy.	2. Turbulence
Characteristics of deposits			
1. Mode of deposition	1. *en masse*	1. Rapid grain-by-grain aggradation from both suspension and traction.	1. Grain-by-grain, dominated by traction processes.
2. Stratification	2. None within depositional units.	2. None or horizontal stratification; *no* cross stratification.	2. Conglomerate: massive or horizontal stratification. Sandstone: cross stratification and horizontal stratification.
3. Grading	3. None; reverse; reverse-to-normal; coarse-tail normal.	3. Frequently, although not always, distribution normal graded.	3. Variable and as a result of sequential processes rather than a single process.
4. Conglomerate framework	4. Matrix-support; rarely clast-support.	4. Clast-support with poorly sorted, polymodal matrix.	4. Clast-support with an open framework or distinctly finer grained matrix of infiltrated sand.
5. Clast long-axis (a) orientation; imbrication.	5. Variable, based on location within flow; parallel to flow is most prominent; minor imbrication.	5. Large cobbles to boulders; usually perpendicular to flow. Pebbles to small cobbles; usually parallel to flow. Poor imbrication.	5. Almost always perpendicular to flow; usually well imbricated.

Table 3.1 Table of lithological criteria for the recognition of the various epiclastic deposit types, as proposed by Smith (1986).

UNIT #	1	2a	2b	3	4	5a	5b	8
THICKNESS (m)	> 24	17 (APPROX)	33 (APPROX)	19	28	36	12	8
TEXTURAL								
- COHERENT OR FRAGMENTAL	FRAGMENTAL	FRAGMENTAL	FRAGMENTAL	FRAGMENTAL	FRAGMENTAL	FRAGMENTAL	FRAGMENTAL	FRAGMENTAL
- WELDING	NO	POSSIBLE, RARE	POSSIBLE	NO	NO	NONE NOTED	NO	NONE NOTED
- GRAIN SIZE RANGE - CLASTS (cm) - MATRIX	0.3-10 MUD	5-20 VCG	SIMILAR TO 2a FG	0.2-3 FG	0.1-2 (RARE 60) MG	0.2-10 NONE-FG (UP)	UP TO 0.8 MUD	0.3-25 -
- SORTING	POOR	POOR	POOR	POOR	POOR	POOR	POOR	POOR
- ANGULARITY - CLASTS - MATRIX	SUBRND-SUBANG -	ANGULAR-SUBANG ANGULAR-SUBANG	ANGULAR ANGULAR-SUBANG	SUBROUND -	ANGULAR-SUBANG ANGULAR-SUBANG	ANGULAR-SUBANG ANGULAR-SUBANG	SUBANG-SUBRND -	ANGULAR -
- FRAMEWORK TYPE	OPEN	CLOSED	CLOSED	OPEN	CLOSED	CLOSED	OPEN	CLOSED
COMPOSITIONAL								
- VOLCANIC CLAST AFFINITY	BASALTIC	BASALTIC	BASALTIC	BASALTIC	BASALTIC	BASALTIC	BASALTIC	BASALTIC
- HOMOGENEITY - CLASTS - MATRIX	HETEROGENEOUS HOMOGENOUS	HETEROGENEOUS HETEROGENEOUS	HETEROGENEOUS HETEROGENEOUS	HETEROGENEOUS -	HETEROGENEOUS HETEROGENEOUS	HETEROGENEOUS HETEROGENEOUS	HOMOGENEOUS HOMOGENEOUS	HOMOGENEOUS -
- CLAST COMPONENTS	MASSIVE BASALT AND QUARIZ PEBBLES	SCORIACEOUS + MASSIVE GLASSY BASALT (RARE SERIATE CLASTS)	SCORIA + MASSIVE MICROXILN-GLASSY BASALT (RARE SERIATE CLASTS)	SCORIA + MASSIVE BASALT (GLOMERO- AND PORPHYRITIC)	MASSIVE(PORPH, GLOM, AND SERIATE) AND LOW SCORIA CONTENT	SCORIA, MASSIVE BASALT + BOMBS AND BOMB FRAGS	MASSIVE BASALT	SCORIA
- MATRIX COMPONENTS	MUD	BASALT FRAGS AS ABOVE + ABD QTZ AND SILTST FRAGS	LOWER OVERALL MATRIX MATERIAL, MAINLY QTZ	-	QTZ SAND AND VOLC FRAGS IN GLASS MATRIX	QTZ SAND IN ASH(?) MATRIX WHERE PRESENT	MUD	-
OTHER NOTES	-STEEPLY INCLINED DEWATERING STRUCTURES(10cm thick,40cm long)	-RARE INTACT BOMBS NEAR BASE -SILTST CONTAINS ASH (?) MATRIX -HIGH QUARIZ CONT IN VOLC CLASTS -CARB PORE-FILL	-SLIGHTLY HIGHER CRYSTALLINITY IN BASALT FRAGS -LESS VOID SPACE AND CARB FILL -PERVASIVELY ALTERED RED	-UNIT GRADES UP INTO A PLATY, MED GRAINED,ANG-SUBANG QTZ SAND IN ASH(?) MATRIX	-UNIT GRADES UP, THROUGH LOSS OF LARGE CLASTS, INTO A FINE-MED GRAIN SST WITH LOCAL CG LENSES (LAGS)	-VARIABLE CLAST SIZE AND COMP THROUGH SECTION -COMMON INTACT BOMBS IN MIDDLE PORTION OF UNIT	-FLAGGY OUTCROP -POSSIBLE SIEVE DEPOSITION INTO UPPER PART OF UNIT 5a	-MAINLY SCORIA FRAGMENTS IN A WIDE GRAIN SIZE RANGE -UNIT SLIGHTLY RED AT TOP

Table 3.2. Table of lithological data for the volcaniclastic deposits from the Bals Fiord section.

3.2.2.2 Observations

Unit 1 This unit contains subangular-subrounded basaltic clasts and subrounded quartz pebbles in a muddy matrix. Elongate lenses of coarse-grained material, steeply inclined to bedding occur within this unit. The coarse grain size of the lenses may be the result of winnowing of the muddy matrix material by dewatering during compaction of this water-saturated deposit. Evidence of water saturation, a massive, poorly sorted lithology, and the presence of rounded quartz pebbles all indicate an open-framework conglomerate classification for this unit. This unit, in genetic terms, is likely an epiclastic mass-flow or pebbly mud flow deposit.

Unit 2 Variations in lithological character allow the subdivision of Unit 2 into two parts, with an indistinct boundary. The lower unit (2a) contains at least two intact pyroclastic bombs. Thin section observations of Unit 2a (AX92-203, Fig. 3.3) show both massive and scoriaceous clasts with cryptocrystalline to glassy textures and high concentrations of detrital angular quartz grains. Rare fluidal structures in the clasts, and the indistinct, interlocking grain boundaries of the some scoriaceous fragments may indicate welding. Secondary carbonate matrix material indicates high porosity upon deposition (Fig. 3.3). This unit is a closed-framework (clast support) breccia of massive and scoriaceous basalt fragments. The presence of intact bombs, and local evidence for hot emplacement (fluidal structures and welding), support the classification of this unit as an agglomerate.

Unit 2b is also a closed-framework breccia of angular massive and scoriaceous

basalt fragments. In thin section (AX92-204, Fig. 3.4), the basalt fragments display cryptocrystalline to slightly porphyritic textures with common plagioclase microphenocrysts. This unit again shows abundant angular quartz grains within the volcanic clasts. A few clasts display fluidal structures, and most clasts have indistinct and interlocking grain boundaries indicative of welding. Two thin igneous sub-units (1.5 and 2 m thick) lie within the upper portion of Unit 2b, parallel to bedding. The upper igneous sub-unit (AX92-205) is a slightly porphyritic, fine-grained basalt containing subangular basaltic clasts of mixed affinity, and abundant, partially resorbed quartz grains. These features are similar to those found in some of the basaltic clasts in this unit, and may indicate a genetic, and possibly temporal link between the volcaniclastic and flow units. A thin dyke (AX92-202) cutting units 1 and 2 is not texturally related to this upper igneous unit. Unit 2b is a closed-framework breccia, and possibly an agglutinate deposit as suggested by its lithology, possible evidence for hot emplacement, lack of pyroclastic bombs, and the occurrence of thin interbedded flow tongues. The bright red weathering of this unit suggests subaerial deposition.

Unit 3 Marked by an abrupt change in clast angularity, Unit 3 grades upward from a poorly sorted volcaniclastic conglomerate, through a rapid transition, to a platy-fractured, medium-grained sandstone. The volcaniclastic conglomerate has an open framework, and displays inverse grading defined by an increase in maximum clast size upward through the unit. The upper sandstone unit (AX92-206) consists of mainly angular to subangular quartz grains (+rare detrital microcline) and porphyritic volcanic fragments in an indistinct brown, cryptocrystalline (glassy ash?) matrix. The matrix

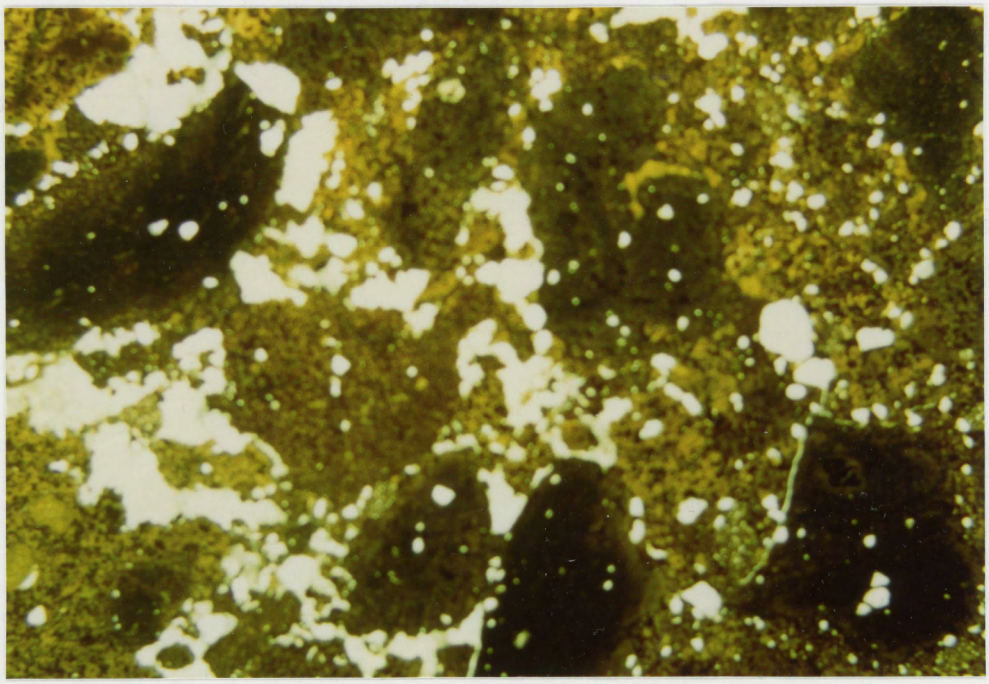

Figure 3.3. Photomicrograph of Unit 2a (AX92-203) in PPL. Note the indistinct, interlocking nature of the clast boundaries for the scoriaceous fragments, the fluidal structure in the clast in the upper left corner, the intraclast angular quartz grains, and the carbonate matrix material. FOV = 10 x 14 mm.

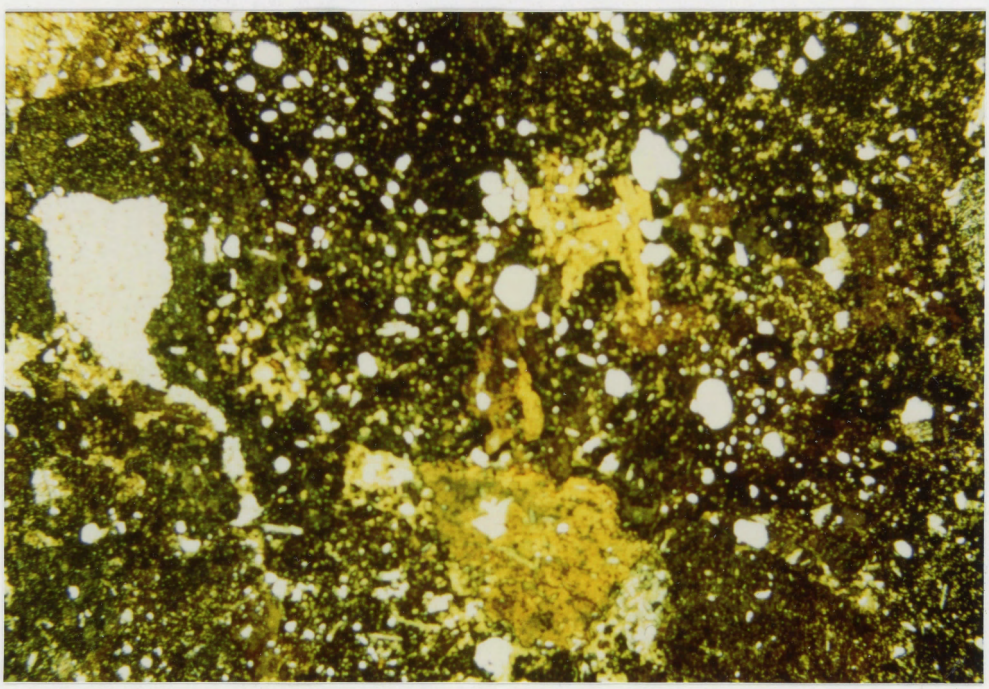

Figure 3.4. Photomicrograph of Unit 2b (AX92-204) in PPL. Note indistinct, interlocking clast boundaries and the high concentration of unresorbed angular quartz grains. FOV = 10 x 14 mm.

material contains sub- to euhedral plagioclase and clinopyroxene crystals indicating a possible crystal tuff origin for this material. Unit 3 is an open-framework conglomerate in sharp contact with Unit 2, probably a mass- flow deposit. The upper sandstone unit likely represents fluvial deposition of angular quartz sand and re-worked volcaniclastic material.

Unit 4 This unit has a sharp basal contact showing considerable relief along strike. Large sand-flame structures (up to 2 m high with 80 cm bases) occur in the base of this unit. The base of this unit is a poorly sorted closed-framework breccia. In thin section (AX92-207, Fig. 3.5) this lower unit consists of massive, subangular basalt clasts in a groundmass of fine-grained angular to subangular quartz sand with an indistinct brown cryptocrystalline (glassy ash?) matrix. Basalt fragments in this unit show considerable textural variety ranging from glassy/cryptocrystalline (+/- plagioclase phenocrysts), to fine-grained holocrystalline. The amount of angular quartz grains in the volcanic clasts is distinctly lower than in the units below. This unit grades up into a fine- to medium-grained sandstone through a decrease in the clast:matrix ratio. Lensoidal trough lag deposits of coarse-grained material (large quartz grains and volcanic clasts) occur locally in the upper sandstone unit. The basal portion of Unit 4 is probably an epiclastic mass-flow breccia. The upper sandstone unit is a fluvial deposit of angular sand and reworked volcaniclastic material.

Unit 5 This unit consists of a lower closed-framework volcanic breccia (5a), and an upper open-framework volcanic conglomerate (5b). Unit 5a displays reverse

grading defined by an increase in maximum clast size, and a corresponding increase in bomb fragment concentration. At 15 m above the base of the unit intact bombs (up to 15 cm in diameter) are common (Fig. 3.1, 3.6), the amount of scoriaceous material increases, and the matrix becomes mud-rich. Thin section analysis of the matrix material (AX92-209, Fig. 3.7) reveals a mixture of subangular-subrounded quartz sand and subangular-angular basalt fragments in an indistinct brown cryptocrystalline (glassy ash?) matrix. The bombs and other basalt fragments again contain subangular to subround quartz grains, but in lower concentrations than in previous deposits. At 20 m above the base of the unit bombs become less common, and the proportion of massive and amygdaloidal basalt clasts (up to 5 cm in diameter) increases. Unit 5a is likely an agglomerate, based on the presence of bombs, however, this unit may have experienced local re-deposition, incorporating the sandy/muddy matrix material.

Unit 5b is an open-framework conglomerate containing rounded basalt clasts in a muddy matrix, likely a pebbly mud-flow deposit. The gradation between Units 5a and 5b may be the result of infiltration of muddy material from the upper lahar deposit into the breccia below, similar to sieve deposition in alluvial fans (Hooke 1967).

One other volcaniclastic unit occurs in the section, within the main flow sequence, between flows #2 and #3 (Fig. 3.1). This unit is a closed-framework breccia containing mainly amygdaloidal basalt fragments. The homogeneous clast composition and the occurrence of a thin discontinuous flow above suggests the classification of this unit as an agglutinate. A slight reddening of this unit indicates subaerial deposition and weathering.

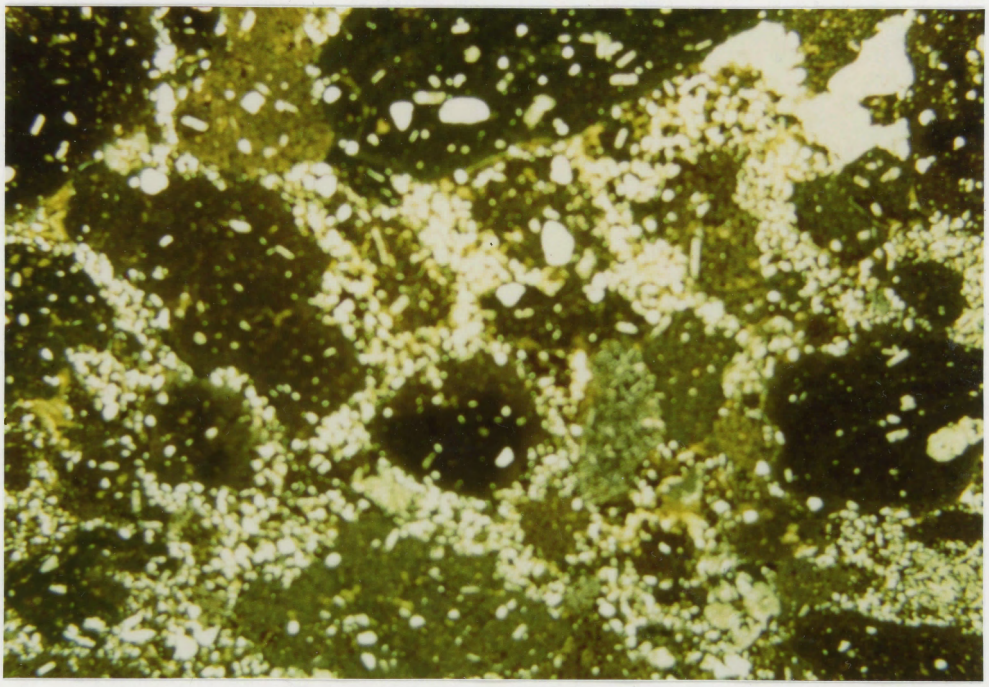

Figure 3.5. Photomicrograph of the basal volcaniclastic breccia of Unit 4 (AX92-207) in PPL. Note the high concentration of angular quartz grains in the matrix and within the clasts, and the similar appearance of the two populations. Local carbonate fill (upper right). FOV = 10 x 14 mm.

Figure 3.6. Photograph of a common pyroclastic bomb from Unit 5a. Note the intact nature of the bomb with a well-developed chilled margin and scoriaceous center. Pen-top = 5 cm long.

3.2.2.3 Regional interpretation

The volcaniclastic deposits in the basal 169 m of the Bals Fiord section have a mixed pyroclastic and epiclastic affinity. The pyroclastic units (Units 2 and 5a) are proximal deposits, while the epiclastic units (Units 1, 3, 4, and 5b) may represent deposits from a more distal source and/or reworking of the local pyroclastic material.

The pyroclastic units 2a and 5a contain intact bombs indicating very close proximity to the source. High concentrations of interstitial angular quartz grains in some parts of the pyroclastic deposits (e.g. AX92-204, 209) may suggest minor reworking of this material, or fall deposition into an area of active sand sedimentation.

The angular quartz grain content of the volcanic clasts in the pyroclastic deposits indicates mixing of magma and unconsolidated sand (Fig. 3.8) just prior to eruption, providing insufficient time for any resorption of the quartz grains (Fisher and Schmincke 1984) (Fig. 3.9). Quartz grains react quickly in mafic magmas, forming an augite corona (Glazner and Ussler 1988). Significant augite crystallization occurs after only a few hours in the magma, and a dense mat forms after 22 hours which protects the remaining quartz and explains their widespread preservation (Glazner and Ussler 1988). An observed decrease in detrital quartz grain concentrations in the volcanic fragments upward through the pyroclastic units indicates isolation of the rising magma from the unconsolidated sediment, perhaps by the coating of the conduit(s) through repeated eruptions.

The presence of interstitial and intraclast detrital sand supports hydrovolcanic activity as the mechanism for eruption of the pyroclastic material (Leat and Thompson

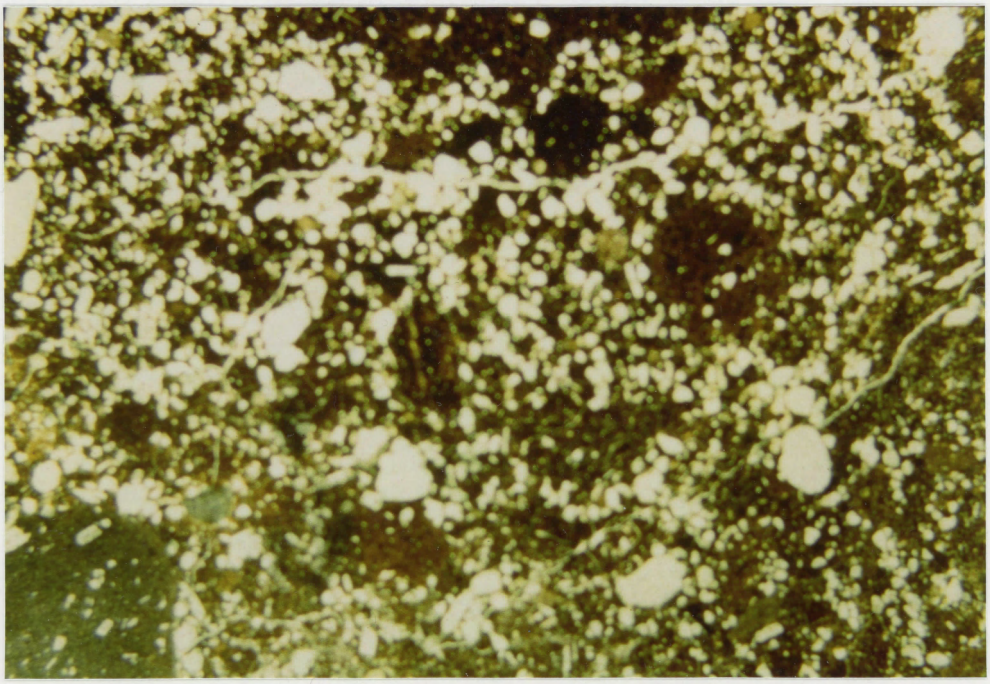

Figure 3.7. Photomicrograph (PPL, FOV = 10 x 14 mm) of the volcaniclastic material in the bomb horizon of Unit 5 (AX92-209) showing the edge of a bomb at the top, and the quartz-rich matrix material with volcaniclastic fragments.

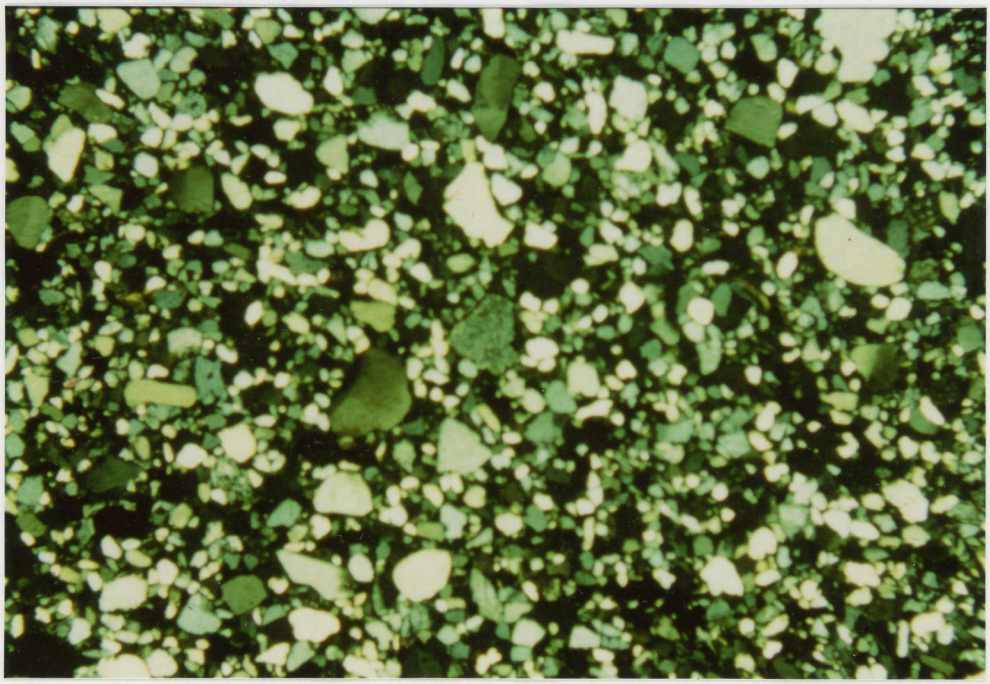

Figure 3.8. Photomicrograph (XN, FOV = 4 x 7 mm) of the immature quartz sandstone typical of the Bals Fiord section (from fluvial sedimentary unit between flows #4 and #6). Note the similarity in size (note scale change) and angularity of the quartz grains to those found within the volcaniclastic fragments in the lower part of the section.

a)

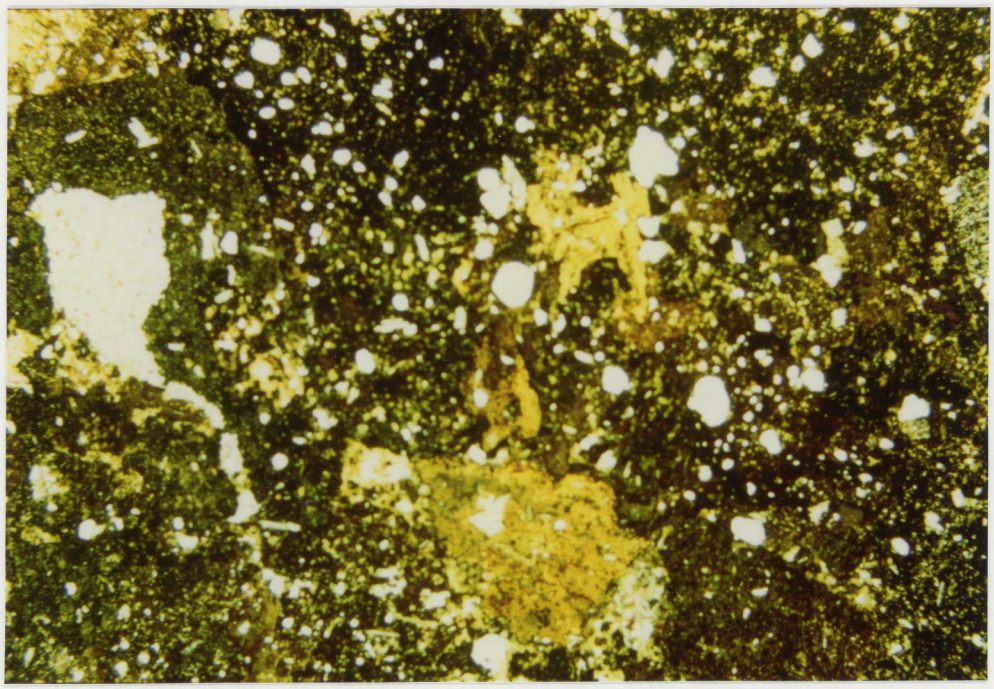

b)

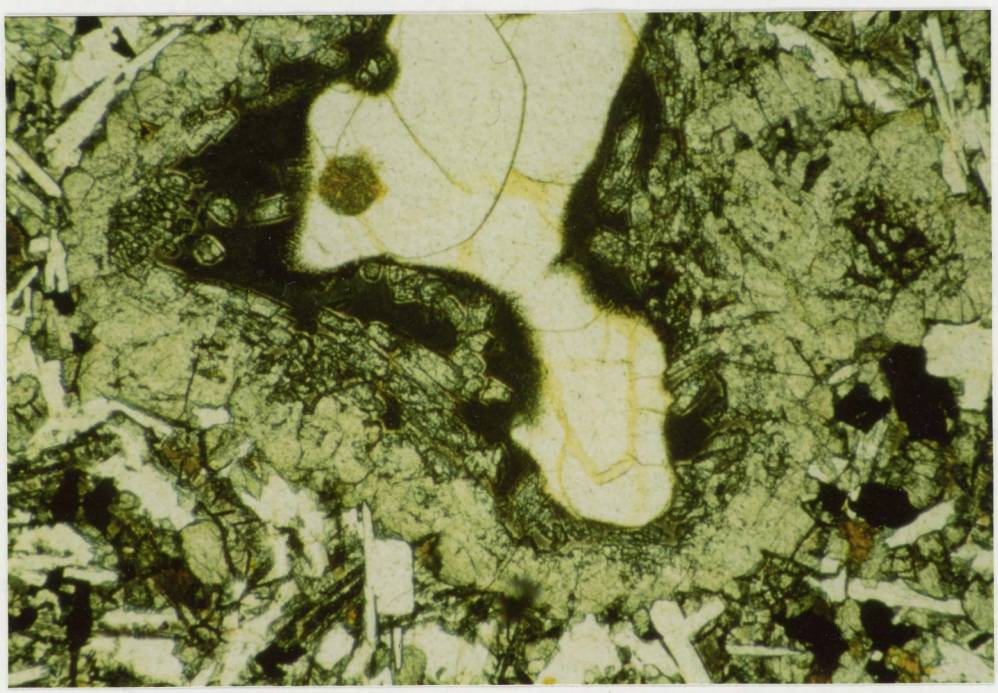

Figure 3.9. Figure illustrating the stability quartz sand in the Bals Fiord basalts; a) pyroclastic material with high concentration of unresorbed angular quartz grains (Unit 2b, AX92-204) (PPL, FOV = 10 x 14 mm), and b) detrital quartz grain from the base of a basalt flow in the main flow sequence (Flow #5, AX92-195) (PPL, FOV = 1 x 2 mm). Note the thick corona of augite formed around the quartz grain in Flow #5, and the lack of any quartz resorption or augite crystallization in the pyroclasts.

1988, Cas and Wright 1987, Kokelaar 1982). The predominance of basalt fragments, and paucity of lithic clasts suggests a phreatomagmatic origin for this material (Cas and Wright 1987).

Increasing crystallinity in the pyroclastic fragments from glassy to microphenocryst-bearing within Unit 2, and to holocrystalline and slightly porphyritic in Unit 5, may indicate cooling and maturation of the magmas within the source vent area for this material. The decrease in quartz grain concentration in the pyroclastic fragments also supports the model of a maturing source for this material.

Interbedded with the pyroclastic deposits in this section are epiclastic deposits, defined as re-deposited volcaniclastic material (Cas and Wright 1987). Movement of epiclastic material is caused by gravitational instability and enhanced by water saturation. The source region for these epiclastic deposits may be the local pyroclastic material, or, more likely, they may represent deposits from a more distal source. These epiclastic units resemble volcaniclastic fan deposits, which may occur at considerable distances from their source (approximately 8 km in Palmer et al. 1993).

All epiclastic deposits in the Bals Fiord section appear to be formed by debris flow because they: (i) are all massive, (ii) are all open-framework (matrix supported) deposits, and (iii) all show no grading, or only poorly developed reverse grading (Table 3.1). Epiclastic units 3 and 4 display a rapid gradation into sandstone deposits. The sandstone above Unit 4 contains coarse-grained lenses of quartz and volcanic fragments, interpreted as lag deposits, indicating fluvial deposition of this material. Fluvial deposition of the sandstone units would suggest that the gradational boundary

with the lower epiclastic material is the result of reworking. The sandstone above Unit 3 is massive, and is also believed to be of fluvial origin, however this may represent the reverse-to-normal grading pattern recognized for hyperconcentrated flood-flow deposits (Smith 1986) (Table 3.1). Sandstone layers above the epiclastic units likely represent the re-establishment of fluvial deposition in the channels which hosted the debris flows. Epiclastic deposits which grade into quartz sandstones could not occur on the flanks of an eruptive edifice, where topography limits the possibility of quartz sand accumulation, rather, they must have accumulated in a low-lying area, possibly a delta plain.

Other volcaniclastic deposits in the Isachsen Formation include epiclastic deposits from the upper portions of Walker Island Member volcanogenic sequences at Strand and Bunde fiords (Fig 1.2b). Ricketts (1985) describes an 80 m thick volcanic breccia, with a thin lahar deposit in the uppermost part of the section, within the Isachsen Formation at Strand Fiord. Work by G.K. Muecke (pers comm) suggests that this volcanic breccia, reported by Ricketts (1985) to be an agglomerate, is actually an epiclastic deposit, and that four flow units, not reported by Ricketts (1985), occur at the base of this sequence with interbedded Walker Island Member sediments. The Camp Five Creek section at Bunde Fiord contains a 45 m thick epiclastic deposit, lying above several flow units, near the top of the section (Hinds 1991).

The Bals Fiord sequence is the thickest of all known Isachsen Formation volcaniclastic deposits, and contains the only known pyroclastic deposits. Both the observations suggest that the Bals Fiord section is closest of these deposits to an

eruptive center. The Bals Fiord section is the westernmost of all known Isachsen Formation volcanogenic sections (Fig. 1.2b), and contains the most proximal volcaniclastic deposits, which may indicate that the source for Isachsen Formation volcanism lies offshore, west of Bals Fiord.

3.2.3 Volcanic Flows and Associated Intrusives

3.2.3.1 Introduction

Eleven fine- to medium-grained mafic igneous units constitute the main flow sequence at Bals Fiord. Their uniform appearance permits a brief summary of common features, followed by a more detailed discussion of features particular to specific flows. The stratigraphic section (Fig. 3.1) provides a summary of the features present in individual units. Where possible, interpretations of volcanological and paleoenvironmental significance follow the description of each feature.

3.2.3.2 Observations

Flows in the main flow sequence at Bals Fiord are 8-50 m thick (22 m average thickness). All units display columnar jointing, either in their lower portion or throughout. The columns in all cases are 80-100 cm in diameter, and occur over various thickness intervals.

Vesiculation is a common feature near both the upper and lower contacts of each flow, with vesicle concentration invariably increasing toward the contacts. Vesicle concentrations are low at the base, but reach very high concentrations in the upper part of some units. Intense vesiculation of the upper portion leads to the development of a

scoriaceous, rubbly flow top, indicating a flow origin for the few units in which it occurs. Nowhere in the Bals Fiord section do flow-top deposits show bole development, a diagnostic feature of prolonged subaerial exposure.

Thin horizons displaying a blocky fracture pattern separate highly vesicular basalt from the zone of column development below. This blocky development also occurs at the base of some units.

The following observations are those particular to specific flows. The presentation of these unique features is in stratigraphic order.

Flow #4 is columnar over its entire thickness, only slightly vesicular at its lower contact, and only slightly altered, all of which suggest that this unit may be a sill. Flow #4 is enveloped in sediments, and a sedimentary unit in the sequence would be the most obvious host for an intrusion.

Flow #5, the thickest unit in the sequence, displays an unusually thick flow top with siltstone lenses which indicate local reworking of the material in the uppermost part of the flow-top. This flow also contains a tree stump, rising 1.5 m above the base of the unit (Fig 3.10). The presence of plant fragments at the base of a flow is unequivocal evidence for subaerial emplacement. The tree stump, rooted in a coal horizon below the flow, tapers from a basal diameter of 55 cm to 38 cm at the top. The tree broke as the flow passed over it, bending slivers at the top of the stump in the direction of flow (Fig 3.11). Tree fragments in the base of the flow, east of the stump, include a branched log of roughly the same diameter as the top of the stump, and possibly from the same plant (Fig 3.12). Highly vesicular basalt surrounds the

a)

b)

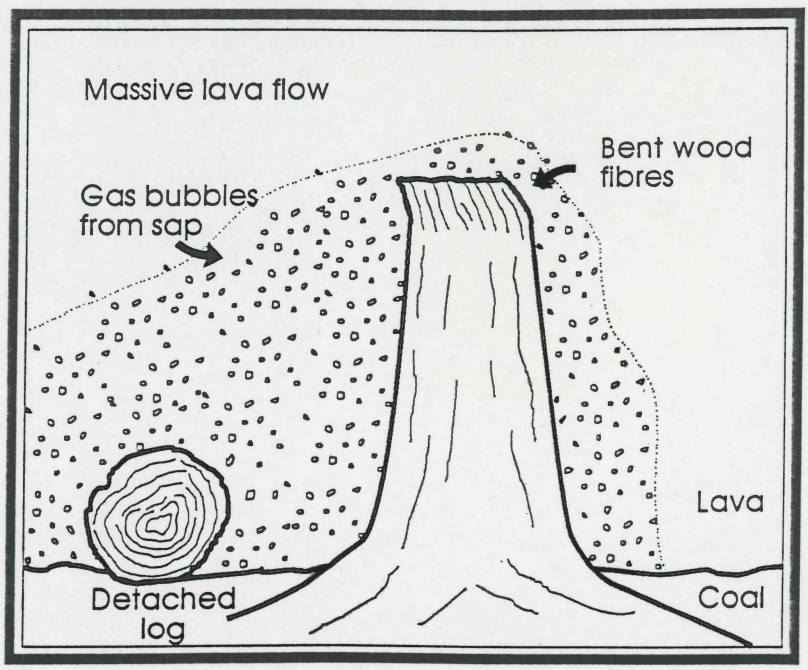

Figure 3.10. Photograph (a), and tracing (b) of the tree stump (1.5 m tall) at the base of Flow #5. Note the location of the tree fragments and the shape of the scoriaceous halo. East is toward the left in this figure.

Figure 3.11. Photograph of the top of the tree stump in the base of Flow #5, in the same orientation as in Figure 3.10, showing the bent slivers which indicate flow movement toward the east (left). Pocket knife is 10 cm long.

stump, forming a tear-shaped halo with its tail toward the east (Fig 3.10). Evidence collected from this location indicates that lava flowed eastward at this location, during the emplacement of Flow #5.

Flow #8 contains rounded clasts of scoriaceous flow-top material (3-150 cm in diameter), from Flow #7, at its base. The inclusion of this material suggests a flow origin for this unit, but does not distinguish between subaerial and subaqueous emplacement.

Sand flame structures rising into the base of Flow #11 (Fig 3.13) also indicate flow emplacement, over unconsolidated sediments. The fluvial nature of the sediments below this flow suggest subaerial emplacement.

3.2.3.3 Interpretation

The 220 m total thickness of basalt flows in this sequence indicates voluminous magmatism occurred at this location during deposition of the Walker Island Member of the Isachsen Formation. Most igneous units occur in pairs, with thin sedimentary or pyroclastic units between them. This stratigraphic pattern may indicate episodic volcanism in the area, separated by periods of clastic sedimentation. Subaerial emplacement of the flow units is most likely, as no evidence exists to support subaqueous emplacement, and various features in the flows support subaerial emplacement (e.g., the incorporation of plant material). The lack of bole development in the flow-top material of flows indicates that deposition in this area was rapid, with each flow being covered by either another flow or sediments before significant weathering could occur.

Figure 3.12. Photograph of the tree fragment on the east side of the stump in the base of Flow #5, in the same orientation as in Figure 3.10. The photograph is centered on the branches of the tree fragment, and the left side of photograph cuts through the trunk. Pocket knife is 10 cm long.

Figure 3.13. Photograph of a sand-flame structure in the base of Flow #11. Ruler is 1.1 m long.

3.2.4 Sedimentary units

3.2.4.1 Introduction

Five sedimentary units occur within the Bals Fiord volcanogenic sequence (Fig. 3.1). These sedimentary units, four fluvial and one marine, are consistent with the fluvial-deltaic plain model for the deposition of the Walker Island Member of the Isachsen Formation (Embry 1991, 1985). Analysis of the sedimentary units in terms of depositional facies models provides important insight into the paleoenvironment and paleogeography at the time of deposition.

3.2.4.2 Observations

The uppermost sedimentary unit, below Flow #11, is the thickest, most complete fluvial deposit in the section (Fig. 3.1). This 24 m thick unit provides the best opportunity to study fluvial deposition in this sequence.

A thin siltstone overlies Flow #10, which is covered in turn by a thin coal horizon. A medium-grained, cross-laminated sandstone, possibly a levee deposit, lies in sharp contact with the coal and contains abundant fossil plant fragments.

A fining-upward sandstone unit follows a 3 m covered interval. The sandstone grades upward from a very coarse-grained platy-fractured horizon, through a massive/platy interval, to a fine-grained, ripple cross-laminated sandstone at the top of the sequence. This fining-upward sequence resembles point bar accretion deposits in a meandering river (Walker and Cant 1984).

A second coal horizon follows another 3 m covered interval and may represent the

re-establishment of vegetation after channel migration or switching. The fine-grained sandstone above the second coal horizon indicates overbank deposition. The shaly interval above the overbank deposits suggests channel migration away from this location. Finally, a medium-grained, laminated sandstone in the upper part of the section indicates renewed overbank deposition.

Three other thin sedimentary units, above flows #3, #4, and #6, are compositionally similar to the thick fluvial sedimentary unit above Flow #10, and contain sedimentary structures consistent with various horizons in the upper fluvial sandstone. The similarity in sedimentary structures and general appearance between all of these units suggest a similar depositional model.

The sandstone unit above Flow #8 is massive, has a distinct yellow color, and contains a trace fossil assemblage indicative of shallow marine deposition. Tubular (Skolithos) and U-shaped (Diplocraterion, Fig. 3.14) vertical burrows are observed in this marine sandstone interval. Both of these trace fossils belong to the Skolithos ichnofacies, which implies deposition in high-energy, shallow marine conditions with a high sediment influx (Frey and Pemberton 1984).

3.2.4.3 Interpretation

The sediments in the Bals Fiord section are consistent with the fluvial-deltaic model for deposition of the Walker Island Member of the Isachsen Formation. The fluvial sediments are consistent with a delta-plain setting for deposition, and the marine sandstone unit represents shoreface deposition in a delta front environment.

The marine sandstone unit signals a rise in sea level, possibly related to the basin-wide regression which defines the top of the Walker Island Member. The occurrence of two subaerial flows and the thick fluvial sedimentary unit above this marine sandstone indicate re-establishment of delta plain deposition.

3.3 Bjarnasson Island Section

Only reconnaissance data are available for the Bjarnasson Island section, on the north coast of the island. The following sections describes, in stratigraphic order, the igneous units sampled and the sediments surrounding each unit.

Reconnaissance data from the south coast of the island show a series of basalts within the Walker Island Member, and only one thin unit within the Paterson Island member. In contrast, the volcanic succession on the north coast lies within Paterson Island Member sediments.

The stratigraphically lowest unit sampled (AX92-215) is a columnar, medium-grained, glomeroporphyritic basalt with slight vesiculation in the upper 1-2 m. The lack of flow-top development, and the unusually coarse-grained nature of this unit suggest an intrusive origin for this unit. This unit is overlain by massive sandstone of the Paterson Island Member.

The second sample (AX92-216) is from a fine-grained basalt flow. This flow displays horizontal to sub-horizontal column development, a feature common to many basalt flows on the north side of Bjarnasson Island. Horizontal column development occurs in ponded flood basalts (Wright 1984).

An unmeasured interval separates the third sampled unit (AX92-217) from the

previous two. This flow unit displays vertical columnar jointing at the base, grading through progressively shallower angles into sub-horizontal columns at the top of the unit (Fig. 3.15). This unit is underlain by a shale with increasing thin sandstone interbeds toward the base of the flow. The sandstones show cross-bedding and intense bioturbation.

The final sample (AX92-218) was taken from the uppermost exposure in the sequence, with a thick interval containing other unsampled basalts between this unit and the previous sample location. The stratigraphic position of these upper units is unknown, and the sequence may be continuous into the Walker Island Member of the Isachsen Formation.

Embry and Osadetz (1988) suggest that two flows occur in the Lower Isachsen Formation on northern Bjarnasson Island, and use this evidence to support a lower Isachsen volcanic episode. The number of flows in this sequence is greater than previously believed, and their stratigraphic relationships are complex. Evidence for ponding, the lateral discontinuity of flows on northern Bjarnasson Island, and the change in flow character and stratigraphic position of flows across the island (approximately 2 km away) all suggest considerable topographic relief on northern Bjarnasson Island at the time of deposition. Topographic relief in this location, caused by erosional incision or faulting, could explain, in part, the lower stratigraphic position of these flows. This area requires more detailed study in order to fully elucidate the volcanological, sedimentological, and structural relationships.

Figure 3.14. Photograph of the shallow marine trace fossil Diplocraterion from the marine sandstone above Flow #8. Pen top=5 cm.

Figure 3.15. Flow #3 (AX92-217) from Bjarnasson Island showing vertical to sub-horizontal column development. Vertical columns approximately 10 m high.

3.4 Summary

The basal portion of the Bals Fiord section contains volcaniclastic deposits of both pyroclastic and epiclastic origin. A distal volcaniclastic fan model for the epiclastic deposits is consistent with the evidence for volcaniclastic-sand mixing, and the fining-upward of epiclastic deposits to sandstones. A volcaniclastic fan setting is consistent with the deltaic model for deposition of the Isachsen Formation sandstone, but the stratigraphic location of the volcaniclastic deposits within the Paterson Island Member or Walker Island Member is unclear. Pyroclastic material interbedded with the epiclastic deposits represents input from a proximal eruptive center(s), possibly the result hydrovolcanic interaction between a high level intrusion and the water-saturated sediments of the volcaniclastic/fluvial fan (Leat and Thompson 1988, Cas and Wright 1987).

A thick sequence of subaerial flows with minor interflow sedimentary and volcaniclastic units forms the upper part of the section. The thin sedimentary units are consistent with deposition in a fluvial-deltaic environment, which suggests low topographic relief. The source region for the flows may be the same as that for the epiclastic deposits, but during a less explosive phase in its development. The youngest pyroclastic deposit occurs early in the flow sequence (between flows #2 and #3), and may represent a final explosive event at the proximal edifice which was the source for the basal pyroclastics. The epiclastic material and flows are likely products of a more distal eruptive edifice, shedding this material into a low-relief depositional environment.

Delta-plain sedimentation continued in this area despite the addition of large thicknesses of igneous and sedimentary material. This indicates rising relative sea level (maintaining accommodation space) during deposition. The shallow marine sandstone in the upper part of the sequence may mark the regional regression which defines the top of the Walker Island Member. Two subaerial flows deposited above the marine sand are subaerial, perhaps as a result of thermal doming related to their emplacement. The 38 m thickness of the two flows would cause emergence of the delta, the re-establishment of delta-plain sedimentation, and deposition of the uppermost sandstone unit.

Reconnaissance work on Bjarnasson Island shows contrasts in flow type and stratigraphic position across the Island. The flows on the north side of Bjarnasson Island show features consistent with ponding, and are laterally discontinuous. These features, along with the apparent change in flow character and stratigraphic position across the island suggest significant paleotopographic relief in this area. The north coast of Bjarnasson Island hosts more volcanic units than previously reported (Embry and Osadetz 1988). The stratigraphic location of the lower flow units within the Paterson Island Member may be, in part, the result of their deposition into an area of topographic relief caused by erosional incision or faulting. Regardless of the mechanism for deposition in the Paterson Island Member, these basalts represent the stratigraphically oldest Isachsen Formation volcanics.

CHAPTER 4: PETROLOGY AND GEOCHEMISTRY

4.1 Introduction

This chapter presents the petrography and geochemistry of the Isachsen basalt samples from Bals Fiord and Bjarnasson Island. The petrology section summarizes the mineralogy and textures, and provides a petrographic classification for these samples. The geochemistry section presents new data, explores alteration effects, and provides a geochemical classification for these rocks.

4.2 Petrography

4.2.1 Introduction

Appendix A contains detailed petrographic descriptions of each sample from Bals Fiord and Bjarnasson Island. This section presents a summary of the petrography for these samples. Two textural varieties exist in these samples: (i) the main sequence basalts from Bals Fiord and one sample from Bjarnasson Island display seriate or semi-seriate textures, and (ii) three of the four samples from Bjarnasson Island and the thin flow in the volcaniclastic sequence at Bals Fiord have porphyritic to glomeroporphyritic textures. Petrographically, most seriate samples are tholeiites, and most porphyritic samples are olivine tholeiites.

4.2.2 Mineralogy

The mineral assemblage in all samples includes predominantly plagioclase and clinopyroxene, with minor amounts of opaques and olivine. Most samples from

Bals Fiord and Bjarnasson Island are relatively fresh, with alteration restricted to olivine crystals and interstitial glass.

Euhedral to subhedral plagioclase crystals constitute 50-100% of the phenocrysts in all samples. Plagioclase phenocrysts commonly have oscillatory zoning and contain numerous inclusions of clinopyroxene, opaque material, and glass (Fig. 4.1). Inclusions occur in the rims, cores, and throughout the crystals, normally parallel to zoning or twin planes. Plagioclase is also a common groundmass phase, occurring as euhedral to subhedral laths. In seriate-textured samples plagioclase crystals form a continuum in grain size from groundmass to phenocryst phases (Fig. 4.2).

Subhedral to anhedral clinopyroxene is a major constituent in the groundmass of all samples, but is normally less abundant in the phenocryst phase. Clinopyroxene occurs as interstitial material between plagioclase laths in the groundmass of the seriate samples (25-45%, Fig. 4.2), and forms an intergranular groundmass in the porphyritic and glomeroporphyritic samples (55-65%, Fig. 4.3). Larger subhedral clinopyroxene crystals commonly constitute 20-40% of the phenocryst phase in seriate samples (Fig. 4.2), but are rare in the porphyritic and glomeroporphyritic samples (Fig. 4.3). Clinopyroxene grain size distribution is approximately bimodal, with a clear division between groundmass and phenocryst phases where both exist (Fig. 4.2). Clinopyroxene phenocrysts are rarely zoned, contain few inclusions, and locally display subophitic textures.

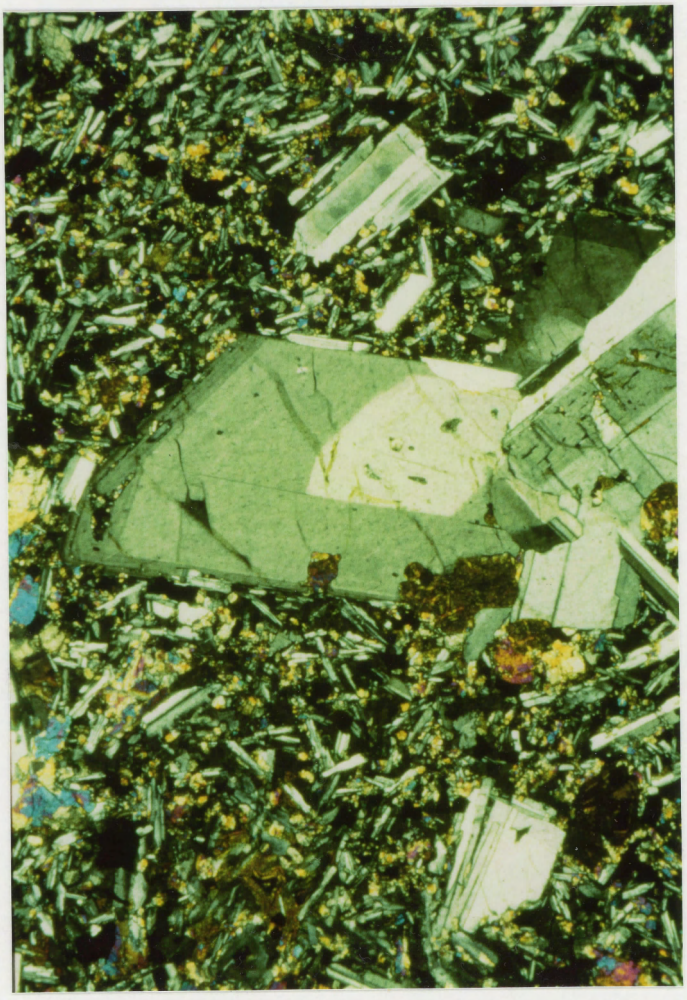

Figure 4.1. Large plagioclase phenocryst (AX92-196, Flow #6) illustrating oscillatory zoning on the rims, and inclusions common in these crystals. FOV = 2 x 3 mm.

a)

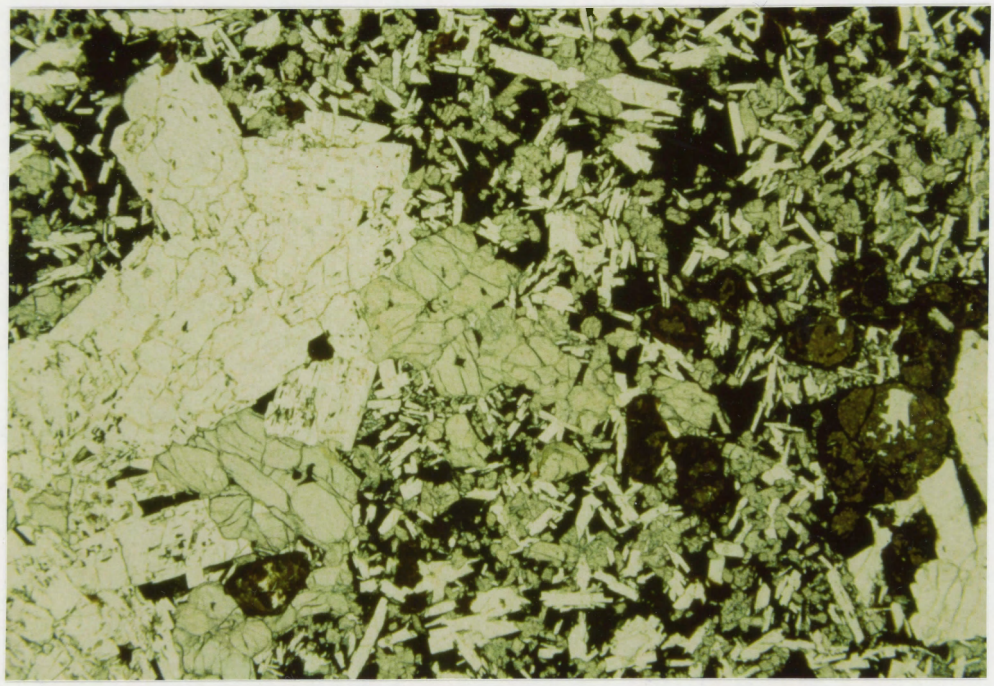

b)

Figure 4.2. Photomicrographs showing common mineral assemblage for seriate-textured samples, including: plagioclase, clinopyroxene, opaques, olivine (iddingsite), and glass (palagonite, dark in photo (AX92-198, Flow #8). Note the gradation in grain size for plagioclase and clinopyroxene which defines the seriate texture. This example also shows the development of glomeroporphyritic texture in the largest phenocrysts. Photomicrographs shown in: a) PPL, and b) XN; FOV = 4 x 6 mm for both.

a)

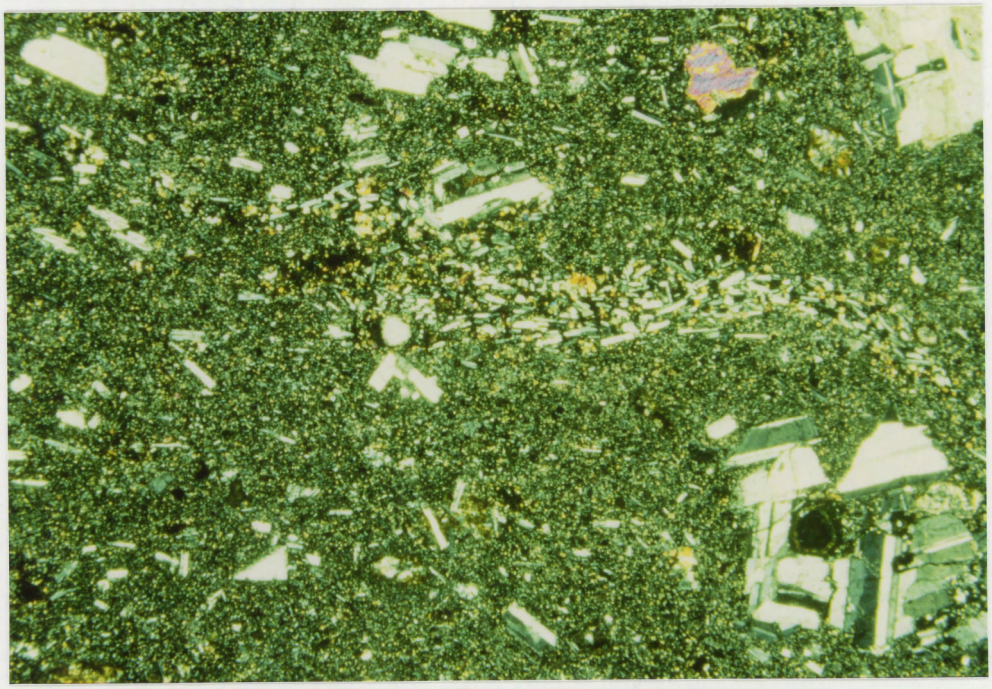

b)

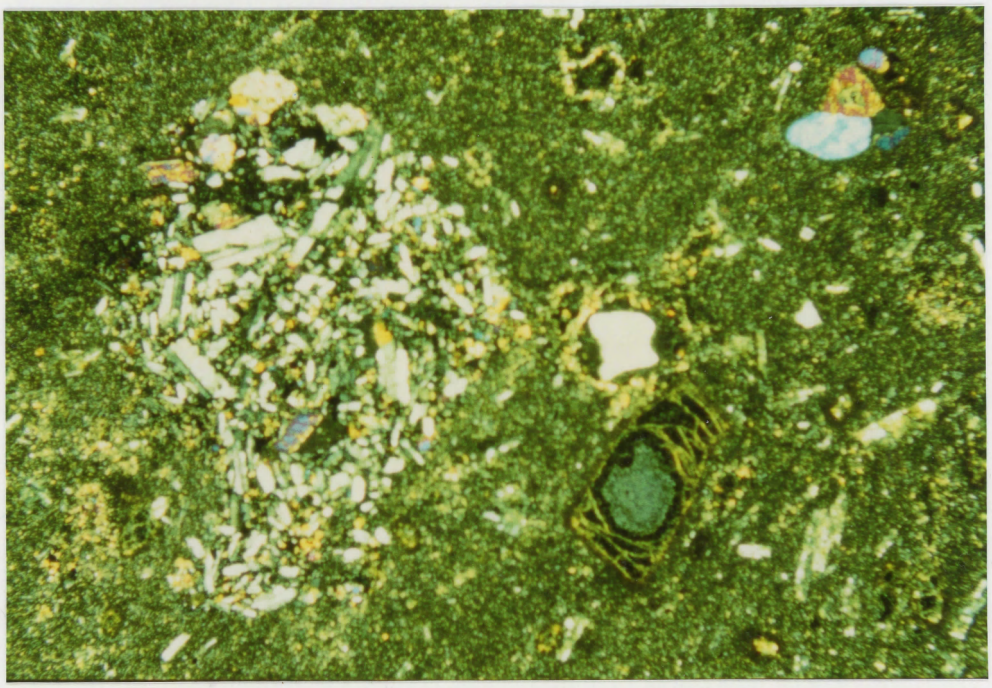

Figure 4.3. Photomicrographs illustrating the common mineral assemblage for the fine-grained porphyritic to glomeroporphyritic samples from Bjarnasson Island, including: plagioclase, clinopyroxene, and olivine (iddingsite) (opaques and glass not visible at this scale). Samples include: a) AX92-216 (XN), and b) AX92-218 (XN), FOV = 4 x 7 mm for both. Note the flow alignment of plagioclase phenocrysts in (a), the large, partially resorbed detrital quartz grain with clinopyroxene rim above the large olivine crystal in the lower right corner of (b), and the seriate-textured inclusion in (b).

Opaque minerals occur in all samples (5-15% modal), but are restricted to the groundmass. Euhedral and subhedral grain shapes are most common.

Olivine occurs in most samples, and constitutes a small percentage of the phenocryst and groundmass phases (trace-10%). The Bjarnasson samples are unique in that they contain 20-30% olivine in the phenocryst assemblage. Pervasive alteration of olivine to iddingsite, or chlorophaeite +/- carbonate, occurs in all samples except AX92-192, in which olivine has altered to chlorite. Iddingsite replacement of olivine indicates high-temperature, probably magmatic, alteration, and chlorophaeite suggests lower-temperature alteration (Cox et al. 1979).

Interstitial glass is a constituent in the groundmass of all samples (trace-25%). Fresh glass is rare, with most samples displaying pervasive palagonitization. Fresh glass is isotropic, pink in plane-polarized light, and locally contains inclusions of plagioclase and/or opaque phases, commonly as crystallites (Fig 4.4). Most commonly the glass alters to massive yellow or brown gel-palagonite, occasionally with dark brown fibro-palagonite rims (Fig. 4.4).

Gel-palagonite indicates high-temperature alteration and fibro-palagonite suggests low-temperature alteration (Mathews 1962). Observations on the interstitial glass in the Bals Fiord samples suggest that alteration is primarily the result of hot hydrothermal activity, possibly during emplacement over water-saturated sediments, with only minor secondary low-temperature alteration.

a)

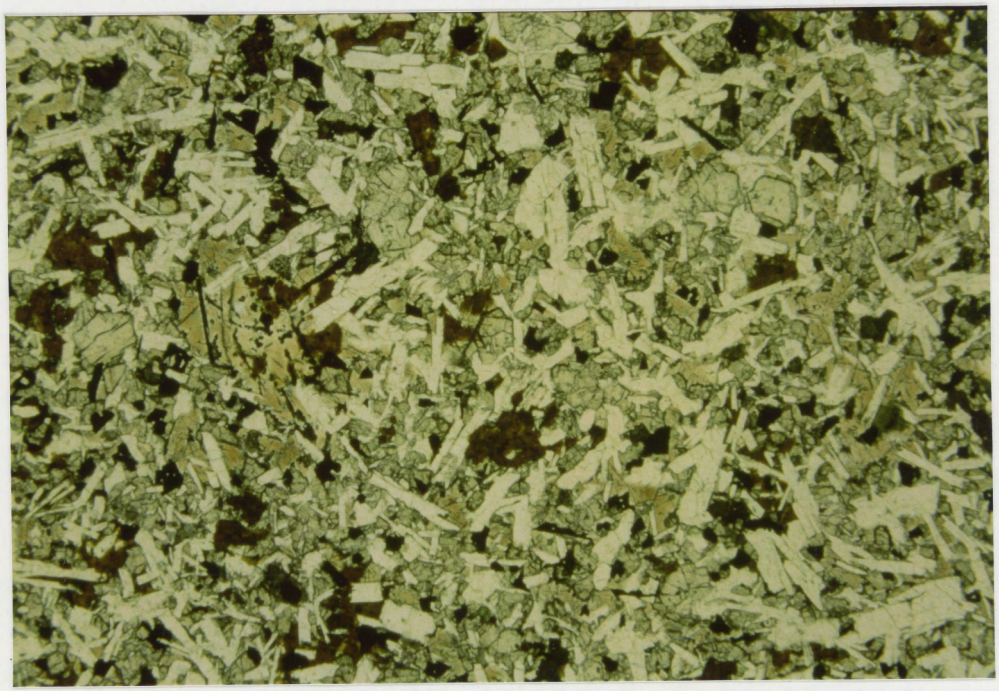

b)

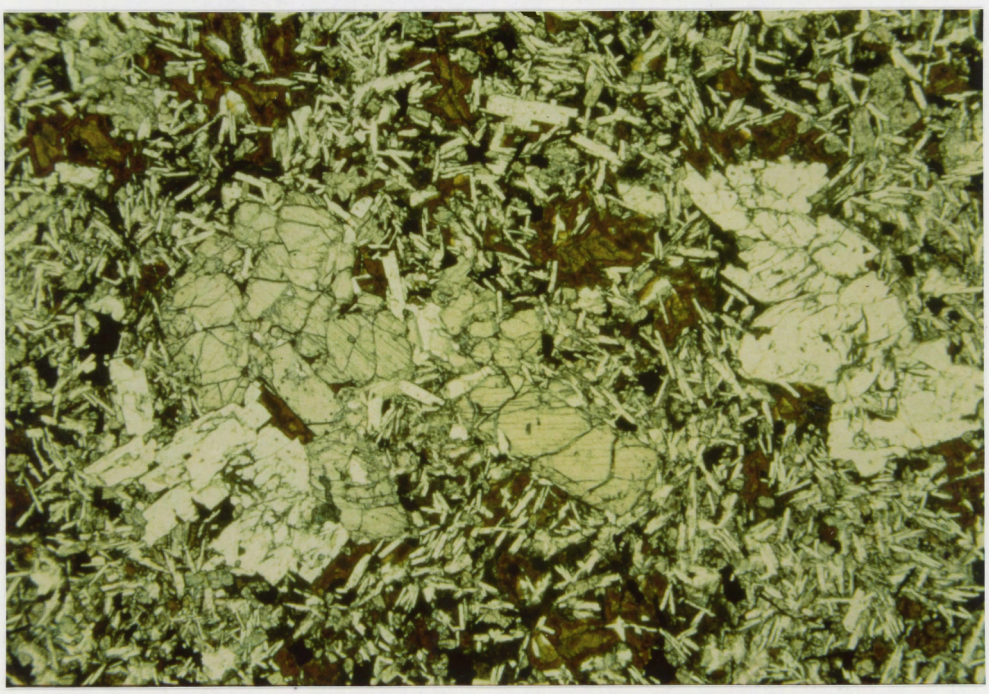

Figure 4.4. a) Fresh glass showing inclusions and crystallites, visible most readily in the large patch of pinkish material in the left-center of the photograph (AX92-192, Flow #4). b) Palagonite-replaced glass, sample showing zoned palagonite replacement with massive gel-palagonite cores, and dark brown fibro-palagonite rims (AX92-188, Flow #1). PPL, FOV = 4 x 7 mm for both.

4.2.3 Textures

The majority of samples in this study display seriate or near-seriate textures. Grain size limits for these samples are somewhat variable: 0.02-0.1 mm minimum grain sizes in the groundmass, and 1.5-6 mm maximum phenocryst grain sizes.
The largest phenocrysts locally define porphyritic and/or glomeroporphyritic textures in some seriate samples (Fig. 4.2). All samples with seriate textures are hypocrystalline, with variable interstitial glass content (trace to 25%), leading to the development of both intergranular and intersertal textures in the groundmass of these samples.

The porphyritic/glomeroporphyritic samples contain the phenocryst assemblage plagioclase + olivine +/- clinopyroxene (5-15%, 0.1-3 mm), set in a hypocrystalline, very fine-grained groundmass. The groundmass in these samples contains a higher proportion of clinopyroxene, and forms intergranular and intersertal textures.

4.2.4 Petrographic Classification

Petrographic classification of these basalts follows the classification scheme of Figure 4.5 (after Mackenzie et al. 1982). These samples invariably contain interstitial glass, and have a mineral assemblage consistent with their classification as tholeiites. These samples are either tholeiites or olivine tholeiites, depending on the abundance of olivine.

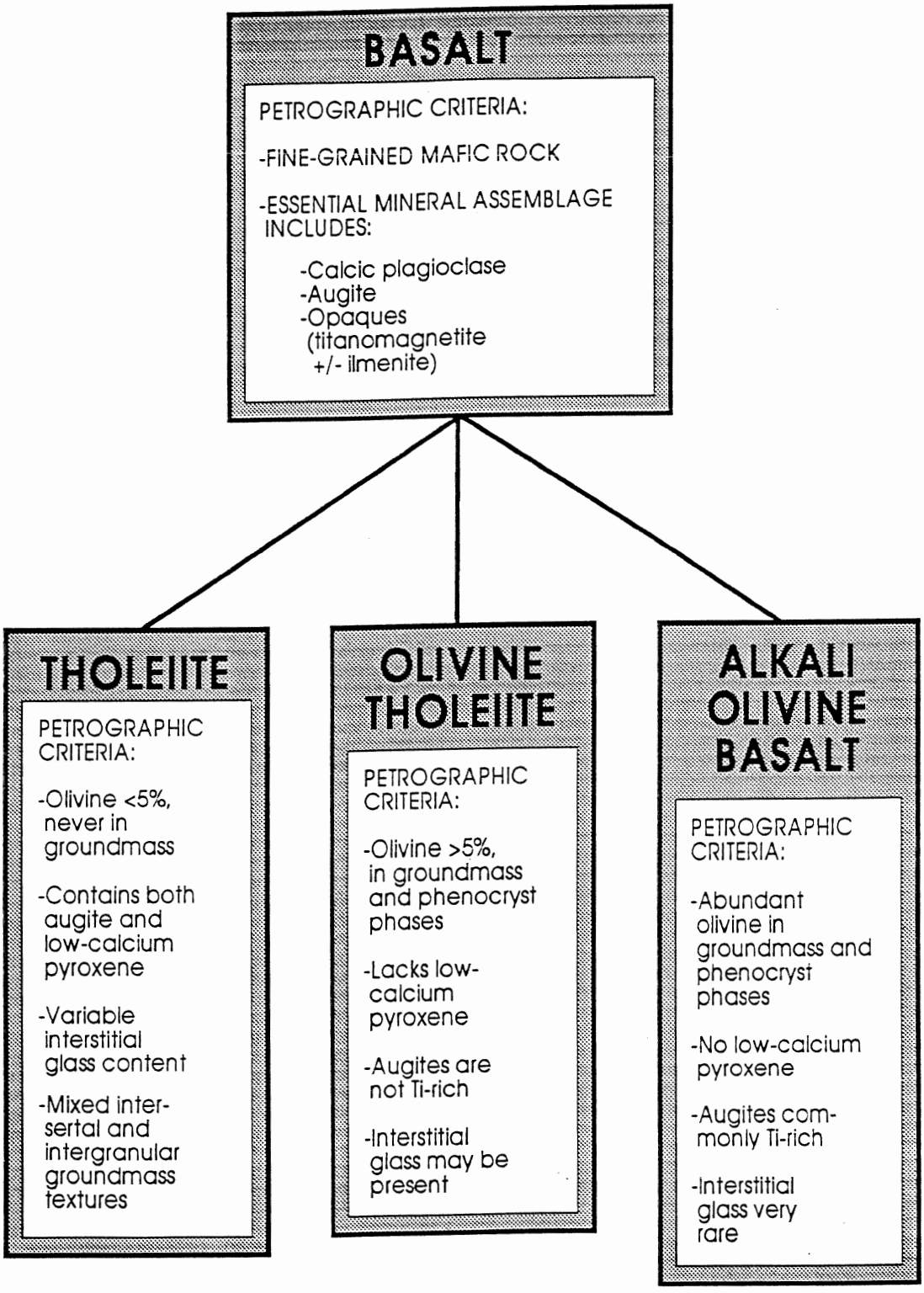

Figure 4.5. Petrographic classification scheme for basalts based on mineralogical and textural criteria (after MacKenzie et al. 1982).

4.3 Geochemistry

4.3.1 Introduction

Geochemical data for all samples in this study include X-ray Fluorescence (XRF) analyses for 10 major and minor element oxides and 15 trace elements (Appendix B). Table 4.1 provides a summary of the geochemical data from Bals Fiord and Bjarnasson Island, as well as previous data from Bunde Fiord (Williamson 1988, Hinds 1991). The following sections describe the geochemical effects of alteration in these rocks, and provide a geochemical classification for these samples.

4.3.2 Alteration

Visible alteration in the Bals Fiord basalts includes the replacement of interstitial glass by palagonite, and of olivine crystals by iddingsite or chlorophaeite +/- carbonate. The exception to this observation is the intense alteration in sample AX92-177, from the base of Flow #11. This sample displays intense carbonatization in thin section, and has a composition very different from all other samples, including AX92-176 from within the same flow. The extreme variation in composition between AX92-177 and all other Bals Fiord samples warrants its removal from the data set. This section deals with the assessment of the more subtle geochemical effects of alteration on these rocks, following the approach of Williamson (1988).

Well-defined chemical changes accompany palagonitization of basaltic glass, including an increase in H_2O content (18-30 wt%), an oxidation of Fe, and a loss of Ca, K, Na, Mg (Fisher and Schmincke 1984). More recent microprobe studies show

	BALS FIORD (N = 12)				BJARNASSON ISLAND (N = 4)				BUNDE FIORD (N = 20)			
ELEMENT	MINIMUM	MAXIMUM	MEAN	STD. DEVIATION	MINIMUM	MAXIMUM	MEAN	STD. DEVIATION	MINIMUM	MAXIMUM	MEAN	STD. DEVIATION
SiO_2	46.69	50.17	49.24	0.95	47.74	51.25	50.04	1.57	46.72	51.24	49.18	1.30
Al_2O_3	12.39	13.66	12.96	0.43	13.11	14.11	13.62	0.51	12.25	14.33	13.14	0.59
Fe_2O_3*	12.74	15.63	14.61	1.05	11.65	12.44	12.03	0.34	11.93	14.74	13.65	0.87
MgO	4.08	5.71	5.05	0.48	6.11	6.52	6.32	0.17	4.30	5.87	5.27	0.47
CaO	8.77	10.79	9.73	0.62	9.80	10.96	10.40	0.48	8.77	11.99	10.31	0.84
Na_2O	2.25	3.44	2.76	0.33	2.01	2.36	2.16	0.15	1.96	2.63	2.28	0.19
K_2O	0.20	0.92	0.44	0.19	0.14	0.31	0.20	0.08	0.14	0.98	0.37	0.23
TiO_2	1.72	3.12	2.17	0.39	1.48	1.59	1.54	0.04	1.68	2.89	2.28	0.33
MnO	0.19	0.27	0.22	0.02	0.14	0.20	0.18	0.03	0.17	0.22	0.20	0.01
P_2O_5	0.16	0.42	0.23	0.08	0.12	0.14	0.13	0.01	0.19	0.34	0.24	0.04
LOI	0.80	4.40	1.95	0.97	0.60	3.70	2.33	1.28	0.70	4.70	2.50	1.02
Ba	60	252	158	60	58	95	84	17	87	284	177	63
Rb	13	35	25	8	5	8	7	1	3	39	14	10
Sr	172	307	214	46	184	224	208	17	171	327	246	51
Y	36	57	47	7	28	30	29	1	26	49	37	6
Zr	134	225	181	33	109	119	116	5	132	270	176	39
Nb	8	23	16	5	7	9	8	1	8	33	14	7
Ga	18	24	21	2	16	19	18	1	17	29	22	3
Zn	94	146	115	13	82	89	86	3	98	151	112	13
Cu	63	236	168	61	109	144	128	16	106	223	176	39
Ni	24	65	47	12	78	89	86	5	28	76	56	13
V	224	447	373	70	305	317	310	5	318	495	388	50
Cr	13	94	45	30	191	209	199	8	11	99	58	27

* Fe_2O_3 + FeO

Table 4.1. Maximum, minimum, mean, and standard deviation statistics for chemical analyses from Bals Fiord, Bjarnasson Island, and Bunde Fiord flows. Note the unique chemical nature of the Bjarnasson Island samples, and the contrast in LOI between Bunde Fiord and Bals Fiord samples. Data for Bals Fiord and Bjarnasson Island samples in Appendix B, data for Bunde Fiord from Williamson (1988) and Hinds (1991).

that most elements are redistributed in palagonitization, with the degree of alteration showing a positive correlation with water content (Fisher and Schmincke 1984). This positive correlation between alteration and water content allows the weight percent LOI (loss on ignition) to be used as an alteration index.

Olivine alters to iddingsite or chlorophaeite, both mixtures of various clay minerals. This alteration, in response to mineral stability rather than hydrothermal activity, should not significantly affect whole-rock geochemistry.

The procedure for evaluating alteration effects involves the comparison of several samples from the main flow sequence at Bals Fiord with AX92-192, a petrographically fresh sample from that section (1.3 wt% LOI). The samples chosen for comparison with AX92-192 have approximately the same modal glass content, but have variations in LOI concentration: (i) AX92-195, Flow #5, 1.4 wt% LOI; (ii) AX92-198, Flow #8, 1.5 wt% LOI; (iii) AX92-200, Flow #9 (upper), 1.8 wt% LOI; (iv) AX92-199, Flow #9 (base), 2.2 wt% LOI; and (v) AX92-188, Flow #1, 4.4 wt% LOI. Systematic chemical changes with increasing LOI concentration indicate alteration, as mentioned above. The analysis used in this evaluation of alteration involves the comparison of various element concentrations in the samples with respect to TiO_2 concentrations. TiO_2 is a good reference element in alteration studies because it has a low solubility in natural waters, and therefore remains relatively immobile during hydrothermal alteration (Cramer and Nesbitt 1983).

Systematic changes in the ratio [element]/[TiO_2] with increasing alteration (increasing LOI concentration), normalized to the ratio for AX92-192 (Equation 4.1)

suggest alteration as the mechanism for these chemical variations (Fig. 4.6, 4.7). Non-systematic changes in element concentrations using this method indicate other processes are responsible for the changes.

$$\%CHANGE = [(X^{A}/TiO_2{}^{A})/(X^{UA}/TiO_2{}^{UA}) - 1] \text{ X } 100 \qquad (4.1)$$

X = Concentration of element

A = Altered sample

UA = Unaltered sample (AX92-192)

This analysis indicates that chemical alteration of the Bals Fiord samples is relatively minor, with clear alteration effects apparent only for barium. The variations in all other elements, although sometimes extreme, are non-systematic, and therefore cannot be attributed to alteration in this treatment.

Limited chemical alteration of the Bals Fiord samples is consistent with their relatively fresh appearance in thin section, and low mean water content (1.95 wt% LOI, Table 4.1). The Bunde Fiord samples, in contrast, have a higher mean water content (2.50 wt% LOI, Table 4.1). The Bunde Fiord samples display much greater alteration in thin section, and show much greater element mobility during alteration in a similar analysis (Williamson 1988).

4.3.3 Geochemical Classification

The geochemical classification of Le Bas et al. (1986) uses the relationship between total alkali content ($Na_2O + K_2O$) and silica. Following this scheme the Bals

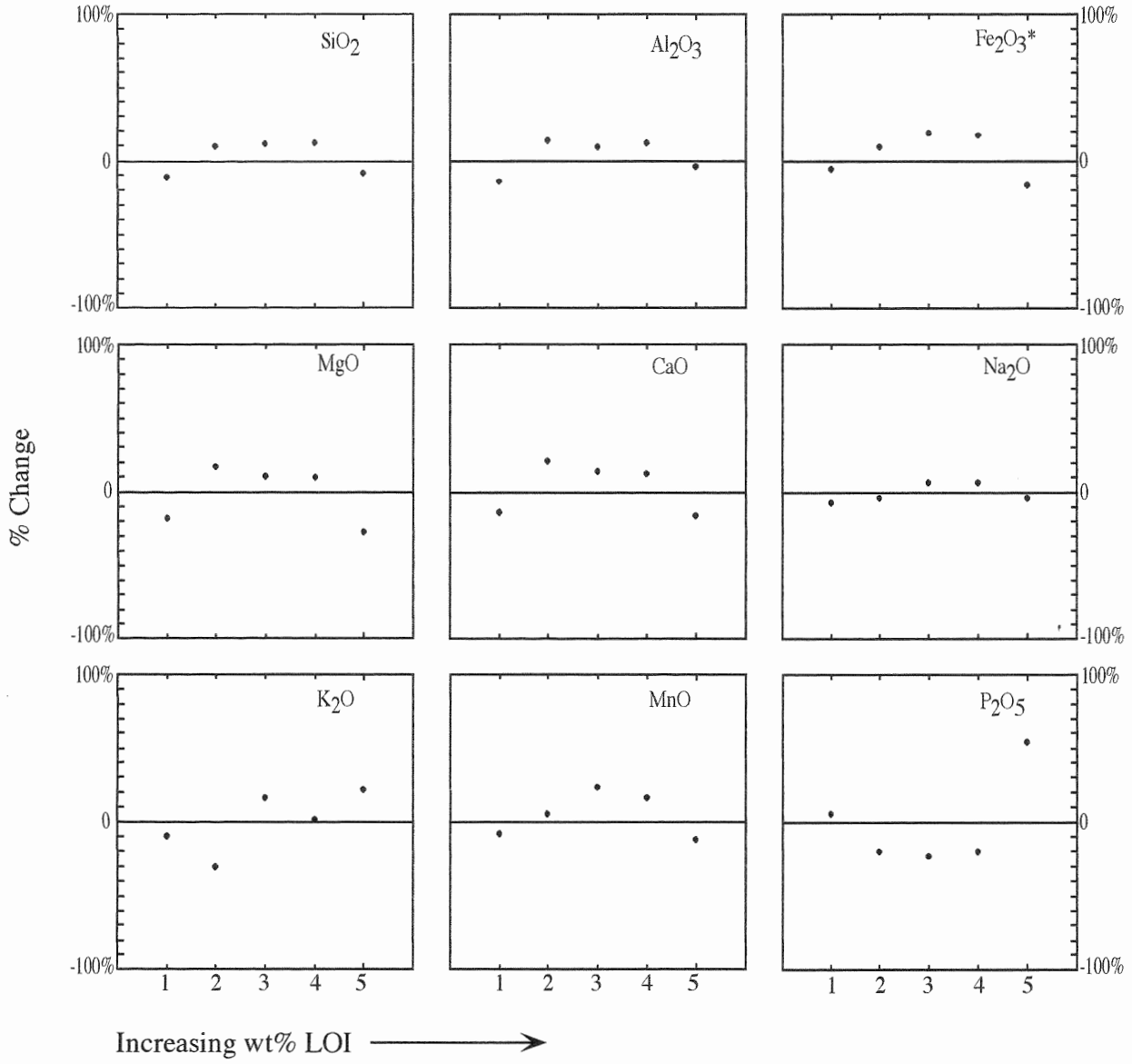

Figure 4.6. Alteration plots for various major elements from selected Bals Fiord basalt samples, plotted as %CHANGE in concentration with respect to a fresh sample (baseline = AX92-192), against a relative alteration index (increasing LOI wt%). * Fe_2O_3 + FeO

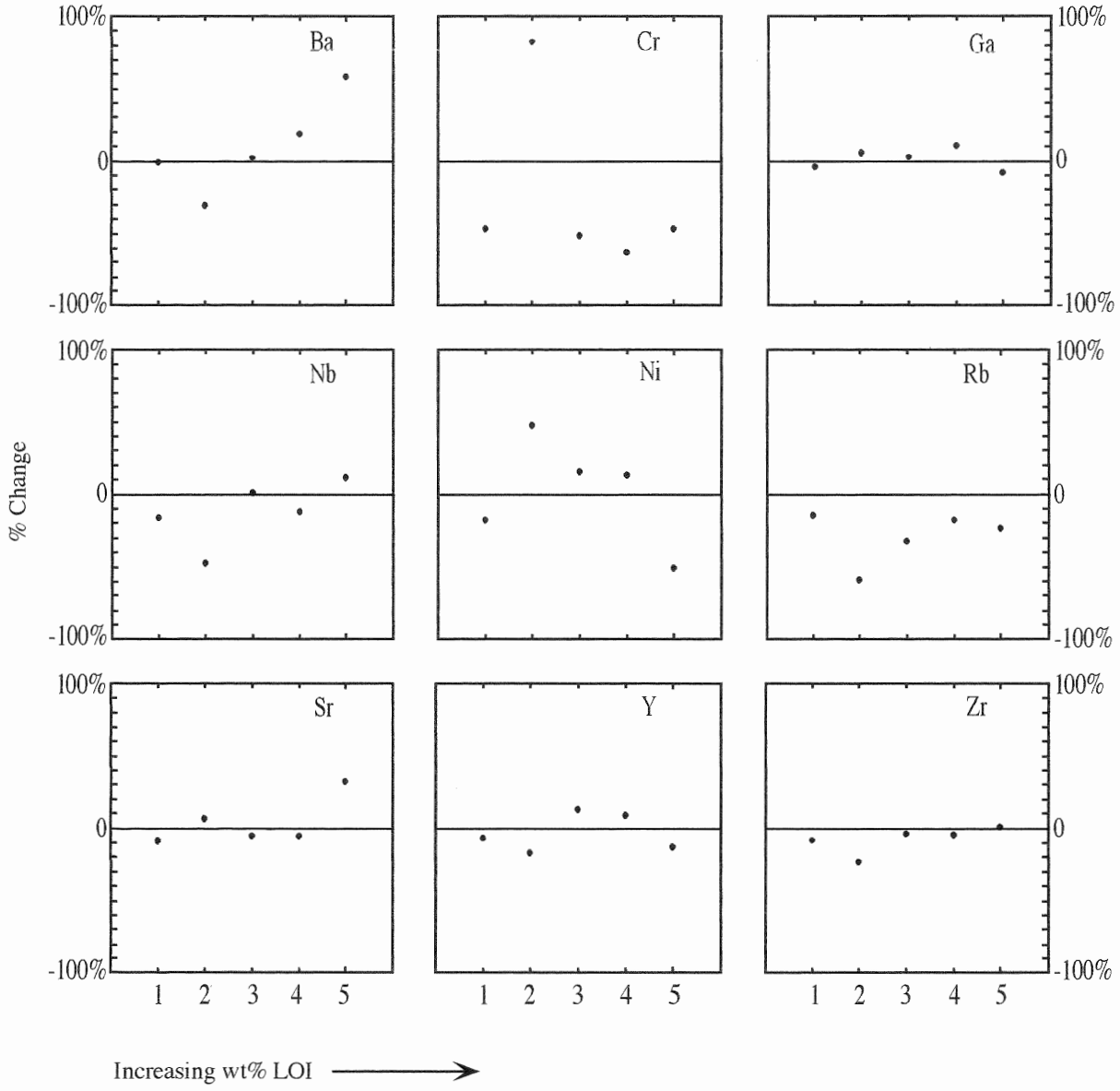

Figure 4.7. Alteration plots for various trace elements from selected Bals Fiord basalt samples, plotted as %CHANGE in concentration with respect to a fresh sample (baseline = AX92-192), against a relative alteration index (increasing LOI wt%).

Fiord, Bjarnasson Island, and Bunde Fiord basalts plot mainly within the basalt field, with a few samples lying just outside the basalt field in the basaltic-andesite field (Fig 4.8). The AFM (alkali-iron-magnesium), and alkali-silica plots of Irvine and Baragar (1971) (Figs. 4.9a and 4.9b) indicate that all Isachsen Formation samples are sub-alkaline (Fig. 4.9b), and tholeiitic (Fig. 4.9a).

4.4 Summary

The basalts from Bals Fiord and Bjarnasson Island contain the same mineral assemblage, but occur in two distinct textural varieties. The Bals Fiord samples are seriate to semi-seriate, with only a few samples from the basal volcaniclastic sequence showing porphyritic and glomeroporphyritic textures. The Bjarnasson Island samples are very different, as only one sample is seriate-textured, and the majority display porphyritic to glomeroporphyritic textures. All samples in this study classify petrographically as tholeiites or olivine tholeiites (less than or greater than 5% olivine, respectively).

An evaluation of element mobility accompanying alteration in the Bals Fiord samples indicates that barium is the only element showing chemical variations related to alteration. This result is consistent with the fresh appearance and low water content (wt% LOI) of the Bals Fiord samples, both indicative of limited alteration.

The majority of Isachsen Formation samples analyzed are basalts, following the classification scheme of Le Bas et al. (1986), with a few samples plotting just outside of the basalt field as basaltic andesites. In the classification of Irvine and Baragar (1971) all Isachsen Formation samples plot within the tholeiitic and subalkaline fields.

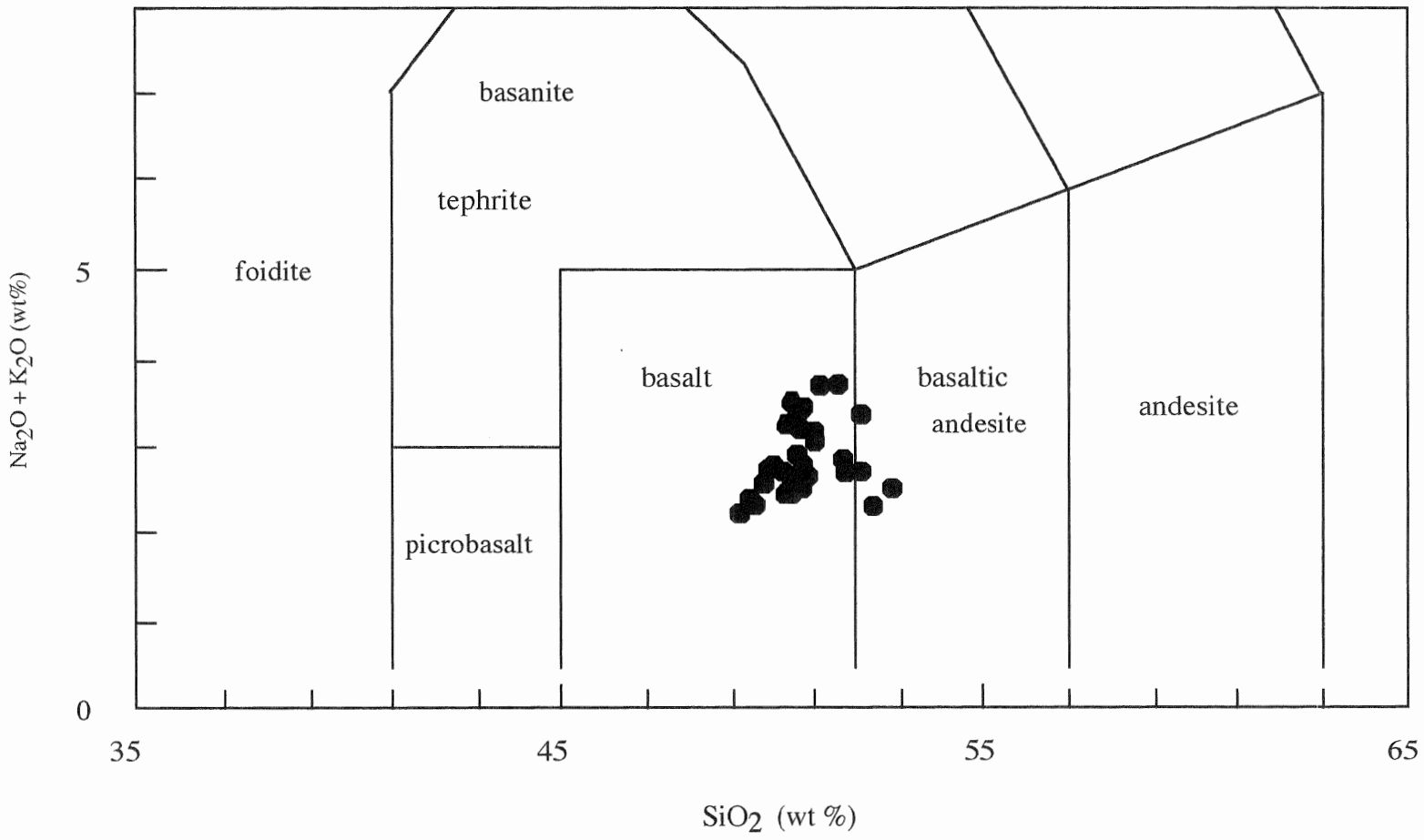

Figure 4.8. Geochemical classification sheme of Le Bas et al. (1986) showing the locations of all Isachsen Formation samples: Bals Fiord and Bjarnasson Island (this study); Bunde Fiord (Williamson 1988, Hinds 1991).

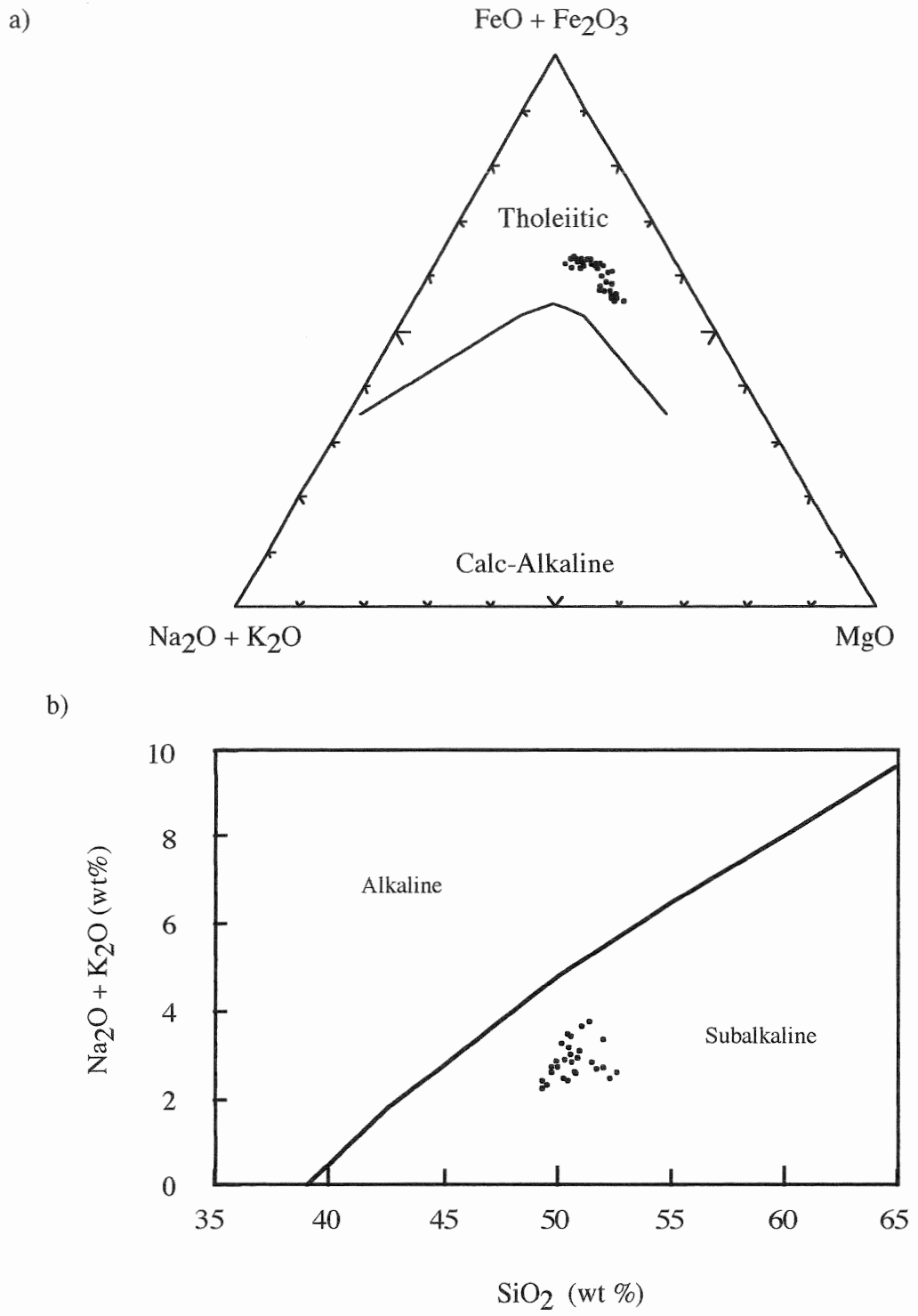

Figure 4.9. Classification diagrams of Irvine and Baragar (1971) showing the location of the Isachsen Formation flow samples.

Using a combination of data collected from Bals Fiord and Bjarnasson Island (this study), and Bunde Fiord (Williamson 1988, Hinds 1991) the following chapter presents a petrogenetic interpretation of Isachsen Formation magmatism.

CHAPTER 5: PETROGENETIC INTERPRETATION OF ISACHSEN FORMATION MAGMATISM

5.1 Introduction

This treatment of Isachsen Formation magmatism employs a combination of geochemical data from the Bunde Fiord region (Williamson 1988, Hinds 1991), and new data from Bals Fiord and Bjarnasson Island (this study). This study uses the analyses for the main flow units in these sections only, and does not include a sill sampled at Bunde Fiord (AX90-61, 62), or the basalt samples from the volcaniclastic succession at Bals Fiord (AX92-202, 205). Also removed from the data set is the highly altered sample AX92-177, as discussed in Chapter 4.

5.2 Major and Trace Element Variation

5.2.1 Introduction

Analysis of chemical variation requires a reliable index element which varies systematically during differentiation, and remains immobile during alteration. For basaltic compositions the highly incompatible elements provide good differentiation indices because they partition strongly to the residual melt during crystallization of all common mineral phases (Cox et al. 1979). Immobile elements have a high charge / radius ratio (high field strength) which makes them resistant to mobilization during alteration (Pearce and Norry 1979). The best differentiation index in this data set is zirconium (Zr), which is both highly incompatible and immobile (Pearce and Norry 1979), and is present in high concentrations in all Isachsen samples (100-300 ppm).

5.2.2 Incompatible and Immobile Elements

The highly incompatible element niobium (Nb) displays a strong linear relationship with Zr in the Isachsen samples (Pearson Correlation Coefficient (r) = 0.9) (Fig. 5.1). This trend suggests a single source may be responsible for all Isachsen Formation volcanics, including those on Bjarnasson Island, which plot at the most primitive end of this trend.

The plot for zirconium (Zr) against titanium (TiO_2), a slightly more compatible element, shows two distinct linear differentiation trends in the Isachsen data (Fig. 5.2). The higher TiO_2 trend intersects the origin and contains most of the samples from the Bunde Fiord region (The Bunde Fiord Trend), and the lower TiO_2 trend contains most of the Bals Fiord samples (The Bals Fiord Trend). The Bjarnasson Island samples are stratigraphically the oldest, and compositionally the most primitive samples, and they lie at the intersection of the Bunde Fiord and Bals Fiord trends. The existence of two distinct differentiation trends indicates that two magma sources, with distinct compositions, contributed to Isachsen Formation volcanism. The intersection of these two trends, and the linear relationship between Zr and Nb suggest that these magmas may have shared a common parent.

Three of the Bunde Fiord samples (AX85-267 and AX90-67,72), unique in that section, lie on the Bals Fiord Trend. These three samples belong to the only flow that correlates across all three Bunde Fiord sections in the multivariate statistical analysis by Hinds (1991). These samples also plot with the Bals Fiord samples in various other element variation diagrams. A second, geochemically distinct source for this

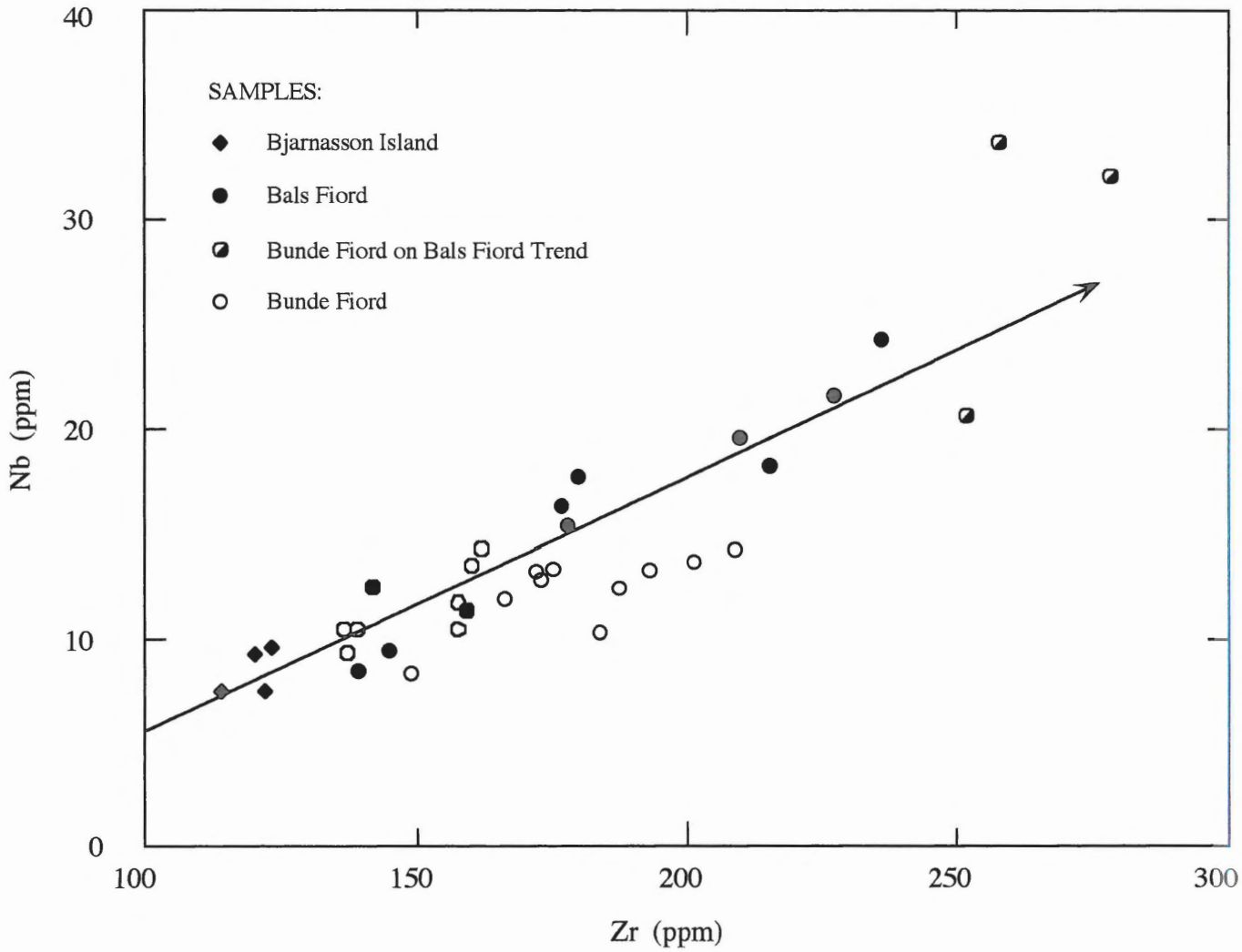

Figure 5.1. Variation diagram for niobium against zirconium with approximate best fit line (Pearson correlation coefficient = 0.904).

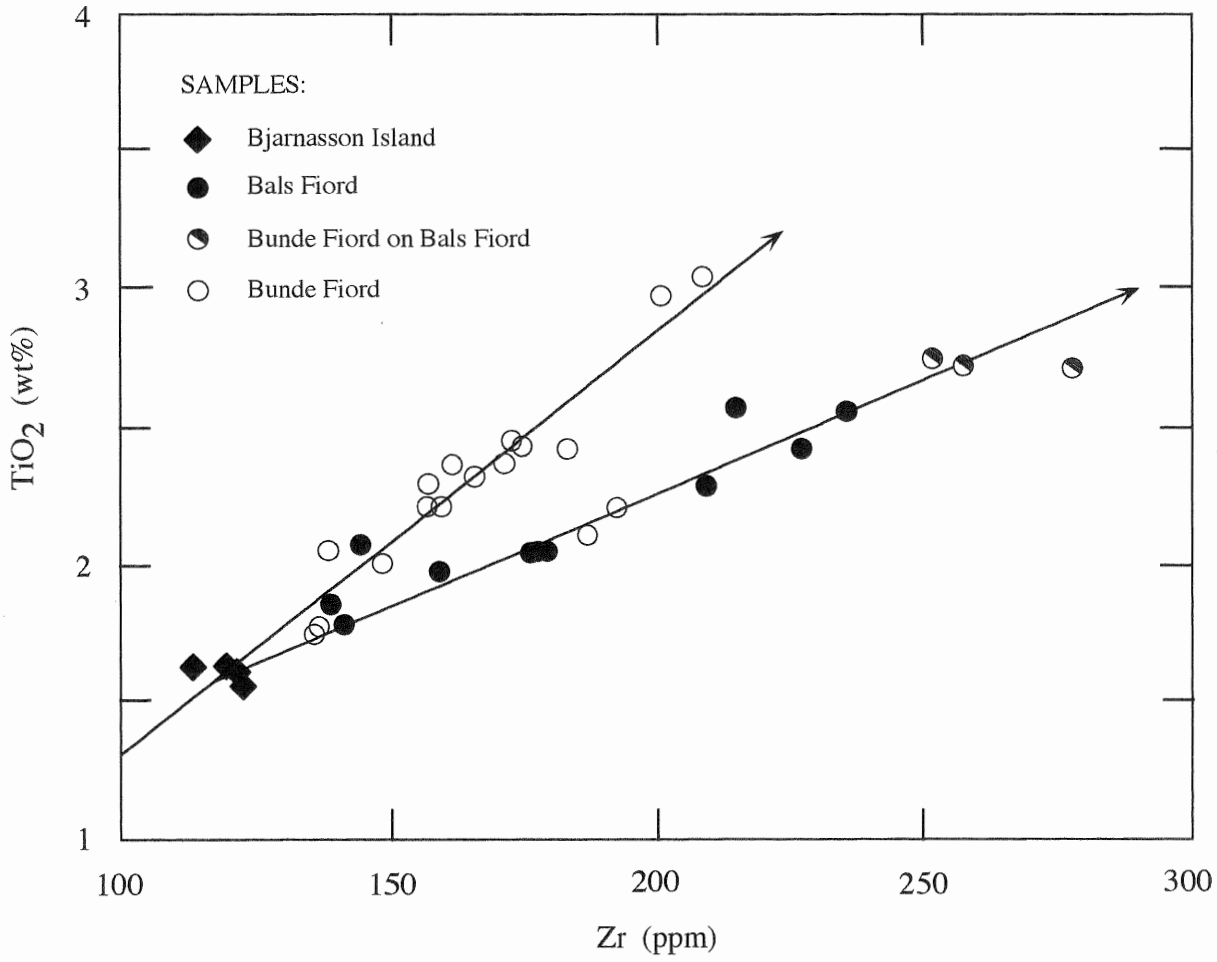

Figure 5.2. Variation diagram for titanium against zirconium with approximate best-fit trend lines for The Bals Fiord Trend and the Bunde Fiord Trend.

flow (The Bals Fiord Trend) would explain its anomalous composition among the Bunde Fiord samples. Other Bunde Fiord samples that plot on the Bals Fiord Trend (AX85-264, 266 and AX90-64, 73) lie closer to the intersection of the two trends. Near the intersection, the separation between the trends approaches analytical uncertainties (+/- 10%) and the effects of within-flow chemical variations, which are documented for repeat samples of a flow in the Bunde sequence (Hinds 1991).

5.2.3 Major Elements

Major element variation diagrams, plotted against zirconium, reveal further evidence to support the existence of two separate differentiation trends. Plots for calcium, sodium, iron, and aluminum (Fig. 5.3) all display considerable scatter because of their inherent susceptibility to alteration. The Bunde Fiord samples show the greatest scatter because they are more highly altered (Chapter 4). Despite their susceptibility to alteration, these element variation diagrams do allow the identification of two distinct populations of data, which correspond to each of the Bals Fiord and Bunde Fiord trends previously identified (Fig. 5.3).

Concentrations of Na and Fe are consistently higher in the Bals Fiord samples, whereas the concentration of Ca is consistently lower. Aluminum concentrations show considerable scatter for both the Bunde and Bals fiord samples and no clear separation of two populations. The broadly linear trend of aluminum against zirconium defines an overall decrease with differentiation.

The Bjarnasson Island samples are the most primitive, and define a third population of samples. The Bjarnasson Island samples have low CaO, Na_2O, and Fe_2O_3

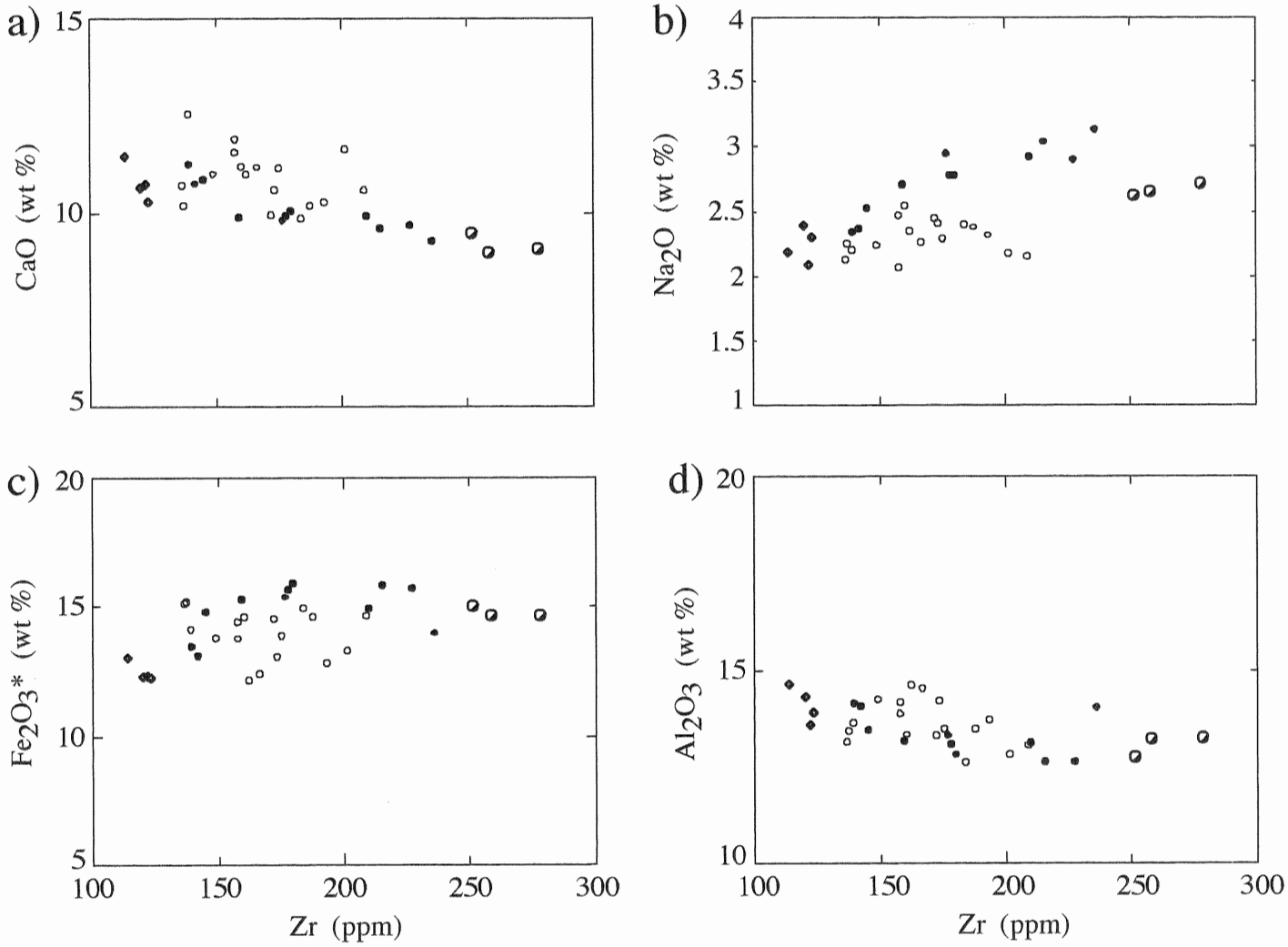

Figure 5.3 Variation diagrams for various major elements against Zr: a) Ca, b) Na, c) Fe, and d) Al. ○ = Bunde Fiord samples, ● = Bals Fiord samples, ◆ = Bjarnasson Island, ◘ = Bunde Fiord samples on Bals Fiord trend. * Fe_2O_3 + FeO

concentrations, and higher Al_2O_3 concentrations relative to the other Isachsen Formation samples.

5.2.4 Trace Elements

Figure 5.4 shows plots for the trace elements Y, Rb, Ni, and Cr against the differentiation index Zr. The Bunde Fiord samples in the Zr-Y plot (Fig. 5.4a) show considerable scatter, and an overall lower concentration. The scatter may be the result of alteration, however, Y is relatively incompatible and immobile, and therefore should not be affected by alteration (Pearce and Norry 1979). The scatter in the Zr-Y and Zr-Rb plots for the Bunde Fiord samples (including those from the Bals Fiord Trend), and the relatively strong linear relationship for the Bals Fiord samples in the same plot provide further evidence that alteration is more intense in the Bunde Fiord samples (Chapter 4).

The trace metal plots of Cr and Ni against Zr show considerable scatter in the data from both Bunde Fiord and Bals Fiord, with overall lower concentrations in the Bals Fiord samples (Fig. 5.4c,d). The most significant feature of these plots is the location of the Bjarnasson Island samples, which have distinctly higher Ni and Cr concentrations than the other Isachsen Formation samples.

5.2.5 Summary

Differentiation plots of various elements against zirconium provide important clues about the origin and evolution of Isachsen Formation magmatism. The incompatible and immobile elements TiO_2 and Nb represent the best clues as these elements are

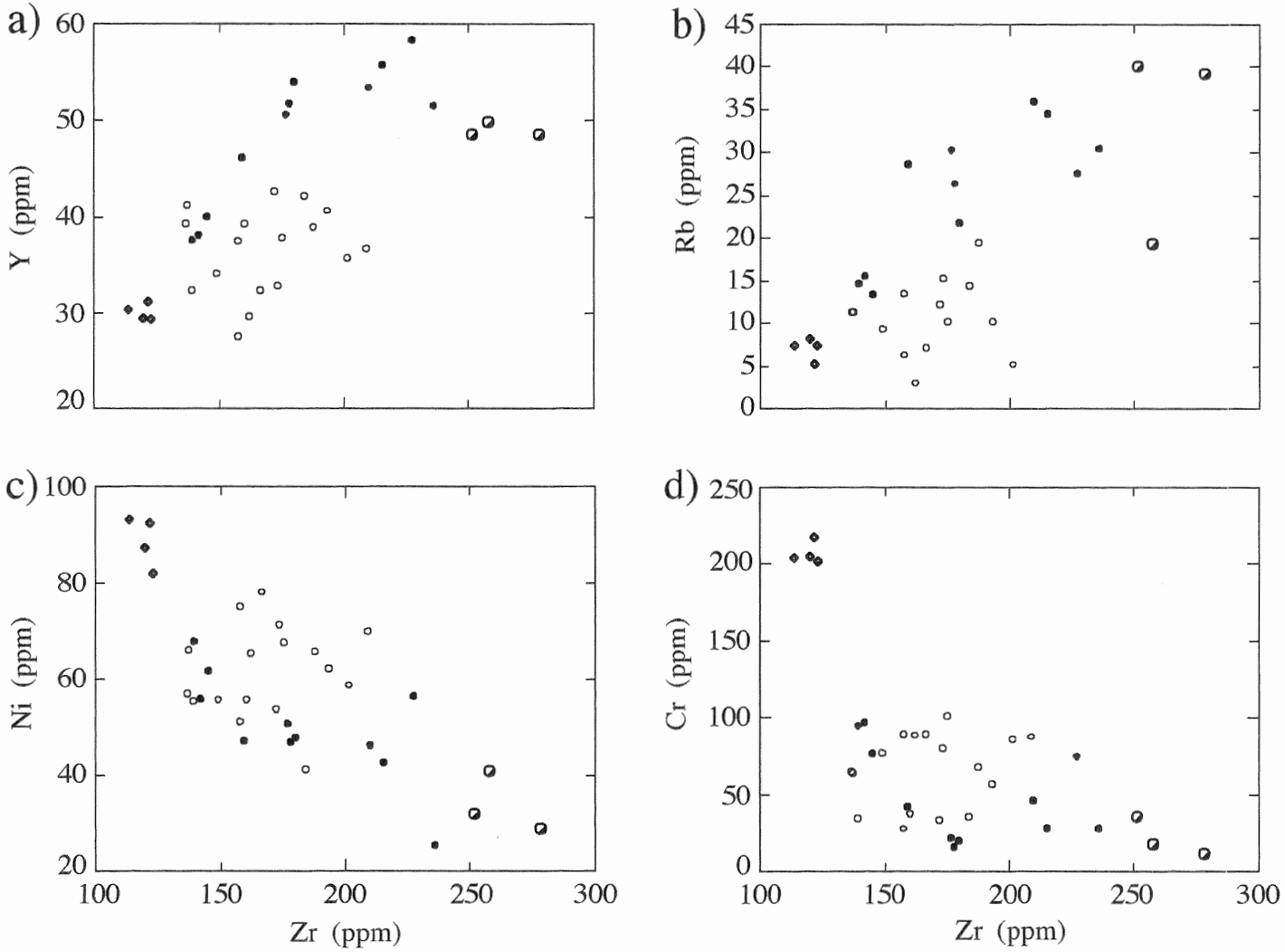

Figure 5.4 Variation diagrams for various trace elements against Zr: a) Y, b) Rb, c) Ni, and d) Cr. o= Bunde Fiord samples, ●= Bals Fiord samples, ◆= Bjarnasson Island, ⊘= Bunde Fiord samples on Bals Fiord trend.

least subject to alteration effects. A strong linear relationship exists between zirconium and niobium, because of the strongly incompatible nature of these two elements. The strong highly significant correlation ($r = 0.9$) of all Isachsen Formation samples in the Zr-Nb plot suggests a common source for all the samples. Two distinct trends in the data set are apparent in the plot of zirconium against titanium. One trend contains the majority of the Bunde Fiord samples, the other the majority of the Bals Fiord samples. The Zr-TiO_2 plot suggests that two sources contributed to Isachsen Formation volcanism. The intersection of the two trends in the Zr-TiO_2 plot, and the linear relationship of these samples in the Zr-Nb plot, suggests that the two sources shared a common parent. The common parental magma for the two populations of Isachsen Formation volcanics likely resembled the composition of the Bjarnasson Island basalts, which: (i) are the most primitive samples, and (ii) plot at the intersection of the two trends in the Zr-TiO_2 plot.

Differentiation plots for several other elements show two distinct populations of samples, dominated by either Bals Fiord or Bunde Fiord samples. The separation of the two populations is less distinct for these other elements because of element mobility during alteration, most notably in the Bunde Fiord samples.

5.3 Petrogenetic Interpretation

5.3.1 Introduction

The petrogenetic analysis of comagmatic basaltic suites involves the examination of magma chamber evolution using simple AFC (assimilation-fractional crystallization)

models. The following discussion of the Isachsen Formation basalts focuses mainly on fractional crystallization as the controlling mechanism for magma evolution, because the role of assimilation is difficult to quantify with the available data.

5.3.2 Trend Analysis

Differentiation trends for various elements in the Isachsen Formation samples display a variety of information useful in petrogenetic interpretation. The most reliable elements for interpretation, as indicated in the previous section, are zirconium, niobium and titanium. The following is a petrogenetic interpretation of Isachsen Formation magmatism, based on work by Pearce and Norry (1979). This discussion centers on the interpretation of niobium and titanium differentiation trends, using variations in other element concentrations as supporting evidence.

Pearce and Norry (1979) evaluate the effects of fractional crystallization, for various minerals, on log-Zr against log-Nb and log-TiO_2 plots. The slope of the trend for the Isachsen Formation samples in the log-Zr against log-Nb plot resembles the trend modelled by Pearce and Norry (1979) for the fractionation of basic rocks (plagioclase (50%) + clinopyroxene (30%) + olivine (20%), Trend #1) (Fig 5.5). The Isachsen Formation samples define slightly steeper trend than that calculated for the above assemblage, and no likely mineral phase can account for this steeper trend. The assimilation of upper crustal material provides a possible explanation for the steeper trend, and is a likely consequence of magma emplacement in the upper crust below the Sverdrup Basin. The average upper crustal concentration of Zr is 190 ppm, and of Nb is 25 ppm (Taylor and McLennan 1985). Mixing of material with this composition

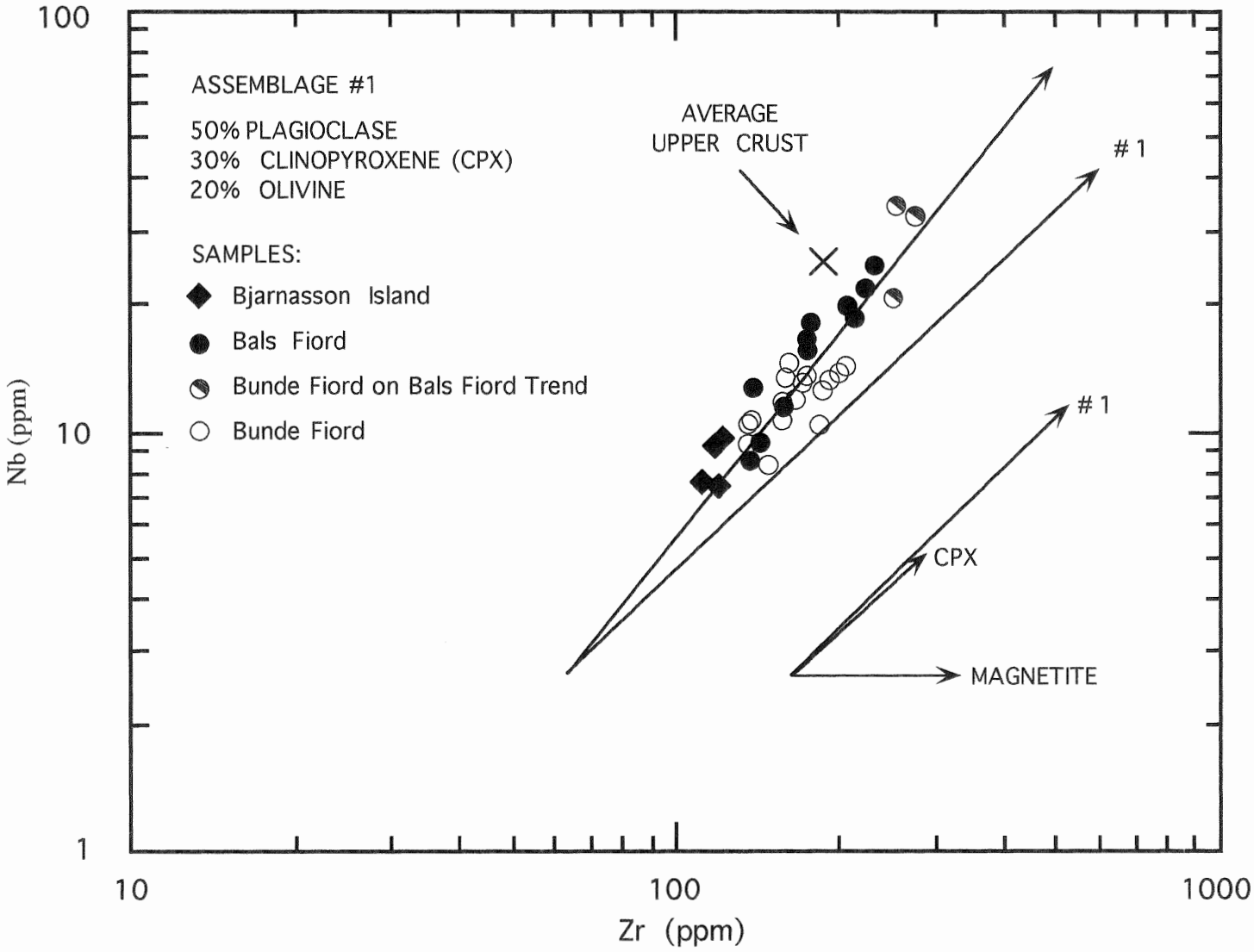

Figure 5.5. Variation diagram of log-niobium against log-zirconium showing the trends for the Isachsen Formation data, and for the fractionation trends calculated by Pearce and Norry (1979) for various minerals and Assemblage #1. Average upper crustal Zr-Nb ratio also shown.

and the Isachsen Formation basalts would result in a steepening of the trend expected for the fractionation of mineral assemblage #1 modelled by Pearce and Norry (1979) (Fig. 5.5). The timing of assimilation, if it did occur, is ambiguous. Assimilation may have occurred prior to fractionation and eruption, during emplacement of the magma into the upper crust, or throughout the fractionation and eruptive history of the magma.

The fractionation trend modelled by Pearce and Norry (1979) for the same mineral assemblage (plagioclase (50%) + clinopyroxene (30%) + olivine (20%), Trend #1) in the plot log-Zr against log-TiO_2 also resembles the trends for the Isachsen Formation samples (Fig. 5.6). Variations in the proportion of clinopyroxene fractionation, or the introduction of magnetite fractionation, could explain the separation between the two trends in the Isachsen Formation samples (Fig. 5.6). The lower TiO_2 Bals Fiord trend could be explained by a higher proportion of clinopyroxene fractionation, or a small proportion of magnetite fractionation (mineral vectors, Fig. 5.6).

A higher proportion of clinopyroxene fractionation in the Bals Fiord magma would explain the decrease in TiO_2 concentration (Fig. 5.2), as well as the depletion of calcium, a major component of clinopyroxene (Fig. 5.3a). Clinopyroxene fractionation may also explain the overall lower concentrations of chromium (Fig. 5.4d), which partitions strongly to clinopyroxene, in the Bals Fiord samples.

Fractionation of a small amount of magnetite would cause a significant depletion of titanium (mineral vector, Fig. 5.6). The effect of magnetite crystallization on other element concentrations, especially iron (Fig. 5.3c), would not be easily detected given the low proportion of magnetite crystallization required to cause a significant depletion

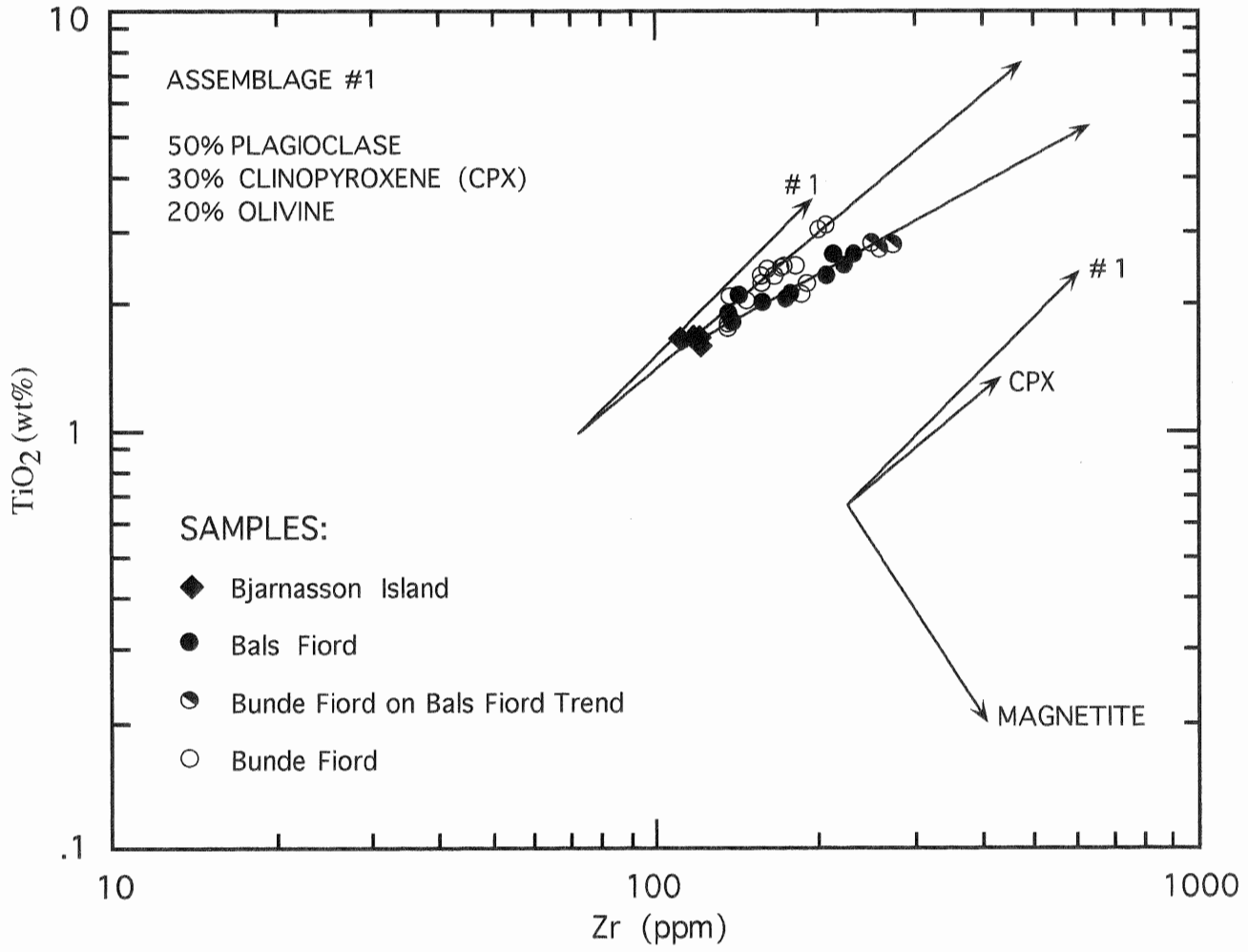

Figure 5.6. Variation diagram for log-titanium against log-zirconium showing the two trends in the Isachsen Formation samples, and the fraactionation trends for various minerals, and Assemblage #1 from Pearce and Norry (1979).

of TiO_2. Magnetite crystallization occurs in response to a slight increase in oxygen fugacity, generally related to crystallization at higher crustal levels (McBirney 1984).

The broad linear decrease in Al concentration for all Isachsen Formation samples (Fig. 5.3d), with no clear separation of two trends, suggests that the fractionation of plagioclase, the major Al-bearing mineral, is roughly equivalent in the two magmas. Two trends exist for sodium against zirconium, which may indicate crystallization of plagioclase with different compositions in each of the two magma sources. Plagioclase composition responds to changes in both pressure and water content (McBirney 1984), but the significance of two trends in the Zr-Nb plot for the Isachsen samples is unclear.

The Bjarnasson Island samples, in most differentiation diagrams, plot at or near the intersection of the two trends in the Isachsen Formation samples. The exceptions are the trace metals Cr and Ni, which show significantly higher concentrations in the Bjarnasson Island samples. Crystallization of clinopyroxene, or spinel, could explain this compositional gap between the Bjarnasson Island samples and the other Isachsen Formation samples. Spinel fractionation would remove Cr and Ni in the ratio 2:1 (Cox et al. 1979). Clinopyroxene crystallization would cause a decrease in Cr (K_d = 10) and Ni (K_d = 2) in the ratio of approximately 10:2, consistent with the observed ratio of approximately 10:1 (Fig. 5.4c,d). Clinopyroxene fractionation is the most likely explanation for the compositional difference between the Bjarnasson Island samples and the other Isachsen Formation samples.

5.3.3 Summary

An examination of differentiation trends in the Isachsen Formation data indicates that two magmas, with distinct evolutionary histories, contributed to this volcanic event, and that these two magmas shared a common parent with a composition similar to the Bjarnasson Island basalts. This study shows that crystal-liquid fractionation can explain the evolution of the two compositionally distinct Isachsen Formation magmas from a common parental magma source. Assimilation may also affect the composition of these samples, but the effect cannot be quantified with the available data.

Fractional crystallization of the mineral assemblage plagioclase (50%) + clinopyroxene (30%) + olivine (20%), as modelled by Pearce and Norry (1979), can explain the general differentiation trends for Nb and TiO_2 against Zr. The cause of the two trends observed in the Zr-TiO_2 plot could be: (i) an increase in clinopyroxene fractionation in the Bals Fiord magma, or (ii) the introduction of magnetite to the fractionation assemblage.

The observed depletion of Ca and Cr in the Bals Fiord samples supports the hypothesis that variations in clinopyroxene crystallization are responsible for the development of two distinct fractionation trends from a common parent. Magnetite crystallization in the Bals Fiord magma is not evident in the differentiation diagram for iron, but the amount of magnetite required to cause the observed TiO_2 depletion may not be sufficient to cause a significant depletion in iron. An increase in magnetite fractionation may indicate a higher oxygen fugacity, and therefore a higher crustal level for this magma.

The Bjarnasson Island samples plot at the intersection of the two fractionation trends in the Zr-TiO_2 plot, indicating that these samples may resemble the common parental composition of the Walker Island Member sources. The lower stratigraphic position of these samples (within the Paterson Island Member) may indicate eruption of an early magma, prior to its segregation at higher crustal levels. The differentiation diagrams for Ni and Cr, against Zr, suggest that clinopyroxene fractionation occurred prior to the separation of the two magmas which contributed to Walker Island Member volcanism.

CHAPTER 6: DISCUSSION AND CONCLUSIONS

This study represents a significant contribution to the understanding of Isachsen Formation volcanism, through the addition of new stratigraphic, petrographic, and geochemical data from Bals Fiord and Bjarnasson Island. Detailed stratigraphic data from Bals Fiord, the thickest, most complete Isachsen volcanogenic sequence available, contributes valuable information on the paleoenvironment and volcanology of the Walker Island Member volcanic episode. The combination of geochemical data from this study with previous data from Bunde Fiord (Williamson 1988, Hinds 1991), allows an evaluation of the petrogenetic history of Isachsen Formation volcanism.

The Bjarnasson Island volcanic sequence, on the north side of the island, contains the stratigraphically oldest, and compositionally most primitive basalts in the Isachsen Formation. This section lies within the uppermost Paterson Island Member (Embry and Osadetz 1988). The horizontal to sub-horizontal column development observed in the Bjarnasson Island flows indicates ponding of the magma. The evidence for ponding magma, along with the laterally discontinuous nature of the flows (both within the section and across the island) indicates considerable topography in this location during early Isachsen Formation volcanism. Erosional incision or faulting, producing topographic relief, may explain, in part, the location of these units within the Paterson Island Member. The composition of the Bjarnasson Island basalts reflects the composition of the common parent magma for the Walker Island Member volcanic sources, with the possible exception of some clinopyroxene fractionation between the

Paterson Island eruptive episode and the segregation of multiple sources for Walker Island Member volcanism.

The Bals Fiord volcanogenic sequence contains deposits which contribute significant information to the understanding of the physical volcanology and paleoenvironment of Walker Island Member volcanism. These deposits include volcaniclastics, flows, and inter-flow sedimentary units.

Volcaniclastic deposits of mixed pyroclastic and epiclastic affinity constitute the basal 169 m of the Bals Fiord section. The pyroclastic units (Units 2 and 5a) are proximal deposits, whereas the epiclastic units (Units 1, 3, 4, and 5b) represent deposits from a more distal volcanic source.

The pyroclastic deposits locally contain intact bombs, indicating deposition in very close proximity to an eruptive source. Locally high concentrations of interstitial sub-angular quartz grains in the pyroclastic deposits may indicate minor reworking, emplacement into an area of active sand deposition, or hydrovolcanic activity. Volcanic clasts in the pyroclastic deposits also contain high concentrations of unresorbed, sub-angular quartz sand, indicating mixing of magma and unconsolidated sand immediately prior to eruption. A hydrovolcanic origin for the pyroclastics may explain both the interstitial and intraclast quartz concentrations.

The overall crystallinity of volcanic clasts in the pyroclastic deposits increases from glassy, to microphenocryst-bearing within Unit 2, to nearly porphyritic and holocrystalline in Unit 5. The concentration of intraclast sub-angular quartz grains in the pyroclastic units decreases at higher stratigraphic levels. Both observations

indicate a maturing source for the pyroclastics through: (i) cooling and crystallization of the magma, and (ii) coating of the conduit through repeated eruption of material, isolating the magma from the unconsolidated material.

Several epiclastic deposits occur in the volcaniclastic sequence, which indicates deposition in a low-lying area with active clastic deposition, consistent with deposition in a deltaic environment. The deposition of volcaniclastic material overwhelms sand deposition at this location, indicating relatively close proximity to the eruptive center producing the epiclastic debris. Pyroclastic activity in this area probably occurred on a much smaller scale, and did not build up significant topography to divert the epiclastic mass-flows. A common source for the epiclastic and pyroclastic material is possible, however, the presence of sandstone units in the volcaniclastic sequence makes the common source model improbable.

The transition between volcaniclastics and basalt flow deposition at Bals Fiord is rapid. This indicates a change from explosive to quiescent volcanism in this region, again reflecting a maturing volcanic source, but in a more regional sense. The change is likely the result of devolatilization of the magma, and establishment of a stable eruptive system.

The Bals Fiord section contains 11 thick (8-50 m) basalt flows, not including the thin, discontinuous units associated with the pyroclastic deposits (Units 2 and 8). Most flows contain evidence for subaerial emplacement, including: flow top development, chilled bases (and not tops), sand flame structures, or plant fragments at their base. Flow #4 lacks any of these flow features, and has an unusually fresh

appearance, suggesting a possible intrusive origin for this unit. The lack of subaqueous flow structures, and the nature of the interbedded sediments, support a subaerial emplacement model for the majority of flows in this section.

Analysis of the five thin sedimentary sequences preserved between flows in the Bals Fiord section provides important clues about the environment of deposition. Four of the sedimentary units display fluvial characteristics, and one contains a trace fossil assemblage indicative of high energy, shallow marine deposition. The combination of fluvial and shallow marine deposition in the Bals Fiord section supports the fluvial-deltaic model for deposition of the Walker Island Member (Embry 1985, 1991).

Isachsen Formation volcanogenic deposits occur only on western Axel Heiberg Island, with the possible exception of one thin flow(?) on eastern Axel Heiberg Island (Embry and Osadetz 1988). The above discussion contains the details of the Bjarnasson Island and Bals Fiord sections. Two other Isachsen Formation volcanogenic sequences occur on western Axel Heiberg Island, one at Bunde Fiord, and another at Strand Fiord (Fig. 6.1). An 80 m thick volcanic breccia with a thin lahar deposit in its uppermost portion occurs in the Isachsen Formation at Strand Fiord (Ricketts 1985). The volcanic breccia displays characteristics indicative of epiclastic deposition, and lies above four flow units with interbedded Isachsen Formation sediments (G.K. Muecke pers comm) (Fig. 6.1). Three Isachsen Formation volcanogenic sections occur at Bunde Fiord. All three Bunde Fiord sections contain basalt flows with interbedded sediments, and the section at Camp Five Creek contains a 45 m thick epiclastic deposit near the top of the section (Hinds 1991) (Fig. 6.1).

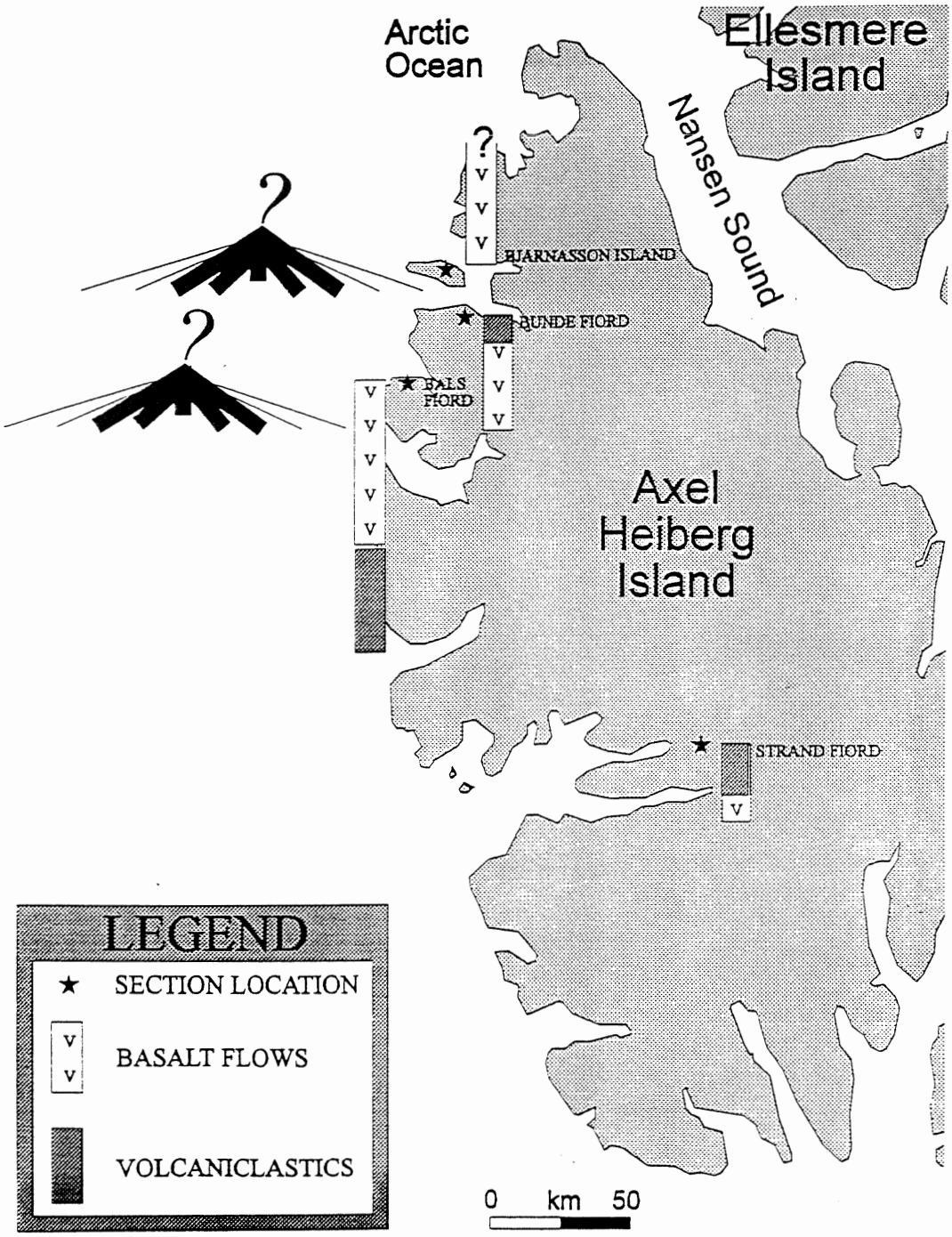

Figure 6.1. Detailed location map showing the locations and rough stratigraphy for the Isachsen Formation volcanogenic sections from western Axel Heiberg Island. Possible edifice locations shown for the Walker Island Member volcanic event.

The thickness of the volcaniclastic sequence at Bals Fiord, its location below the main flow sequence, and the occurrence of interbedded pyroclastic deposits suggest this section is the closest to an eruptive center. The Bals Fiord section is the furthest west on Axel Heiberg Island (Fig. 6.1), and one unit in the sequence (Flow #5) contains evidence for eastward flow movement at this location, both of which suggest that the source for the Isachsen Formation volcanics lies just off the west coast of present-day Axel Heiberg Island (Fig. 6.1). The linear distribution of volcanic deposits along the west coast of Axel Heiberg, and paucity of Isachsen Formation volcanics in central and eastern Axel Heiberg Island suggests a possible linear distribution of eruptive centers, possibly fissure-related, off the west coast of Axel Heiberg Island.

The linear trend for all Isachsen Formation samples in the Zr-Nb plot suggests a comagmatic origin for Isachsen Formation volcanics. The plot of titanium (wt% oxide) against zirconium shows two trends in the data set, each trend containing predominantly Bals Fiord or Bunde Fiord samples, with the Bjarnasson Island samples falling near the intersection of the two trends. Several other element differentiation diagrams support the existence of two distinct populations of samples. Two fractional crystallization theories can explain the observed development of two compositionally distinct magmas from a common parent: (i) crystallization of different proportions of clinopyroxene in the two magmas, or (ii) the addition of magnetite to the fractionating assemblage. The subtle nature of the differences in titanium concentration, and

evidence from other differentiation diagrams support changes in clinopyroxene crystallization in explaining the two distinct fractionation trends.

The Bjarnasson Island basalts are the most primitive Isachsen Formation samples, and plot near the intersection of the two fractionation trends for Walker Island Member basalts. Both of these observations, along with the lower stratigraphic location of the Bjarnasson Island basalts, support the existence of an early Isachsen volcanic event, as proposed by Embry and Osadetz (1988). The compositionally primitive Bjarnasson Island basalts may approximate the common parental magma composition for the multiple Walker Island Member volcanic sources.

REFERENCES

Balkwill HR (1978) Evolution of the Sverdrup Basin, Arctic Canada. The American Association of Petroleum Geologists Bulletin 62: 1004-1028

Cameron BI (1989) Petrochemistry and origin of altered Permian basalts in the Sverdrup Basin, Arctic Canada. Unpubl Master's thesis, Dalhousie University

Cas RAF, Wright JV (1987) Volcanic successions. Allen and Unwin, London

Cox KG, Bell JD, Pankhurst RJ (1979) The Interpretation of igneous rocks, vol.1. Allen and Unwin, London

Cramer JJ, Nesbitt HW (1983) Mass-balance relations and trace-element mobility during continental weathering of various igneous rocks. Sciences Geologiques, Memoire 73: 63-73

Embry AF (1985) Stratigraphic subdivision of the Isachsen and Christopher formations (Lower Cretaceous), Arctic Islands. In: Current Research, Part B, Geological Survey of Canada, Paper 85-1B, pp 239-246

Embry AF (1991) Mesozoic history of the Arctic Islands. In: Geology of the Innuitian Orogen and Arctic Platform of Canada and Greenland. Trettin HP (ed) Geological Survey of Canada, Geology of Canada #3 (also Geological Society of America, The geology of North America vE) pp 371-420

Embry AF, Osadetz KG (1988) Stratigraphy and tectonic significance of Cretaceous volcanism in the Queen Elizabeth Islands, Canadian Arctic Archipelago. Canadian Journal of Earth Science 25: 1209-1219

Fisher RV, Schmincke HU (1984) Pyroclastic Rocks. Spinger-Verlag, Berlin

Frey RW, Pemberton SG (1984) Trace fossil facies models. In: Facies Models, Walker RG (ed). Geological Association of Canada, Geoscience Canada Reprint Series 1, pp 189-208

Glazner AF, Ussler W, Mies JW (1988) Fate of granitic minerals in mafic magmas. EOS 69 (#44): 1504

Hellinger SJ, Sclater JG (1983) Some comments on two-layer extensional models for the evolution of sedimentary basins. Journal of Geophysical Research 88: 8251-8269

Hinds SJ (1991) The correlation and 40Ar/39Ar age dating of the Early Cretaceous Walker Island Member Basalts Axel Heiberg Island, Canadian Arctic. Unpubl honours thesis, Dalhousie University

Hooke RLeB (1967) Processes on arid-region alluvial fans. Journal of Geology 75: 438-60

Irvine TN, Baragar WRA (1971) A guide to the chemical classification of the common volcanic rocks. Canadian Journal of Earth Science 8: 523-548

Kokelaar BP (1982) Fluidization of wet sediments during the emplacement and cooling of various igneous bodies. Journal of the Geological Society of London 139: 21-33

Lajoie J (1984) Volcaniclastic rocks. In: Facies Models. Walker RG (ed) Geological Association of Canada, Geoscience Canada Reprint Series 1. pp 39-52

Leat PT, Thompson RN (1988) Miocene hydrovolcanism in NW Colorado, USA, fuelled by explosive mixing of basic magma and wet unconsolidated sediment. Bulletin of Volcanology 50: 229-243

Le Bas MJ, LeMaitre RW, Streckeisen A, Zanettin B (1986) A chemical classification of volcanic rocks based on the total alkali-silica diagram. Journal of Petrology 27: 745-750

Mackenzie WS, Donaldson CH, Guilford C (1982) Atlas of igneous rocks and their textures. fourth edition. Longman Scientific, New York

Mathews DH (1962) Altered lavas from the floor of eastern north Atlantic. Nature 194: 368-369

McBirney AR (1984) Igneous petrology. Freeman, Cooper and Company, San Francisco

Merrett DC, Muecke GK (1989) Preliminary observations on the volcanics of Phillips Inlet, Ellesmere Island: The last phase of Cretaceous volcanism in the Sverdrup Basin. Musk-ox 37: 28-38

Muecke GK, Reynolds PH, Avison HA (1990) $^{40}Ar/^{39}Ar$ geochronology of episodic magmatism during the late phases of Sverdrup Basin development, Canadian Arctic Islands. Geological Association of Canada, Annual Meeting, Program With Abstracts 15: A93

Palmer BA, Purves AM, Donoghue SL (1993) Controls on accumulation of a volcaniclastic fan, Ruapehu composite volcano, New Zealand. Bulletin of Volcanology 55: 176-189

Pearce JA, Norry MJ (1979) Petrogenetic implications of Ti, Zr, Y, and Nb variations in volcanic rocks. Contributions to Mineralogy Petrology 69: 33-47

Ricketts BD (1985) Volcanic breccias in the Isachsen Formation near Strand Fiord, Axel Heiberg Island, District of Franklin. In: Current Research, Part A, Geological Survey of Canada, Paper 85-1A, pp 609-612

Ritcey DH (1989) A geochemical study of the Carboniferous Audhild volcanics, Northwestern Axel Heiberg Island, Arctic Canada: Initial volcanism in the Sverdrup Basin. Unpubl honours thesis, Dalhousie University

Smith G A (1986) Coarse-grained nonmarine volcaniclastic sediment: Terminology and depositional processes. Geological Society of America Bulletin 97: 1-10

Taylor SR, McLennan SM (1985) The continental crust: its composition and evolution. Blackwell Scientific Publications

Trettin HP (1989) Chapter 13: The Arctic Islands. In: The Geology of North America-An Overview. Bally AW, Palmer AR (eds), Geological Society of America, The Geology of North America, vA., Boulder, Colorado, pp 349-370

Trettin HP, Parrish R (1987) Late Cretaceous bimodal magmatism, northern Ellesmere Island: isotopic age and origin. Canadian Journal of Earth Science 24: 257-265

Walker RG, Cant DJ (1984) Sandy fluvial systems. In: Facies Models. Walker RG (ed) Geological Association of Canada, Geoscience Canada Reprint Series 1. pp 71-90

Williamson MC (1988) The Cretaceous igneous province of the Sverdrup Basin, Canadian Arctic: field relations and petrochemical studies. Unpubl PhD thesis, Dalhousie University

Wright TL (1984) Origin of basalt plateaus, with emphasis on flood basalts. In: Growth and evolution of volcanic edifices. Easton RM and Gasswinkler M (eds), Geological Association of Canada Short Course Notes 4. pp 43-60

APPENDIX A: PETROGRAPHIC DESCRIPTIONS

PART 1: BALS FIORD BASALTS

AX92-188 Flow #1: Tholeiitic Flow

Texture:

Hypocrystalline, seriate textured sample, intergranular patches in intersertal groundmass. Microcrystalline groundmass (0.1-1mm), with larger phenocrysts of plagioclase and clinopyroxene (1-4mm) locally defining porphyritic and glomeroporphyritic textures.

Phenocrysts (10%):

Plagioclase (70%): Sub- to euhedral crystals, with ubiquitous oscillatory zoning at the rims, and occasional inclusion-rich cores (opaques, clinopyroxene, and glass).

Clinopyroxene (30%): Euhedral to anhedral crystals, locally containing fine-grained inclusions of clinopyroxene and plagioclase.

Olivine (rare): Iddingsite replaced pseudomorphs.

Groundmass:

Glass (15%): Mainly replaced by gel-palagonite with darker fibro-palagonite rims. Rare fresh glass (isotropic, pink in PPL) containing abundant crystallites.

Plagioclase (45%): Sub- to euhedral laths.

Clinopyroxene (30%): Sub- to anhedral crystals, locally subophitic.

Opaque (10%): Sub- to euhedral magnetite (cubic), and ilmenite (acicular).

Olivine (rare): Only euhedral crystals recognisable, iddingsite replaced.

AX92-189 Flow #2: Tholeiitic/Olivine-Tholeiitic Flow

Texture:

Hypocrystalline, semi-seriate texture overall, with gradation in grainsize. Larger phenocrysts (0.5-3mm) of plagioclase, clinopyroxene, and olivine define porphyritic and glomeroporphyritic textures in a fine-grained seriate groundmass. Largely intergranular groundmass, with a grain size range from 0.05-0.5mm, with local patches of intersertal texture.

Phenocrysts (10%):

Plagioclase (80%): Sub- to euhedral crystals, almost invariably zoned, containing microcrystalline clinopyroxene, plagioclase, and glass inclusions. Microcrystalline inclusions occur in the cores and parallel to zoning, and cryptocrystalline material fills microfractures in the crystals.

Clinopyroxene (20%): Largely anhedral crystals, locally subophitic growth around groundmass plagioclase laths.

Olivine (Few %): Euhedral (partly resorbed) olivine crystals present in the phenocryst grainsize fraction (one skeletal crystal), Iddingsite replaced, with darker material defining typical olivine fracture patterns locally.

Groundmass:

Glass (5% overall, locally up to 20%): Invariably replaced by palagonite, higher concentrations of glass occur as patches throughout the thin section.

Plagioclase (45%): Occurs as sub- to euhedral laths.

Clinopyroxene (40%): Largely fine-grained, sub- to anhedral crystals, filling interstices between, and surrounding plagioclase laths in groundmass.

Opaque (5%): Sub- to euhedral magnetite (cubic) and ilmenite (acicular).

Olivine (5%): Euhedral, iddingsite pseudomorphs (partially resorbed boundaries).

Notes:

One vesicle observed, slightly elongate and palagonite-filled.

AX92-192 Flow #4: Tholeiitic Flow/Sill (?)

Texture:

Hypocrystalline seriate-textured sample has a fresher appearance, and overall increase in grainsize relative to other samples. Only one cluster of unusually large plagioclase phenocrysts (1.5-4mm) observed, defining rare glomeroporphyritic texture development. Intergranular and intersertal textures observed throughout groundmass (0.05-1.5mm).

Phenocrysts (5%):

Plagioclase (100%): All crystals in the largest grainsize range are plagioclase, many laths only reaching this size range in their greatest dimension. Zoning ubiquitous in all grainsizes of plagioclase, and microcrystalline inclusions of plagioclase, clinopyroxene, opaque, and glass are common in cores and parallel to zoning.

Groundmass:

Glass (20%): Largely fresh (isotropic, pink in PPL) glass with ubiquitous crystallite development. Patchy, localized chlorite and palagonite replacement (few % replaced).

Plagioclase (35%): Sub- to euhedral crystallization as laths, common zoning and inclusions (as described above).

Clinopyroxene (25%): Sub- to anhedral crystallization, largely as finer-grained groundmass material, but locally large crystals observed (up to 1mm).

Opaque (10%): Sub- to euhedral crystals of magnetite (cubic) and ilmenite (acicular).

Olivine (5-10%): Sub- to euhedral pseudomorphs observed with iddingsite and chlorite replacement.

Notes:

This sample shows several unique features, including: limited alteration of interstitial glass, much larger overall grainsize, local replacement of glass and olivine(?) by chlorite. These features suggest a possible intrusive origin for this unit.

AX92-195 Flow #5: Tholeiitic Flow

Texture:

Seriate-textured hypocrystalline groundmass, with slight porphyritic and glomeroporphyritic development in the phenocryst phase (1-4mm). The groundmass (0.1-1 mm) displays intersertal and intergranular development.

Phenocrysts (5%):

Plagioclase (80%): Sub- to euhedral crystals commonly display good zoning, and locally inclusion-rich cores and rims (microcrystalline clinopyroxene).

Clinopyroxene (20%): Sub- to anhedral crystal development.

Olivine (Rare): Sub- to euhedral pseudomorphs with iddingsite replacement.

Groundmass:

Glass (20%): Glass occurs both as fresh glass with common crystallite development (isotropic, pink in PPL), and palagonite replaced. Approximately 50/50 split between fresh and altered glass. Glass occurs as fresh or altered patches throughout the slide.

Plagioclase (40%): Sub- to euhedral lath crystallization, zoning common, recognizable in larger crystals, and inclusion rich rims (microcrystalline clinopyroxene).

Clinopyroxene (30%): Sub- to anhedral crystallization, largely as finer-grained interstitial material.

Opaque (10%): Sub- to euhedral development of magnetite (cubic) and ilmenite (acicular). Ilmenite locally skeletal in patches of fresh glass.

Olivine (Few %): Sub- to euhedral where identified, iddingsite replacement.

Notes:

A single detrital quartz grain observed (1.2mm diameter), resorbed grain boundaries rimmed by dark (PPL) glass, and surrounded by a 0.3mm-thick rim of equigranular clinopyroxene. This extreme alteration illustrates the silica undersaturated nature of this melt.

AX92-196 Flow #6: Tholeiitic Flow

Texture:

Nearly holocrystalline sample displaying semi-seriate texture, with a distinctly larger phenocryst phase (1-4 mm plagioclase and clinopyroxene) defining porphyritic to glomeroporphyritic textures. The groundmass is largely intergranular, with patchy intersertal development. Groundmass grainsize range from 0.05-0.5mm, with a few crystals in 0.5-1mm size range defining the semi-seriate texture.

Phenocrysts (15%):

Plagioclase (60%): Sub- to euhedral development of crystals which commonly display zoning, and microcrystalline inclusions (clinopyroxene, opaque, and glass) in cores and parallel to zoning, especially in rims.

Clinopyroxene (40%): Sub- to anhedral crystals, commonly display zoning.

Groundmass:

Glass (Few %): Patchy occurrence, pervasive palagonite replacement (locally gel- to fibro-palagonite zonation from core to rim).

Plagioclase (45%): Sub- to euhedral laths, commonly zoned and containing inclusions (as described for phenocryst phase).

Clinopyroxene (45%): Sub- to anhedral crystals, occurs largely as finer-grained interstitial material between plagioclase laths.

Opaque (10%): Sub- to euhedral crystals of magnetite (cubic).

Olivine (Rare): One cluster of olivine crystals found, a few others throughout groundmass, all iddingsite-replaced.

AX92-197 Flow #7: Olivine-Tholeiitic Flow

Texture:

Hypocrystalline sample with glomeroporphyritic and porphyritic textures developed with larger plagioclase and clinopyroxene phenocrysts (1-4mm). Seriate, intergranular, and intersertal textures developed in the microcrystalline groundmass (0.01-0.5mm).

Phenocrysts (15%):

Plagioclase (80%): Subhedral to euhedral crystals, commonly zoned, with common cryptocrystalline inclusion patches, both blebby and fracture controlled occurrences.

Clinopyroxene (20%): Subhedral to anhedral crystals developed.

Olivine (Rare): A few large crystals observed, iddingsite replaced.

Groundmass:

Glass (10%): Pervasive palagonite replacement of interstitial glass with euhedral plagioclase and opaque inclusions.

Plagioclase (45%): Sub- to euhedral laths, zoning and inclusions common.

Clinopyroxene (30%): Sub- to anhedral, largely fine-grained interstitial material.

Opaque (15%): Sub- to euhedral, fine-grained intergranular and interstitial (as inclusions in glass) crystals.

Olivine (Few %): Scattered groundmass-size, sub- to euhedral olivine crystals observed, altered to iddingsite.

AX92-198 Flow #8: Olivine-Tholeiitic Flow

Texture:

Glomeroporphyritic texture developed with large clusters of plagioclase +/- clinopyroxene +/- olivine crystals (1-6 mm), set in a finer-grained semi-seriate groundmass. Hypocrystalline, overall coarser-grained (relative to other samples) crystal development. Largely intersertal groundmass (0.1-0.5mm) but local clusters of clinopyroxene and plagioclase develop intergranular textures.

Phenocrysts (15%):

Plagioclase (60%): Sub- to euhedral crystals, commonly zoned, locally contain inclusions of fine-grained plagioclase and glass in cores and parallel to zoning.

Clinopyroxene (30%): Euhedral to anhedral crystals developed, normally in clusters.

Olivine (10%): Sub- to euhedral olivine crystals observed in the phenocryst grainsize range, resorbed to variable degrees, observed within and outside clusters.

Groundmass:

Glass (25%): Mainly opaque, presumably by cryptocrystalline opaque crystal development, with crystallites locally visible. Glass locally shows complete palagonite replacement (gel- to fibro-palagonite replacement core to rim). Other glass patches show partial palagonite replacement.

Plagioclase (30%): Sub- to euhedral laths, commonly display faint zoning.

Clinopyroxene (30%): Sub- to anhedral, largely finer-grained groundmass material in the interstices between plagioclase laths.

Opaque (10%): Occurs almost invariably as inclusions in the interstitial glass, ilmenite (acicular) where distinguishable.

Olivine (5%): Subhedral olivine crystals, with resorbed grain boundaries recognizable in the groundmass size fraction, altered to iddingsite.

AX92-199 Flow #9 (base): Olivine-Tholeiitic Flow

Texture:

Porphyritic and glomeroporphyritic textures developed with large phenocrysts (0.4-2mm) set in a finer-grained seriate groundmass. Hypocrystalline, largely intergranular microcrystalline groundmass (0.03-0.4mm), with spotty interstitial glass.

Phenocrysts (15%):

Plagioclase (60%): Sub- to euhedral laths, commonly zoned, locally inclusion-rich cores and rims (glass/palagonite and clinopyroxene).

Clinopyroxene (30%): Sub- to euhedral crystals, commonly faintly zoned, and inclusion-rich throughout (glass and fine-grained plagioclase).

Olivine (10%): Sub- to euhedral, locally partially resorbed, and pervasively altered to iddingsite (rims and fractures) and carbonate (cores).

Groundmass:

Glass (15%): High concentration in groundmass apparent at high power much more pervasive in the groundmass. Occurs as fresh glass (isotropic, pink in PPL) with crystallites common, and palagonite replaced.

Plagioclase (40%): Sub- to euhedral laths with common fine-grained glass inclusions.

Clinopyroxene (40%): Largely anhedral, very fine-grained (0.03-0.1mm) crystal development in the interstices of plagioclase laths.

Opaque (5-10%): Sub- to euhedral magnetite (cubic) +/- ilmenite (acicular) with rare plagioclase and clinopyroxene inclusions.

Olivine (Few %): Some groundmass-sized olivine crystals observed, sub- to euhedral, and iddingsite-replaced.

Notes:

A few round amygdules observed, range from 0.3-2mm, palagonite-replaced (dark fibro-palagonite rims, lighter gel-palagonite cores).

AX92-200 Flow #9 (upper): Olivine-Tholeiitic Flow

Texture:

Overall seriate texture, with large range of grainsizes (0.02-0.5 mm) in groundmass. Clusters defining glomeroporphyritic texture consist of both fine-grained and very large crystals (0.5-1.5 mm), porphyritic texture largely defined by single, large plagioclase phenocrysts. Hypocrystalline sample with intergranular and intersertal textures developed in the groundmass.

Phenocrysts (15%):

Plagioclase (55%): Largely euhedral laths developed in all grainsizes, commonly zoned, and normally contain scattered inclusions of clinopyroxene and glass, parallel to zoning.

Clinopyroxene (40%): Euhedral to subhedral crystal development with rare faint zoning and common inclusions (glass and/or plagioclase) throughout crystals.

Olivine (5%): Sub- to euhedral crystals observed, pervasive iddingsite replacement, with rare carbonate inclusions.

Groundmass:

Glass (10%): Palagonite-replaced and fresh (isotropic, dark grey in PPL).

Plagioclase (40%): Sub- to euhedral laths, commonly zoned and containing scattered glass and fine-grained clinopyroxene inclusions.

Clinopyroxene (40%): Sub- to anhedral crystals, largely in the finer grainsize range, as interstitial material to groundmass plagioclase laths.

Opaque (10%): Euhedral to anhedral crystals of magnetite (cubic) and possible ilmenite (acicular), with fine-grained plagioclase and clinopyroxene inclusions.

Olivine (Few %): Scattered subhedral, iddingsite-replaced olivine crystals observed in groundmass grainsize fraction.

AX92-201 Flow #10: Tholeiitic/Olivine-Tholeiitic Flow

Texture:

Overall seriate-textured sample, with larger crystals of plagioclase, clinopyroxene, and olivine (0.5-2 mm) locally producing porphyritic and glomeroporphyritic textures. Hypocrystalline, mainly intersertal groundmass texture, with local clusters of intergranular plagioclase and clinopyroxene.

Phenocrysts (15%):

Plagioclase (55%): Sub- to euhedral laths with common zoning, and locally inclusion-rich (clinopyroxene and glass inclusions at rims).

Clinopyroxene (40%): Sub- to anhedral crystals, inclusion-rich with opaques and fine-grained plagioclase.

Olivine (5%): Sub- to euhedral crystals, mainly iddingsite-replaced, with carbonate locally at the cores.

Groundmass:

Glass (15%): Mainly opaque, very difficult to distinguish between opaque minerals and glass material, locally orange hue indicates partial palagonite replacement. Local patches of complete alteration with gel-palagonite cores, and fibro-palagonite rims.

Plagioclase (40%): Sub- to euhedral laths, locally zoning recognised, inclusions common.

Clinopyroxene (35%): Sub- to anhedral crystallization, largely in the finer grainsize range.

Opaque (10%): Magnetite (cubic) and ilmenite (acicular) crystallization as intergranular fill between plagioclase laths, or as inclusions in interstitial glass.

Olivine (Few %): Scattered olivine crystals observed in groundmass size fraction, iddingsite-replaced.

AX92-176 Flow #11: Tholeiitic Flow

Texture:

Semi-seriate texture, with continuous grainsize range for plagioclase. Recognisable phenocryst phase above 0.5mm, defining porphyritic and glomeroporphyritic texture over a largely fine-grained clinopyroxene groundmass. Nearly holocrystalline, intergranular groundmass with grainsize range 0.02-0.5mm (mainly 0.02-0.15).

Phenocrysts (10%):

Plagioclase (60%): Sub- to euhedral crystals, commonly zoned, and fine-grained clinopyroxene inclusions common at rims, parallel to zoning.

Clinopyroxene (40%): Sub- to anhedral crystals with scattered fine-grained clinopyroxene and opaque inclusions.

Olivine (Rare): A few subhedral olivine crystals observed, carbonate-replaced.

Groundmass:

Glass (Few %): Spotty occurrence of palagonite- and carbonate-replaced glass, rare spots of fresh glass (isotropic, pink in PPL).

Plagioclase (50%): Sub- to euhedral laths of variable grainsize defining seriate texture, locally zoned, and with common inclusions (glass, opaque, and possible clinopyroxene).

Clinopyroxene (40%): Largely anhedral development, composing finer-grained fraction in groundmass, interstitial to plagioclase laths.

Opaque (10%): Sub- to euhedral magnetite (cubic) with larger grainsize than groundmass clinopyroxene.

Note:

AX92-177 is a sample from the base of the same flow, displaying a similar texture and mineralogy, but is strongly and pervasively carbonate altered with plagioclase as the only remaining original mineral.

AX92-202 Tholeiitic Dyke Cutting Lower Two Volcaniclastic Units

Texture:

Hypocrystalline, aphyric, seriate-textured sample. Largely intersertal texture observed in groundmass, with a high proportion of palagonite-replaced glass present.

Groundmass:

Glass (25%): Glass, partially palagonite-replaced, contains abundant inclusions of opaques and plagioclase, and common crystallites.

Plagioclase (30%): Sub- to euhedral laths, faintly zoned, and commonly inclusion-rich at cores and rims (clinopyroxene, opaque, and glass).

Clinopyroxene (30%): Sub- to anhedral crystal development, locally subophitic.

Opaque (15%): Sub- to euhedral crystals, commonly within, or surrounding interstitial glass, both magnetite (cubic) and ilmenite (acicular) observed.

AX92-205 Mafic Flow/Sill (?) in Basal Volcaniclastic Sequence

Texture:

Porphyritic and glomeroporphyritic textures developed with phenocrysts of clinopyroxene, plagioclase and possible olivine (carbonate replacement) (0.2-1mm), set in a near-cryptocrystalline, hypocrystalline groundmass of plagioclase, pyroxene, opaques, and glass. A few resorbed detrital quartz grains (with clinopyroxene halos), and a few sub-rounded igneous xenoliths occur as inclusions.

Phenocrysts (5%)

Plagioclase (50%): Euhedral laths, occur as carbonate-replaced pseudomorphs only.

Clinopyroxene (40%): Sub- to euhedral crystals, both fresh and carbonate-altered examples, commonly form glomeroporphyritic clusters with plagioclase.

Olivine (10%?): Possible olivine pseudomorphs with subhedral grainshapes as the result of resorption, altered to an iddingsite + quartz +/- carbonate assemblage. Possibly much higher percentage of sample, but difficult to identify unequivocally.

Groundmass:

Glass (25%): Interstitial glass replaced by palagonite and carbonate (?).

Plagioclase (15%): Sub- to anhedral crystallization, some lath-like forms, positive identification difficult.

Clinopyroxene (30%): Near-cryptocrystalline development, difficult to identify unequivocally.

Opaque (30%): Sub- to euhedral crystallization, largely magnetite (cubic), but ilmenite (acicular) locally observed.

Notes:

Mafic igneous xenoliths (up to 8 mm, truncated by edge of slide) include one highly amygdaloidal sample, one holocrystalline, seriate-textured samples, and others texturally similar to groundmass. Detrital quartz grains up to 1 mm are partially resorbed and have rims of fine-grained clinopyroxene.

PART 2: BJARNASSON ISLAND BASALTS

AX92-215 Olivine-Tholeiitic Sill

Texture:

Hypocrystalline seriate texture with largely intergranular, locally intersertal textures in the groundmass (0.1-1 mm). Phenocrysts (1-3 mm) occur alone and in clusters defining porphyritic to glomeroporphyritic textural overprint.

Phenocrysts (10%):

Plagioclase (80%): Sub- to euhedral crystals commonly display oscillatory zoning and opaque inclusions parallel to zoning and twin planes. Local inclusion concentrations in cores.

Olivine (20%): Euhedral to subhedral crystals, invariably and pervasively altered to iddingsite +/- carbonate.

Clinopyroxene (rare): Sub- to anhedral crystals with common fine-grained glass(?) inclusions.

Groundmass:

Glass (15%): Both fresh (isotropic, pink in PPL) cryptocrystalline material with opaque and plagioclase crystallites, and palagonite- or carbonate-replaced material.

Plagioclase (35%): Euhedral to subhedral laths.

Clinopyroxene (30%): Sub- to anhedral crystallization in interstices of plagioclase laths, local subophitic development.

Opaque (10%): Mainly magnetite (equant) with rare ilmenite (acicular).

Olivine (10%): Sub- to euhedral crystals invariably altered to iddingsite +/- carbonate.

AX92-216 Olivine-Tholeiitic Flow

Texture:

Glomeroporphyritic to porphyritic development with plagioclase, olivine, and rare clinopyroxene phenocrysts (0.1-1.5 mm). Near holocrystalline, fine-grained groundmass (0.01-0.1 mm) with rare glass-rich pockets.

Phenocrysts (15%):

Plagioclase (80%): Sub- to euhedral crystals, local weak oscillatory zoning and opaque inclusions parallel to zoning and twin planes.

Olivine (20%): Euhedral to subhedral crystals, invariably and pervasively altered to iddingsite + carbonate.

Clinopyroxene (rare): Sub- to anhedral crystals.

Groundmass:

Glass (rare): Few percent only, palagonite-replaced.

Plagioclase (30%): Euhedral to subhedral laths.

Clinopyroxene (55%): Very fine-grained, subhedral equant crystals.

Opaque (10%): Euhedral magnetite (equant).

Olivine (5%): Sub- to euhedral crystals invariably iddingsite-replaced.

Notes:

Abundant quartz inclusions (up to 5% of groundmass) showing varying degrees of resorption from complete replacement by clinopyroxene, to partial replacement with fine clinopyroxene halos.

AX92-217 Olivine-Tholeiitic Flow

Texture:

Porphyritic to glomeroporphyritic texture, with 0.15-3 mm phenocrysts in a near-holocrystalline, microcrystalline groundmass (0.01-0.15 mm). Contains sub-rounded seriate-textured xenoliths.

Phenocrysts (10%):

Plagioclase (70%): Euhedral to subhedral crystals, commonly display oscillatory zoning. Rare glass and opaque inclusions.

Olivine (30%): Euhedral to subhedral crystals with a wide range in grainsize, invariably and pervasively altered to iddingsite +/- carbonate.

Clinopyroxene (rare): Anhedral crystals, locally appear resorbed, and possibly xenocrysts.

Groundmass:

Glass (rare): A few percent of groundmass, occurs as patches of isotropic (pink in PPL) material with opaque and plagioclase (?) crystallites.

Plagioclase (30%): Euhedral to subhedral laths.

Clinopyroxene (65%): Sub- to anhedral, very fine-grained, equant crystals.

Opaque (5%): Largely euhedral, possibly magnetite.

Olivine (rare): Rare groundmass olivine, iddingsite-replaced.

Notes:

Few % quartz inclusions in groundmass, clinopyroxene rims or complete recrystallization, as noted in previous sample.

AX92-218 Olivine-Tholeiitic Flow

Texture:

Porphyritic, locally glomeroporphyritic texture defined by phenocrysts (0.1-2 mm) in a holocrystalline, microcrystalline (0.01-0.1 mm) groundmass.

Phenocrysts (15%):

Plagioclase (80%): Sub- to euhedral laths, intensely altered to fibrous chlorite (?) with varying proportions of original crystal preserved as fragments.

Olivine (20%): Euhedral to subhedral crystals, invariably and pervasively altered to iddingsite + carbonate.

Clinopyroxene (rare): Locally resorbed, possibly xenocrysts.

Groundmass:

Glass (rare): Rare pink, isotropic and palagonite-replaced glass, normally associated with quartz grain inclusions.

Plagioclase (25%): Subhedral laths.

Clinopyroxene (65%): Very fine-grained, subhedral, equant crystallization.

Opaque (10%): Very fine-grained magnetite (?) (equant).

Olivine (rare): Some possible olivine in groundmass.

Notes:

Approximately 5% phenocryst-sized quartz inclusions, again displaying varying degrees of resorption and clinopyroxene crystallization. Fresh and palagonite-replaced glass between quartz grain and clinopyroxene rim.

Common subangular, seriate-textured xenoliths.

APPENDIX B: GEOCHEMICAL DATA

ELEMENT	AX92-176	AX92-177	AX92-188	AX92-189	AX92-192	AX92-195	AX92-196	AX92-197	AX92-198	AX92-199	AX92-200	AX92-201
MAJOR ELEMENTS (wt% oxide)												
SiO_2	49.53	32.90	49.18	49.72	49.54	50.03	49.75	48.66	48.91	50.02	50.17	48.73
Al_2O_3	12.86	14.65	13.36	13.66	12.80	12.48	12.39	13.59	13.13	12.92	13.18	12.39
Fe_2O_3*	14.94	10.08	13.29	12.74	14.55	15.63	15.36	12.93	14.43	15.42	15.20	15.32
MgO	5.22	1.01	4.08	5.71	5.18	4.84	4.88	5.59	5.47	5.13	5.05	5.08
CaO	9.64	18.04	8.80	10.43	9.66	9.48	9.46	10.79	10.58	9.78	9.70	9.70
Na_2O	2.64	2.45	2.98	2.30	2.85	3.00	2.84	2.25	2.46	2.74	2.91	2.68
K_2O	0.56	0.49	0.49	0.60	0.37	0.38	0.46	0.20	0.23	0.34	0.37	0.38
TiO_2	1.92	2.11	2.42	1.72	2.22	2.53	2.36	1.77	2.01	2.01	2.01	1.97
MnO	0.24	0.19	0.20	0.19	0.21	0.22	0.22	0.19	0.20	0.22	0.22	0.23
P_2O_5	0.22	0.27	0.42	0.17	0.25	0.30	0.24	0.16	0.18	0.18	0.19	0.17
LOI	2.4	17.9	4.4	1.3	1.3	1.4	0.8	2.1	1.5	2.2	1.3	1.8
TRACE ELEMENTS (ppm)												
Ba	252	197	246	139	143	161	158	60	89	153	125	129
Rb	28	8	29	15	35	34	27	14	13	26	30	21
Sr	176	195	305	223	212	219	190	208	204	180	172	177
Y	45	44	49	37	52	55	57	36	39	51	50	52
Zr	156	168	225	138	205	213	223	134	142	176	175	174
Nb	11	13	23	12	19	18	21	8	9	15	16	17
Ga	20	22	22	18	22	24	21	19	21	22	22	20
Zn	110	128	124	94	110	122	123	100	109	112	116	112
Cu	116	125	71	127	176	203	212	160	191	229	236	227
Ni	46	54	24	54	45	42	55	65	60	46	50	46
V	391	441	224	289	330	387	441	326	351	441	433	418
Cr	41	46	26	94	45	27	73	91	74	15	21	19

* Fe_2O_3 + FeO

ELEMENT	AX92-202	AX92-205	AX92-215	AX92-216	AX92-217	AX92-218

MAJOR ELEMENTS (wt% oxide)

SiO_2	44.92	46.69	47.74	50.65	51.25	50.53
Al_2O_3	12.95	12.81	14.01	13.11	14.11	13.26
Fe_2O_3*	16.22	15.50	12.44	11.88	12.51	11.65
MgO	5.47	4.33	6.32	6.52	6.32	6.11
CaO	10.54	8.77	10.69	10.35	10.51	9.80
Na_2O	2.78	3.44	2.09	2.01	2.36	2.19
K_2O	0.65	0.92	0.31	0.14	0.21	0.14
TiO_2	3.30	3.12	1.54	1.54	1.59	1.48
MnO	0.42	0.27	0.19	0.20	0.18	0.14
P_2O_5	0.38	0.32	0.13	0.13	0.14	0.12
LOI	2.9	2.9	2.5	2.5	0.6	3.7

TRACE ELEMENTS (ppm)

Ba	273	238	92	91	95	58
Rb	11	29	7	5	8	7
Sr	255	307	224	217	206	184
Y	58	46	29	30	29	28
Zr	259	208	109	118	119	118
Nb	24	22	7	7	9	9
Ga	25	22	19	18	18	16
Zn	134	146	82	86	89	86
Cu	208	63	144	120	137	109
Ni	65	27	89	89	86	78
V	422	447	308	317	311	305
Cr	82	13	195	209	202	191

* Fe_2O_3 + FeO